POLITECNICO DI MILANO

Scuola di Ingegneria Industriale e dell'Informazione

Corso di Laurea Magistrale in Ingegneria Energetica

POLITECNICO
MILANO 1863

Biodiesel Production from Chilean Macroalgae: Techno-Economic Feasibility Analysis of Cogenerative and Solar Technologies Integrated in the Transesterification Process

Relatore: Prof. Paolo SILVA

Tesi di Laurea di:

Nicolò GIOSTRA Matr. 858698

Anno Accademico 2017-2018

“Cosa importa se è finita

E cosa importa se ho la gola bruciata, o no

Ciò che conta è che sia stata

Come una splendida giornata…”

A Bi e Fi

Table of contents

TABLE OF CONTENTS 3

ABBREVIATION INDEX 6

ABSTRACT 7

SOMMARIO 8

INTRODUCTION 9

CHAPTER 1 12

CLASSIFICATION OF MACRO-ALGAE 12
CULTIVATION OF MACRO-ALGAE 13
ALGAE CHEMICAL COMPOSITION 15
MACRO-ALGAE SCENARIO IN CHILE 17
FOCUS ON *DURVILLAEA ANTARCTICA AND LESSONIA NIGRESCENS* 20

CHAPTER 2 23

OIL EXTRACTION PROCESS AT "UNIVERSIDAD TECNICA FEDERICO SANTA MARIA" 23
SOXHLET EXTRACTOR 23
CONSTITUENTS 24
OPERATION 25
PREPARATION PHASE 28
EXTRACTION PROCESS AND RESULTS 31
FIRST SIMULATION 32
SECOND SIMULATION 32
THIRD SIMULATION 33

CHAPTER 3 34

TRANSESTERIFICATION PROCESS 34
TRANSESTERIFICATION PROCESS ON ASPEN PLUS SOFTWARE 37
I SIMULATION: PRODUCTION OF AROUND 1000 KG/H OF FAME 41
II SIMULATION: PRODUCTION OF AROUND 6000 KG/H OF FAME 42
RESULTS: ENERGY DEMAND AND WORKING TEMPERATURES 43

CHAPTER 4 47

CONVENTIONAL TECHNOLOGIES TO SUPPLY POWER TO THE PROCESS 47

COGENERATION TECHNOLOGIES **49**
COGENERATIVE INTERNAL COMBUSTION ENGINE (ICE) **54**
FEASIBILITY OF COGENERATION ICE IN BIODIESEL PRODUCTION PROCESS 57
COGENERATION GAS TURBINE **58**
FEASIBILITY OF COGENERATION GAS TURBINE IN BIODIESEL PRODUCTION PROCESS 61
COGENERATION STEAM TURBINE **61**
FEASIBILITY OF COGENERATION STEAM TURBINES 63
COGENERATION COMBINED CYCLE **65**
FEASIBILITY OF COGENERATION COMBINED CYCLE 65

CHAPTER 5 **66**

SOLAR TECHNOLOGIES TO SUPPLY POWER TO THE PROCESS **66**
THERMAL ENERGY STORAGE SYSTEMS (TES) **69**
FLAT PLATE SOLAR COLLECTORS **74**
I CONFIGURATION 79
II CONFIGURATION 84
III CONFIGURATION 85
CONCENTRATING SOLAR PANELS (CSP) **86**
I SCENARIO 93
II SCENARIO 96

CHAPTER 6 **99**

ECONOMIC ANALYSIS **99**
ECONOMIC ANALYSIS OF THE TRANSESTERIFICATION PROCESS **101**
I SCENARIO 103
II SCENARIO 104
ECONOMIC ANALYSIS OF "BASE-CASE" WITH BOILER **106**
I SCENARIO 106
II SCENARIO 107
ECONOMIC ANALYSIS OF THE INTEGRATION BETWEEN BIODIESEL PROCESS AND GAS TURBINE **107**
ECONOMIC ANALYSIS OF THE INTEGRATION BETWEEN BIODIESEL PROCESS AND STEAM TURBINE **109**
ECONOMIC ANALYSIS OF THE INTEGRATION BETWEEN BIODIESEL PROCESS AND SOLAR TECHNOLOGIES **110**
ECONOMIC ANALYSIS OF THE INTEGRATION BETWEEN BIODIESEL PROCESS AND SOLAR FLAT PLATE COLLECTORS **111**
ECONOMIC ANALYSIS OF THE INTEGRATION BETWEEN BIODIESEL PROCESS AND CONCENTRATING SOLAR PANELS **115**

CHAPTER 7 **119**

CONCLUSIONS 119

LIST OF FIGURES 122

LIST OF TABLES 125

REFERENCES 126

Abbreviation Index

FAO	Food and Agriculture Organization
d.w.	Dry Weight
FAs	Fatty Acids
FFAs	Free Fatty Acids
MUFAs	Mono Unsaturated Fatty Acids
PUFAs	Poly Unsaturated Fatty Acids
HC	HydroCarbons
CO	Carbon Monoxide
PM	Particulate Matter
NOx	Nitrogen Oxides
EPA	Environmental Protection Agency
FAME	Fatty Acid Methyl Esters
T-METHANOL	Distill. Column for Methanol Recovery
T-FAME	Distill. Column for FAME Purification
T-GLYCEROL	Distill. Column for Glycerol Purification
HX1	Heat Exchanger no 1
HX3	Heat Exchanger no 3
SEP1	Separator no1
ROIL	Recovered Oil
ME	Methanol
ME-H20	Methanol-Water
NEUTR	Neutralization Reactor
CHP	Combined Heat and Power
CSP	Concentrating Solar Power
ESI	Energy Savings Index
ICE	Internal Combustion Engine
DNI	Direct Normal Irradiance
TES	Thermal Energy Storage
HTF	Heat Transfer Fluid
PCM	Phase Change Material
APEA	Aspen Process Economic Analyzer
OPEX	Operating Costs
CAPEX	Capital Costs
EPC	Equipment Purchasing Cost
PBP	Pay-Back Period
NPV	Net Present Value
IRR	Interest Rate of Retur

Abstract

The present work is born with the aim of finding a solution to the conspicuous accumulation of algae on the Chilean coasts. Every year the coastal communities are forced to employ huge economic efforts for the collection and disposal of the algae. An effective solution is to exploit their energy potential for biodiesel production. In fact, biodiesel is considered a promising alternative to conventional diesel, in a world increasingly threatened by climate changes caused by the excessive exploitation of fossil resources. However, it is common practice to supply the necessary energy to the biodiesel process by means of fossil fuels, contributing to environmental disasters. This is why the present paper aims to analyze possible solutions in order to make the process the greenest possible. The first part of the study involves the simulation on Aspen of the whole oil-FAME transesterification process, with the aim of assessing the demanded energy flows. It continues with the analysis of conventional cogeneration and solar technologies (solar thermal collectors and concentrating plants) that can provide the process with this energy, exploiting the same biodiesel produced *in loco* and the wide Chilean solar potential. The elaborate ends with the economic analysis of the various technologies with the aim of indicating the optimal solution that allows exploiting the energy potential of algae in such a way as to free the process from an extreme dependence on fossil sources and to make it as renewable as possible. The results show how the integration between the steam turbine and solar collectors makes the process sustainable, clean and even self-sufficient. On the contrary, concentrating solar technology, despite being fascinating, appears to be the least indicated solution, given its non-maturity on Chilean soil.

KEY WORDS: Algae; Biodiesel; Transesterification process; Fossil fuels; FAME; Cogeneration technologies; Solar technologies; Thermal solar collectors; Concentrating solar panels; Economic analysis.

Sommario

Il presente lavoro nasce con l'obiettivo di trovare una soluzione al cospicuo accumulo di alghe sulle coste cilene. Ogni anno le comunità costiere si trovano costrette ad impiegare ingenti sforzi economici per la raccolta e lo smaltimento delle stesse. Un'efficace soluzione sarebbe quella di sfruttare il potenziale energetico delle alghe per la produzione di biodiesel. Il biodiesel è infatti considerato una promettente alternativa al diesel convenzionale, in uno scenario mondiale sempre più minacciato dai cambiamenti climatici causati dall'eccessivo sfruttamento delle risorse fossili. È però prassi comune quella di fornire l'energia necessaria al processo di conversione del biodiesel tramite combustibili fossili. È per questo che il presente elaborato si prepone l'obiettivo di analizzare possibili soluzioni per rendere il processo il più "green" possibile. La prima parte dello studio in esame prevede la simulazione su Aspen dell'intero processo di transesterificazione da olio a FAME, con l'obiettivo di valutare i flussi energetici richiesti dal processo. Prosegue con l'analisi di tecnologie convenzionali cogenerative e solari (collettori solari termici e impianti a concentrazione) che possano fornire tale energia al processo, sfruttando lo stesso biodiesel prodotto *in loco* e l'enorme potenziale solare del Cile. L'elaborato si conclude con l'analisi economica delle varie tecnologie con lo scopo di indicare la soluzione ottima che permetta di sfruttare il potenziale energetico delle alghe in modo tale da svincolare il processo da un'estrema dipendenza dalle fonti fossili e di rendere lo stesso il più rinnovabile possibile. I risultati mostrano come l'integrazione tra turbina a vapore e collettori solari renda il processo sostenibile, pulito e anche auto-sufficiente. Al contrario, la tecnologia solare a concentrazione, seppur affasciante, appare la meno indicata data la non maturità della stessa sul suolo Cileno.

PAROLE CHIAVE: Alghe; Biodiesel; Processo di transesterificazione; Fonti fossili; FAME; Tecnologie cogenerative; Tecnologie solari; Collettori solari termici; Pannelli solari a concentrazione; Analisi economica.

Introduction

The present work is born as a way to find a solution to the problem related to macro-algae accumulation on the Chilean coasts. Over the last years, Chile has experienced an increasing difficulty in disposing of all those algae that each year increase their amount. This problem is especially evident in the *V region*, the region of Valparaiso, where in the small city of *Algarrobo* is becoming a serious issue since 2014. The reason, according to the inhabitants of the village, is clear: the owners of yachts, with the support of the authorities, managed to join a small island near the city, causing the water to stagnate and, therefore, the algae to increase. In addition to the presence of algae, recent is the problem of the strong smell that makes tourism unbearable in the sector, causing economic losses to the merchants of the city.

A way to face the high costs of harvesting and disposing of algae is by exploiting their energy content and turning them into bio combustibles. In fact, algae are an important source of energy and they can be used in the production of biodiesel and biogas. Algal biomass can be considered a sustainable and cost-effective solution for the present and future obstacles.

In addition, over the last decades, the world is facing serious energy and economic issues related to environmental concerns (GHG emissions, global warming, receding of glaciers, rising of sea levels and loss of biodiversity [1]) due to the massive use of fossil fuel sources and their following depletion for an increase in the demand of oil, gas and coal as a consequence of world's population increment.[1] What follows is a growing attention towards R&D with the aim of finding possible solutions that, above all, are renewable and sustainable. As a matter of fact, renewable sources are receiving an important attention as an attractive alternative in producing biofuels.

Marine biomass shows important advantages as it can grow on fresh, brackish, saline and wastewater streams and does not require use of arable land for the cultivation[2]. Macro-algae can convert solar energy into chemical energy with higher photosynthetic efficiency (6–8%) than terrestrial biomass (1.8– 2.2%) (FAO, 1997). In addition, algae can reach 2–20 times the production potential of conventional terrestrial energy crops. A negligible or low amount of lignin makes them less resistant to degradation than lignocellulosic feedstocks, and avoids

the need for energy-intensive pretreatments.[3] Macro-algae can tolerate a wide variety of environmental conditions and can be produced all over the year. [4]

The work focuses on the production of biodiesel starting from oil extracted from macro-algae. The most used method is through a transesterification process by which the lipids contained in the biomass react with an alcohol (generally methanol or ethanol) in presence of a catalyst (generally potassium or sodium hydroxide) to form esters and glycerol. A big obstacle in using marine biomass for the production of clean combustibles is the huge expenditure of energy, that goes from the extraction of the oily part from the algae to the transesterification process itself. What makes the process extremely energy-costing is the methanol recovery stage[5] and the purification of biodiesel and glycerol, in order to get a product that is the cleanest possible and a by-product with an high level of purity to be used for other purposes. Traditionally all the energy demanded by the process is provided with fossil fuels, and this represents a possibility to switch to renewable sources. The present work aims at considering the installation of conventional technologies that implement the same biodiesel produced and a solar field by which ensuring the provision of the energy required by the biodiesel production process. The idea is born on the consideration of making the entire process as greener as possible, getting rid of fossil fuels-based technologies as well as accounting for the high potential that central and northern Chile has in terms of solar power.

First part of the study is the analysis of Chilean macro-algae scenario with an important focus on the two species of *Durvillaea Antarctica* and *Lessonia Nigrescens*, their chemical composition and energy potential. It follows a study performed at Universidad Técnica Federico Santa María of Valparaiso, Chile, that sees the extraction of oil content from the two above-cited algae. The third chapter of the study is totally related to the transesterification process of the extracted oil to get biodiesel and glycerol; the process has been entirely simulated on Aspen Plus software to get all the energy variables to perform the following analysis. It follows the central part of the study where different technologies are proposed to provide the biodiesel process with the necessary energy inputs: among the cogenerative conventional technologies, internal combustion engine, gas turbine, steam turbine and combined cycles are studied giving a look at the "base-case" of conventional boilers; solar technologies are studied as well, such as flat plate collectors and concentrating solar panels to exploit the high

solar potential of Chile. Last part of the present work is focused on the economic analysis of the transesterification process and the different technological configurations, with the aim of assessing which one can be considered the most suitable even from an economic point of view.

The result would be a scenario in which two problems are overcome: the serious issue of the excessive algae accumulation along Chilean coasts and the need to get rid of an undue use of fossil fuels in a world increasingly threated by environmental disasters.

Chapter 1

Classification of Macro-algae

Macro-algae are large aquatic multicellular photosynthetic plants that can be seen without the aid of a microscope (differently from micro-algae). Macro-algae are classified as green, red, brown and blue algae (Cyanophyta)[6] according to the thallus color derived from natural pigments and chlorophylls.

Figure 1.1 Botryocladia Sp.

There are about 4500 species of green algae including 3050 species of freshwater-favorable algae (class *Trebouxiophyceae* and *Chlorophyceae*) and 1500 species of seawater-favorable algae (class *Bryopsidophyceae, Dasycladophyceae, Siphoncladophyceae*, and *Ulvophyceae*) (Guiry, 2012). Red algae are all included in a single class (i.e., *Rhodophyceae*) consisting of two subclasses: *Florideophycidae* and *Bangiophycidae*. The red color is given by chlorophyll a, phycoerythrin and phycocyanin. There are 4000–6000 species of red algae in over 600 genera, and most of them exist in tropical marine environments. Brown algae are classified as *Phaeophyceae* under phylum *Chrysophyta*. Their principal photosynthetic pigments are chlorophyll a and c, b-carotene, and other xanthophylls. Exist 1500–2000 species. [7]

Figure 1.2 Laminaria digitata

The pigment, growth, and chemical composition of macro-algae are significantly affected by their habitat conditions such as light, temperature, salinity, nutrient, pollution, and even water motion, particularly depending on their taxonomical classes and species. Among the conditions, light is the most principal contributor. Thus, the classes of macro-algae are vertically distributed from the upper zone (close to the sea surface) to the lower sublittoral zone.[8] This is because macro-algae have their respective pigments, which absorb selectively the light with specific wavelengths: for instance, while most macro-algae live in the littoral

zone near coastal line, some red algae inhabit the deep sea where sunlight availability is limited.

Cultivation of Macro-algae

Algal biomass can be cultured or acquired from natural, eutrophicated and degraded water bodies. In 2010, the world production of seaweeds was estimated at 19 million tons, where *Laminaria Japonica* was the most cultivated at 6.8 million tons.[9] The current uses of seaweeds are predominantly in the food, feed, chemicals, cosmetics and pharmaceutical sectors in Asian countries such as China, the Philippines, North and South Korea, Japan and Indonesia.

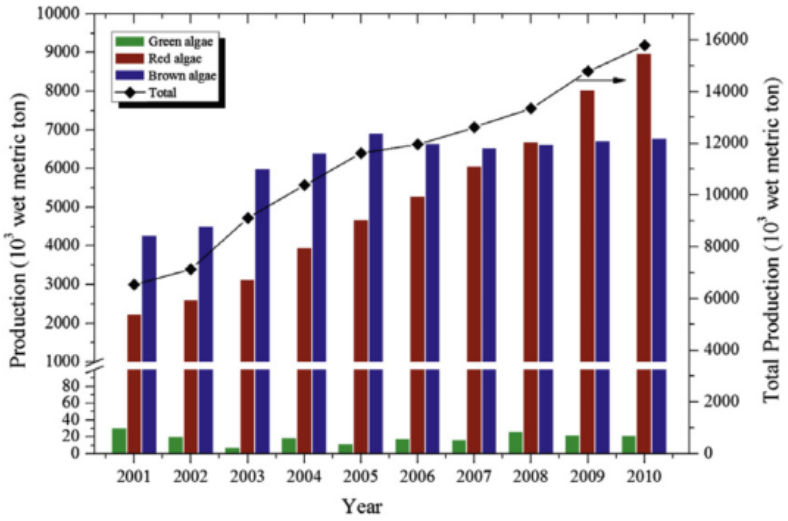

Figure 1.3 Production of algae

When the only outcome product is energy, the cultivation of algal biomass is unlikely to be economically viable, and thus many studies have been carried out in order to make it feasible.[3]

Although only a dozen of algae is commercially cultivated among over 20000 species reported worldwide (Critchley et al., 1998), the amount of macro-algae mass-cultivated in the world has continuously increased over the last 10 years at an average of 10% (FAO, 2012).

World production of macroalgae, microalgae, energy crops, and lignocellulosic biomass.

Species	Group (or phylum)	Production	% of total
Macroalgae[a]			
Laminaria japonica	Brown algae	5,146,883	32.61
Eucheuma spp.	Red algae	3,489,388	22.11
Kappaphycus alvarezii	Red algae	1,875,277	11.88
Undaria pinnatifida	Brown algae	1,537,339	9.74
Gracilaria verrucosa[b]	Red algae	1,152,108	7.30
Porphyra spp.	Red algae	1,072,350	6.79
Gracilaria spp.[b]	Red algae	565,366	3.58
Porphyra tenera	Red algae	564,234	3.57
Eucheuma denticulatum	Red algae	258,612	1.64
Sargassum fusiforme	Brown algae	78,210	0.50
Phaeophyceae	Brown algae	21,747	0.14
Enteromorpha clathrata	Green algae	11,150	0.07
Monostroma nitidum	Green algae	4,531	0.03
Caulerpa spp.	Green algae	4,309	0.03
Codium fragile	Green algae	1,394	0.01
Gelidium amansii	Red algae	1,200	0.01
Total		15,784,098	100.00
Microalgae[c]			
Arthrospira sp.	Cyanophyta	3000	
Chlorella sp.	Chlorophyta	2000	
Dunaliella salina	Chlorophyta	1200	
Haematococcus pluvialis	Chlorophyta	3000	
Energy crops[d]			
Corn		844,405,181	
Palm oil		45,097,422	
Rapeseed		59,071,197	
Sugar cane		1,685,444,531	
Soybean		261,578,498	
Lignocellulosic biomass[e]			
Corn stover		12.6	
Switchgrass		9.0	

Figure 1.4 World production of different kinds of biomass

The figure easily shows that brown and red algae are cultivated more than green algae. The amount of the mass-cultivated macro-algae is four and six orders of magnitude greater than for the micro-algae and lignocellulosic biomass, respectively. This implies that with current farming technology, macro-algae can be more mass-cultivated to sufficiently supply feedstocks for biorefinery. At present the most promising macro-algae species for biorefinery feedstock are *Laminaria japonica, Eucheuma spp., Kappaphycus Alvarezii, Undaria Pinnatifida,* and *Gracilaria Verrucosa*. For brown algae, only two species, *L. Japonica* and *U. Pinnatifida*, account for over 40% of the total. For red algae, *Eucheuma, Kappaphycus* and *Gracilaria spp.* account for about 40%. In contrast, the production number of green algae is negligible. Considering current mass-cultivation technology and market demand, macro-algae-based refinery technology needs to be focused on utilizing brown and red algae rather than green algae. To increase the amount of macroalgal biomass for biorefinery globally,

international cooperation activities must intervene and improve the farming technology and experience of the East Asian countries (i.e., China, Korea, Japan, Indonesia, and the Philippines), which are the principal macro-algae producers (FAO, 2012). These countries accounted for 95% of the world's supply in 2010.[7]

There is potential for macroalgal cultivation in offshore renewable energy facilities, such as wind farms, on the idea of sharing the infrastructure with an offshore enterprise that can be beneficial from planning, design and operation perspectives. The challenge includes the feasibility of growing fast rate macro-algae in the open ocean, cutting costs of collection and avoiding environmental damage. If farming methods were improved, marine biomass could become a potentially viable energy crop. Inshore seaweed aquaculture is well established and has less challenges.[10]

Another option is represented by the collection of storm cast weed from beaches, which is more developed in countries such as the UK and Ireland. That is considered as the most readily available feedstock for the generation of biofuel on a small, localized scale. However, it is underlined that the biomass of beach-cast would unlikely be sufficient for larger scale exploitation of this resource for bioenergy purposes. Besides, it must be considered that this source of biomass does not guarantee a constant and homogeneous feedstock supply as it depends on variable climatic conditions.

Algae Chemical Composition

Knowing the algal chemical composition permits to calculate the biodiesel potential yields that can be obtained through a whatever process that converts algae in biofuels.

Algal biomass is rich in nutrients such as carbon, nitrogen and phosphorus. Nevertheless, several key factors have been identified in the biochemical composition of algal biomass affecting diesel or gas production, such as *moisture content*, *lipids, carbohydrates, proteins, ash content* and *lignin fraction*.[3]

Obviously algal biomass exhibits very high level of moisture content: it typically ranges between 78% and 90%.[11] Thus, the compatibility of this kind of biomass with esterification

process: a drying step is always mandatory, that would negatively impact on the overall process cost.

As a general rule, macro-algae are extremely rich in proteins, whose content goes from 30 to 70% on dry basis, followed by carbohydrates whose content ranges between 3% and 40% d.w., depending on genera and season.[3] The carbohydrates synthesis is related to the periods of maximum growth, increased photosynthetic activity and a reduction in proteins content. For instance, the carbohydrates content of *Laminaria digitata* peaked in June (69.1% d.w.) as result of the increased rate of photosynthesis, whereas the lowest level of carbohydrates was reached in early spring since most carbohydrates have been used up during winter.[12] Lipids level in macro-algae has been found to be very low, in general between 0.4% and 5% d.w., but appreciable exceptions of algae with high lipid content exist, making them more suitable for a biodiesel production process. Macro-algae contain different types of carbohydrates with respect to terrestrial plants.

Carbohydrate composition of macroalgae, microalgae, and lignocellulosic biomass.

Macroalgae[a]			Microalgae[b]	Lignocellulosic biomass
Green algae	Red algae	Brown algae		
Polysaccharide	*Polysaccharide*	*Polysaccharide*	Starch	Cellulose
Mannan	Carrageenan	Laminarin	Total carbohydrate	Hemicellulose
Ulvan	Agar	Mannitol	Arabinose	Lignin
Starch	Cellulose	Alginate	Fucose	
Cellulose	Lignin	Fucoidin	Galactose	
Monosaccharide	*Monosaccharide*	Cellulose	Glucose	
Glucose	Glucose	*Monosaccharide*	Mannose	
Mannose	Galactose	Glucose	Rhamnose	
Rhamnose	Agarose	Galactose	Ribose	
Xylose		Fucose	Xylose	
Uronic acid		Xylose		
Glucuronic acid		Uronic acid		
		Mannuronic acid		
		Guluronic acid		
		Glucuronic acid		

Figure 1.5 Carbohydrate composition of macroalgae, microalgae and lignocellulosic biomass

It is worthy to note that macro-algae almost do not include lignin because they do not need to stand rigidly in the water (being lignin the constituent needed for the rigidity of terrestrial plants). Thus, due to their low lignin content, macro-algae can provide many benefits for biorefinery: no need for complex processes such as lignin removals and detoxification of lignin-originated inhibiting compounds. Compared to the terrestrial biomass, macro-algae have higher contents of water (70–90% fresh wt.) and minerals such as alkali metals (10–50% d.w.) (Ross et al., 2008). In contrast, they have lower contents of protein (7–15% d.w.) and lipids (1–5% d.w.) (Jensen, 1993).

Macro-algae Scenario in Chile

Over the last years, Chile is facing important problems related to the excessive accumulation of algae along its coasts. The problem is extremely evident in the region of Valparaiso where, for the local community of *Algarrobo*, it is becoming a serious issue by threatening summer tourism.

The excessive presence of algae is an important issue all the way long from Antofagasta to Chilean Patagonia, such that specific types of algae are used in Chilean culture as edible food as a consequence of their high richness of organic constituents. They are known to be of nutritional value regarding vitamin, protein and mineral contents (with sodium, calcium, potassium, chlorine, sulfur and phosphorus)[13]. It has been said that 100 g of seaweed provides more than the daily requirement of Vitamin A, B2 and B12 and two thirds of the Vitamin C requirement [14], as well as an important source of dietary fiber, important in preventing constipation, colon cancer, cardiovascular disease and obesity, among others. [15] In addition, the presence of Fatty Acids has been proved to be able to reduce heart diseases, thrombosis and atherosclerosis. [16] Their proteins are rich in glycine, arginine, alanine and glutamic acid; they contain amino acids essential at levels comparable to those indicated by FAO, they have a low Na/K ratio, of the order 0.14-0.16, which helps to reduce the incidence of hypertension.[13] That is the case of *Durvillaea Antarctica*, most commonly known as *ochayuyo,* that is sold and consumed in almost every part of Chile and it is found from Coquimbo region to Cabo de Hornos.[17]

The following image has been taken from Chilean SARNAPESCA (*Servicio Nacional de Pesca y Acuicultura – National Fishing and Aquaculture Service*) and shows the variety of Chilean algal species (micro and macro) as well as their accumulation every year on the beach shores. It's worthy to take a special look to *Chascón* and *Cochayuyo*, that are respectively *Lessonia Nigrescens* and *Durvillaea Antarctica*, the two macro-algae studied in the present work.

ESPECIE	2001	2002	2003	2004	2005	2006	2007	2008	2009	2010	2011
TOTAL ALGAS	299.791	315.668	349.008	410.850	425.343	339.334	339.938	412.266	456.225	380.759	418.031
CAROLA	5	12	5	10	-	17	13	-	-	-	-
CHASCA	402	533	392	402	683	310	494	292	375	219	222
CHASCON	87.508	96.428	108.899	151.752	203.897	161.834	136.766	202.262	222.628	190.746	241.633
CHICOREA DE MAR	3.325	5.677	4.986	4.642	1.517	1.590	980	1.031	2.001	914	998
COCHAYuYO	2.098	2.312	1.764	2.733	2.562	2.292	4.274	4.872	5.872	6.048	6.468
HAEMAtOCOCCuS	-	-	-	-	-	1.444	7	16	38	12	5
HuIRO	9.672	9.774	11.501	9.543	8.786	9.319	10.950	17.061	14.097	11.735	19.400
HuIRO PALO	18.457	25.956	69.272	65.290	46.923	27.552	31.010	33.754	54.120	62.734	46.239
LIQuEN GOMOSO	-	-	-	93	187	215	-	2	-	-	-
LuCHE	-	8	31	16	9	4	33	87	102	16	41
LuGA CuCHARA O CORtA	-	7.329	6.247	5.954	4.930	3.731	5.108	4.372	4.225	1.172	2.096
LuGA NEGRA O CRESPA	-	20.047	21.135	18.414	24.942	17.135	12.297	14.941	34.289	30.194	29.559
LuGA-LuGA	37.606	99	9	24	13	8	-	-	-	-	-
LuGA-ROJA	22.717	21.301	30.952	33.308	42.541	33.331	41.879	41.896	29.159	19.725	14.616
PELILLO	117.969	126.184	93.809	118.669	88.353	77.336	93.402	85.653	89.316	57.239	56.732
SPIRuLINA	-	-	-	-	-	3.189	2.712	6.000	3	5	22
OtRAS ALGAS	32	8	6	-	-	27	13	27	-	-	-

Figure 1.6 Algae accumulation along Chilean coasts every year

It can be noticed that *Lessonia Nigrescens* is widely the most abundant all over the Chilean coasts with an accumulation in 2011 of more than 240 thousand tons.

By looking at the 2011 as it is the most recent year with available data, the algae accumulation according to the months is reported as follows:

ESPECIE	ENE	FEB	MAR	ABR	MAY	JUN	JUL	AGO	SEP	OCT	NOV	DIC	Total
CHASCA	45	19	57	7	13	-	-	1	9	36	22	13	222
CHASCON O HuIRO NEGRO	20.821	25.648	25.613	23.751	18.476	17.113	15.033	20.244	18.163	14.564	19.034	23.173	241.633
CHICOREA DE MAR	88	56	65	39	60	21	40	62	119	217	108	123	998
COCHAYuYO	963	855	1.092	881	364	197	135	134	115	317	462	953	6.468
HAEMAtOCOCCuS	-	-	-	-	-	-	-	-	-	2	2	1	5
HuIRO	1.769	2.167	2.217	1.800	1.646	1.009	755	1.267	1.536	1.494	1.715	2.025	19.400
HuIRO PALO	3.268	4.405	5.970	3.883	5.958	3.600	3.145	5.252	3.369	2.085	2.012	3.292	46.239
LuCHE	2	2	1	2	2	5	4	6	6	6	3	2	41
LuGA CuCHARA O CORtA	338	384	471	113	15	7	2	1	6	26	263	470	2.096
LuGA NEGRA O CRESPA	5.200	6.197	7.354	4.641	2.686	359	119	8	36	53	382	2.524	29.559
LuGA-ROJA	1.251	2.029	1.585	632	878	587	189	1	566	1.567	2.347	2.984	14.616
PELILLO	3.995	7.319	8.807	4.766	4.709	3.869	1.591	2.502	1.894	3.454	6.293	7.533	56.732
SPIRuLINA	2	2	2	2	2	2	2	-	2	2	2	2	22

Figure 1.7 Algae accumulation along Chilean coasts in year 2011

Where it can be seen that algae mostly accumulate on beaches during summertime, from November to April.

The following image shows the situation according to the regions:

ESPECIE	XV	I	II	III	IV	V	VI	VII	VIII	IX	XIV	X	XI	XII	RM	AI	BF	Total
CHASCA	-	-	-	-	6	-	166	14	-	-	-	36	-	-	-	-	-	222
CHASCON O HuIRO NEGRO	-	9.974	61.890	120.046	43.753	5.533	220	46	171	-	-	-	-	-	-	-	-	241.633
CHICOREA DE MAR	-	-	-	32	35	-	-	-	748	-	-	183	-	-	-	-	-	998
COCHAYuYO	-	-	-	-	-	215	424	204	3.573	250	729	1.073	-	-	-	-	-	6.468
HAEMAtOCOCCuS	-	5	-	-	-	-	-	-	-	-	-	-	-	-	-	-	-	5
HuIRO	-	460	2.232	2.244	5.329	423	334	55	172	-	27	8.124	-	-	-	-	-	19.400
HuIRO PALO	-	632	3.992	10.866	26.583	3.511	301	-	2	-	148	204	-	-	-	-	-	46.239
LuCHE	-	-	2	-	-	-	-	3	33	-	2	1	-	-	-	-	-	41
LuGA CuCHARA O CORtA	-	-	-	-	2	84	1.111	-	246	-	263	390	-	-	-	-	-	2.096
LuGA NEGRA O CRESPA	-	-	-	-	-	2	-	-	4.522	-	372	24.315	348	-	-	-	-	29.559
LuGA-ROJA	-	-	-	-	-	-	-	47	7	3	134	11.081	1.561	1.783	-	-	-	14.616
PELILLO	-	-	4	1.223	2.543	-	-	-	68	-	845	52.046	3	-	-	-	-	56.732
SPIRuLINA	-	22	-	-	-	-	-	-	-	-	-	-	-	-	-	-	-	22

Figure 1.8 Algae accumulation according to regions

By focusing on the *V Región*, that is the Valparaiso region, it can be seen that only 2.3% of the entire *Lessonia Nigrescens* accumulation and 3.3% of *Durvillaea Antarctica* is recorded in that region, while the very northern part of Chile presents much higher numbers (the third region accounts for half the total accumulation of *Lessonia*).

Finally, by looking at the only city of Valparaiso, the situation is described below:

ESPECIE	ENE	FEB	MAR	ABR	MAY	JUN	JUL	AGO	SEP	OCT	NOV	DIC	Total
CHASCON O HuIRO NEGRO	28	62	11	19	15	12	8	4	16	23	9	36	243
COCHAYuYO	-	-	-	-	-	17	-	-	8	6	1	13	45
HuIRO	-	-	-	-	-	-	-	12	-	-	-	-	12
HuIRO PALO	5	4	6	4	6	12	16	6	2	1	2	-	64
LuGA CuCHARA O CORtA	-	-	-	-	-	-	-	-	-	-	1	6	7

Figure 1.9 Algae accumulation in the city of Valparaiso

Focus on *Durvillaea Antarctica and Lessonia Nigrescens*

As already said, in the present work two different types of macro-algae have been taken into account since they're among the most present in Chile.

Durvillaea Antarctica, commonly known as *cochayuyo*, is an edible brown large and robust kelp species, dominant seaweed that inhabits the coast of the sub-Antarctic seas, especially southern New Zealand and Chile. It can reach up to 15 meters in length. Its leaves are green-brown when they are in the sea and red-brown after drying, have fleshy consistency and its interior is a honeycomb structure that gives them great resistance to support the strength of the waves. Its stem is circular and does not have spaces full of air, its color is light green and measures about one meter long until the first leaf. The basal disc is a very strong structure that adheres to rocks, as it must be able to withstand the continuous blow of the waves without detaching from the substrate.

Lessonia Nigrescens is a brown kelp, smaller than *cochayuyo*, extremely diffused along Chilean coasts. It has a blackish color that becomes very dark after desiccation. Among the Chilean kelps of economic interest, it represents near 70% of the national annual brown algae harvest.[19] For what concerns their chemical composition, it is shown as follows:

		Moisture content %	Ash % d.w.	Protein % d.w.	Lipid % d.w.	Carbohydrate % d.w.	References
DURVILLAEA ANTARCTICA	Leaves	72,3±1,5	17,9±1,2	10,4±0,3	0,8±0,1	70,9±2,7	[13]
DURVILLAEA ANTARCTICA	Stem	82,2±0,7	25,7±2,5	11,6±0,9	4,3±0,6	58,4±1,2	[13]
LESSONIA NIGRESCENS	-	-	34,9±2,46 28,7±1,9	11,9±1,7 13,3±1,1	0,2±0,1 0,6±0,4	53 57	[18] [19]

Table 1.1 D.Antarctica and L.Nigrescens chemical composition

Despite what has been said before, the two species of algae that have been taken into consideration, present a mostly carbohydrates composition, with the leaves of *D. Antarctica* that are almost completely constituted by carbohydrates. It's easy to notice that only the stem of the above-mentioned alga presents an appreciable composition of lipids.

A special focus will be done on the lipids content of the two species, since in the fatties relies the energy potential of the seaweeds, that make them suitable in biofuels production.

Although macro-algae in general present a lower percentage of lipids composition if compared to most of earth vegetables, it is worthy to mention their lipid fraction considering the large amount of algae along Chilean coasts. For what concerns *D. Antarctica,* the above table shows in detail the lipid composition.[15]

Fatty acids composition of macroalga *Durvillaea antarctica*		
Fatty acids	Methyl ester (%)	
	Durvillaea antarctica (leaves)	*Durvillaea antarctica* (stem)
C12:0	0.22 ± 0.01	1.08 ± 0.02
C14:0	5.60 ± 0.23	4.23 ± 0.04
C14:1	0.45 ± 0.01	–
C15:0	0.90 ± 0.01	–
C15:1	2.00 ± 0.08	–
C16:0	12.12 ± 1.11	18.33 ± 1.15
C16:1	2.19 ± 0.06	–
C16:1ω7	2.22 ± 0.02	–
C16:2	0.14 ± 0.00	–
C17:0	0.16 ± 0.01	–
C17:1	0.25 ± 0.01	–
C18:0	3.18 ± 0.01	8.78 ± 1.02
C18:1ω9*trans*	0.32 ± 0.01	0.32 ± 0.02
C18:1ω9*cis*	25.36 ± 1.81	25.83 ± 2.52
C18:1ω7*cis*	0.85 ± 0.04	1.43 ± 0.02
C18:2	1.34 ± 0.12	8.78 ± 2.13
C18:2ω6	10.77 ± 0.08	15.65 ± 1.09
C18:3ω3	3.93 ± 1.12	1.10 ± 0.03
C20:0	0.67 ± 0.01	1.78 ± 0.02
C20:1	3.92 ± 0.21	1.63 ± 0.22
C18:4ω3	0.23 ± 0.11	–
C20:2	0.17 ± 0.00	–
C20:4ω6	11.23 ± 1.81	–
C22:0	0.40 ± 0.01	2.08 ± 0.02
C22:1	0.39 ± 0.01	–
C20:5ω3	4.95 ± 0.11	2.69 ± 0.02
C24:0	2.75 ± 0.06	–
C22:6ω3	1.66 ± 0.02	–
ni	1.62 ± 0.02	5.28 ± 2.23
Saturated FAs	25.84 ± 1.92	36.28 ± 2.90
MUFAs	38.11 ± 0.12	29.21 ± 1.13
PUFAs	34.42 ± 1.90	29.23 ± 2.20
PUFAs ω6	22.00 ± 0.22	15.65 ± 1.09
PUFAs ω3	10.77 ± 0.01	3.79 ± 0.12
Ratio ω6/ω3	2.0	4.1

Figure 1.10 Fatty content of D. Antarctica

From the table it can be assessed that the most present fatty acid both in leaves and stem is C18:1ω9cis, that is the Oleic Acid, with a concentration of 25.36%, followed by Palmitic Acid (C16:0), Arachidonic Acid (C20:4ω6) and Linoleic Acid (C18:2ω6). Among these, only Palmitic Acid is a Saturated Fatty Acid, while the others are Mono and Poly Unsaturated

Fatty Acids. Generally, the leaves contain a higher level of lipid content if compared to the stem. Variations in fatty acid contents are attributable both to environmental and genetic differences.

Regarding *Lessonia Nigrescens*, it has been recently demonstrated by Tellier et el. (2009) that the alga is a complex species, basically constituted by *Lessonia berteroana* and *Lessonia Spicata.*[19] The same study show the lipid composition of the species.

Fatty acid	Species	
	L. berteroana	*L. spicata*
14:0	4.0±0.2	4.1±0.1
16:0*	22.7±0.7	20.8±0.4
16:1(n-7)	4.3±0.2	5.1±0.1
18:0	1.1±0.2	0.9±0.1
18:1(n-9)	17.5±1.0	14.8±0.6
18:2(n-6)	6.0±0.2	6.7±0.2
18:3(n-6)	1.0±0.1	1.4±0.1
18:3(n-3)	4.6±0.3	4.3±0.2
18:4(n-3)	8.0±0.5	8.4±0.4
20:0	1.1±0.0	0.8±0.0
20:4(n-6)	18.5±0.6	20.6±0.3
20:4(n-3)	0.9±0.1	1.0±0.1
20:5(n-3)	8.0±0.5	7.7±0.4
SFA	29.6±0.8	27.5±0.5
MUFA	22.3±0.9	20.6±0.6
PUFA	48.1±1.6	51.9±1.0
Sat/unsat FA	0.4±0.0	0.4±0.0
Total lipids	2.04±0.09	1.97±0.08

Table 1.11 Fatty acid content of L. Nigrescens

From the picture it can be easily seen that the lipid composition of both the species are very similar, coming from the same macro species. Differently from *D. Antarctica,* the most abundant fatty acid is now C16:0 (Palmitic Acid) with a concentration of 22.7/20.8%, followed by the Arachidonic Acid (C20:4(n-6)), and the Oleic Acid (C18:1(n-9)).

From a quick comparison between *D. Antarctica* and *L. Nigrescens*, it can be seen that they mainly differentiate from the Unsaturated Fatty Acids content: MUFAs in the former are 38.11 and in the latter 22.3, while PUFAs are 34.42 against 48.1.

Chapter 2

Oil Extraction Process at "Universidad Tecnica Federico Santa Maria"

The following extraction process has been performed in order to evaluate the potential of the oil extracted from the two different kinds of macroalgae analyzed before: *Durvillaea Antarctica* and *Lessonia Nigrescens*. The process has been repeated three times considering a dried and pressed *Durvillaea Antarctica* for the first simulation, the same macroalga dried only for the second one and finally a dried *Lessonia Nigrescens* for the third process. The use of two different algae and the different treatment of the *Durvillaea Antarctica* has been performed to see which one is more suitable in providing oil and if a pre-pressing step can improve the extraction or not.

In all the cases, the same extraction technology has been used: a Soxhlet extractor has been implemented with the use of n-hexane solvent. Once the extraction process seemed to be completed, a rotaevaporator has been used to separate the solvent from the oil.

Three different samples have been obtained that showed quite different extraction efficiencies, as a result of the macroalga implemented and the preliminary processes used.

Soxhlet Extractor

The Soxhlet extractor was developed by Franz von Soxhlet in 1879 as a way to study the fats in milk, in a similar way as Pasteur's study of pasteurization. It has been used then to extract lipids from solid samples – biological and inorganic materials - that have the characteristics of having soluble components.

Constituents

1. Boiling flask (in the orange square): made of glass for chemical inertness and recently made of heat-resistant borosilicate glass; it is filled with the extraction solvent – where it's even possible to put some boiling stones in order to facilitate the boiling of the solvent.
2. Soxhlet itself (in the green square): made of three parts that are *percolater*, *thimble* (where the sample is placed – it has to work as a filter, it may be made of cellulose and it has to be slightly higher than the siphon) and the *siphon*.
3. Reflux condenser (in the yellow square): it permits the condensation of the solvent vapor that can go back to the sample.

A schematic representation of a Soxhlet extractor can be seen in detail.

1. Stirrer bar 2. Still pot (the still pot should not be overfilled and the volume of solvent in the still pot should be 3 to 4 times the volume of the Soxhlet chamber) 3. Distillation path 4. Thimble 5. Solid 6. Siphon top 7. Siphon exit 8. Expansion adapter 9. Condenser 10. Cooling water in 11. Cooling water out.

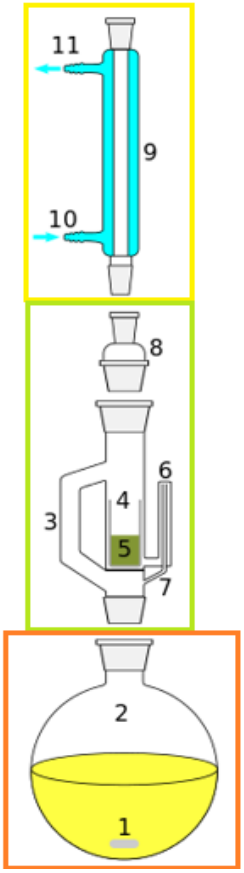

Figure 2.1.Parts of Soxhlet extractor

Operation

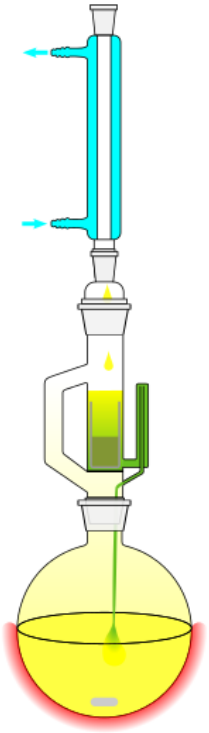

Figure 2.2 Operation of Soxhlet extractor

Hot, fresh solvent is collected in the boiling flask where it is heated up, evaporates and passes into the Soxhlet. Then the vapor of solvent continues in the condenser reflux where it goes down again in the Soxhlet – this time going in the thimble -, it percolates over the sample and allows extraction of lipids.

Once the thimble is filled up, i.e. when percolator fills up with condensed solvent above the siphon, it then returns in the boiling flask to evaporate again. When the solvent re-evaporates, only evaporates fresh solvent so that all the extractables remain in the flask while fresh solvent travels up and down indefinitely extracting more.

To make sure the device works as efficiently as possible, it is important that the sample is dry. In a study performed on algal samples, it seemed evident that the best oil recovery is met when the alga was 100% dry.[20]

Parameters: Algae powder (50 gm), time (3 hr), temperature (50°C) for all sample

Parameters	100% dry sample	75% dry sample	50% dry sample
Algae oil obtained	1.92 g	1.58 g	1.13 g

Figure 2.3 Oil recovery from algae at different rate of dryness

Soxhlet extractors are autonomous (they work on their own without needing a supervising - no need to extract lipids continuously); recycle the solvent (use of a fixed volume of solvent); are scalable (a variety of different sizes of Soxhlet can be implemented); are easily varied in the operation parameters (highly versatile in examining the effects of increasing the amount of sample, the solvent etc..)

The Soxhlet extractor for its versatile nature, can be employed for different purposes such as biofuel production, according to the collection of lipids; to obtain essential oils and

fragrances; for any laboratory experiences; for environmental analysis in the examination of soil, seawater, marine species, content of fats of an environmental sample etc..

In the boiling flask can be collected: neutral lipids – not charged - such as FFA (Free Fatty Acids) and TAGs (triacylglerycides); polar lipids (fatty acids + polar head group); other classes (such as lipoproteins, steroids, cellular debris – as well as chlorophyll when the sample is a vegetable species like algae).

The solvents that can be utilized are:

1. n-hexane $CH_3(CH_2)_4CH_3$ (boiling temperature: 69 °C @ atmospheric pressure)
2. ethyl acetate $CH_3COOC_2H_5$ (boiling temperature: 77 °C @ atmospheric pressure)
3. ethanol $CH_3{-}CH_2{-}OH$ or C_2H_6O (boiling temperature: 78,4 °C @ atmospheric pressure)
4. dichloromethane (DCM) CH_2Cl_2 (boiling temperature: 40 °C @ atmospheric pressure)

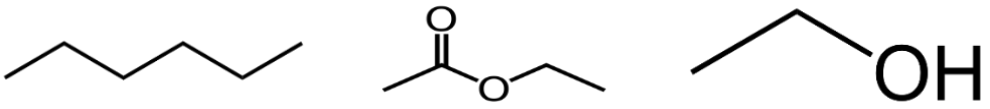

1. *2.* *3.*

These solvents are characterized by different polarities and it's possible to vary the ratios of solvents to get the best mixtures. It's worth to assess that the use of a determined solvent has implications on the content of the extractables that will be collected. For instance, n-hexane is very non-polar and, as a result of its strongly hydrophobic nature, only neutral lipids will be collected. On the other hand, ethanol is polar and contains a hydroxyl head group that makes it "stronger" than n-hexane in the way that it can extract neutral lipids and polar lipids as well. It has two carbon tail with a slight hydrophobic character, that allows the collection of neutral lipids, but the hydroxyl head group helps to extract polar lipids and it can also permeate the cell wall with a better access to the cellular lipids.

As a general rule:

- On a small scale, it does not really matter which solvent is implemented;
- On an industrial scale, it matters a lot because of the higher costs and because of the fact that, at the end of the process, the solvent must be recovered in order to make the operation economically feasible.

In fact, n-hexane is not miscible with water, whereas ethanol is, that makes n-hexane pretty more attractive. If there was the will to recover ethanol from extractables, the only way should be to distill it, and if the sample contains water (or if water is used in the process), the ethanol implemented would no longer be 100% ethanol because of the water in it. In addition, distillation requires a lot of energy and a lot of equipment. Since n-hexane is not miscible with water, in order to recover it, it's simply possible to put it in a separatory funnel where two phases are obtained - an organic and an aqueous – and by easily decanting the organic phase, the n-hexane is recovered. So, in order to eliminate the solvent, the flask is simply put on a rotary evaporator where it's easy to recover the extractable since the solvent evaporates at very low temperature.

From a study on pistachio oil to assess how the compositions of the oily extractables vary according to the solvent used (n-hexane Hx, dichloromethane DCM, ethyl acetate EtAc and ethanol EtOH), it has been proved that saturated and unsaturated fatty acid profiles extracted by Soxhlet method were not different but their content was statistically different. [21]

Extraction method	Solvent	Unsaturated fatty acids (%)				
		Palmitoleic	Oleic	Linoleic	Linolenic	Total
Soxhlet	Hx	0.914 ± 0.01 a	49.850 ± 0.02 b	35.478 ± 0.2 d	0.379 ± 0.4 b	86.621 ± 0.02 c
Soxhlet	DCM	0.925 ± 0.3 a	51.939 ± 0.03 c	34.670 ± 0.3 c	0.391 ± 0.2 b	87.925 ± 0.06 b
Soxhlet	EtAc	0.899 ± 0.02 a	53.263 ± 0.2 f	33.948 ± 0.5 a	0.383 ± 0.09 b	88.493 ± 0.08 a
Soxhlet	EtOH	0.914 ± 0.04 a	52.904 ± 0.06 e	34.0788 ± 0.01 b	0.392 ± 0.01 b	88.289 ± 0.2 a

Figure 2.4 Unsaturated fatty acid content of pistachio oil obtained by Soxhlet technique

It's easy to see from the table that the highest production of Linoleic is given by hexane, while EtAc provides the highest rate of Oleic, being the substance that extracts more as an overall. [21]

Preparation Phase

In order to use the algal samples in the extraction phase, a preparation phase is mandatory where, above all, the macroalgae must lose all the water they contain.

The following steps have been followed:

- *Washing and cutting of the algae:* as marine organisms, algae contain an appreciable amount of salt that must be eliminate because salt could produce distortions in the measurements of the final oil components. For this reason, the algae have been accurately washed. After being washed, the macroalgae have been cut in order to get small pieces, much easier to be handled and used in the following steps.

Figure 2.5 Durvillaea Antarctica

Figure 2.6 Lessonia Nigrescens

- *Pressing of a part of macroalga Durvillaea Antarctica:* it has been decided to press some samples of the *Durvillaea* as a consequence of the need to destroy the cell wall of the alga and facilitate the following extraction process. In this phase, a pressing machine has been implemented, by means of which a resinous waste has been collected and set aside.

Figure 2.7-8. Pressing phase with pressing machine

- *Drying phase*: all the three different samples have been put in a stove at a temperature of 110-120 °C to eliminate all the water content. The algae were left drying in the oven overnight. The pressed alga was the one which needed less time to dry, since a big amount of water was already gone in the pressing machine. The sample which remained the most time in the oven was the *Lessonia Nigrescens* (more than 24 hours).

Figure 2.9 Drying stove

Figures 2.10-11-12 Drying of pressed Durvillaea, non-pressed Durvillaea and Lessonia Nigrescens

- *Grinding phase*: all the samples were put in a common mixer to get a thin dust.

Figure 2.13 Mixer

- *Dehumidification phase*: after the grinding step, the dust was left resting in a dehumidifier with absorbent particles of silica to definitively eliminate all the water content.

Figure 2.14 Dehumidifier

Figure 2.15 Thin algal dust

Extraction Process and Results

In all the simulations, the dust has been collected in two thimbles made of paper texture, that have been used at the same time in the extractor.

As already said, the Soxhlet extractor works making circulate the hexane solvent that, passing through the distillation zone, extracts the oil part contained in the algae. The circulating loop is made possible by heating the solvent collected in the boiling flask. Oily residue is then collected by separating it from the n-hexane in a rotoevaporator.

Figure 2.16 At the beginning of the process

Figure 2.17 During the process

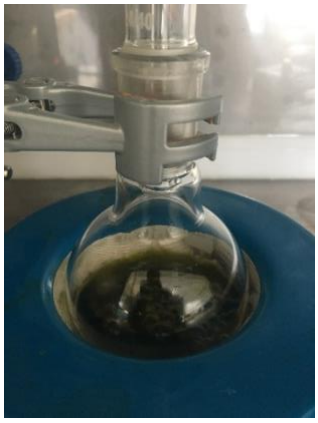

Figure 2.18 At the end of the process

Figure 2.19 Rotoevaporator

First Simulation

In the first simulation, the dried and pressed *Durvillaea Antarctica* has been used.

- A first thimble of 2,2043 gr has been filled with 15,2036 gr of dust while a second thimble of 1,6183 gr has been filled with 10,1601 gr of dust. An overall amount of the dust of 25,3637 gr has been considered
- An amount of 70 ml of n-hexane has been put in the spherical vessel of the Soxhlet, while 120 ml have been put from the top of the extractor. An overall amount of 190 ml of hexane has been implemented.
- After the extraction and the following evaporation, 1,8518 gr of oil have been collected with the following process efficiency:

$$\eta = \frac{1{,}8518}{25{,}3637} = 7{,}3\%$$

- An amount of 112 ml of hexane was left at the end.

Second Simulation

In the second simulation, the same *Durvillaea Antarctica* has been used without being pressed.

- A first thimble of 1,8238 gr has been filled with 10,0095 gr of dust while a second thimble of 1,9247 gr has been filled with 10,0948 gr of dust. An overall weight of the dust of 20,1043 gr has been considered
- The same amount of hexane has been used at the beginning. But an additional amount of 40 ml has been put from the top of the Soxhlet, since the solvent was not able to reach the minimum level to fall down in the bottom vessel. As a consequence, a total quantity of 230 ml has been used.
- After the extraction and the following evaporation, 1,9432 gr of oil have been collected with the following process efficiency:

$$\eta = \frac{1{,}9432}{20{,}1043} = 9{,}66\%$$

- An amount of 122 ml of hexane was left at the end.

It's important to point out that this second simulation lasted more time to perform the extraction: the extractor gave much more laps because the solvent inside the distillation path got every time a yellow-green color.

Finally, it's worthy to assess that this second process was more efficient from the point of view of the oil extracted to the initial mass of algae. That could be seen as a hint to assess that the pressing phase worked worsening the overall efficiency.

Third Simulation

The final simulation has been performed using the only dried *Lessonia Nigrescens* alga.

- A first thimble of 1,8389 gr has been filled with 10,1270 gr of dust while a second thimble of 1,8740 gr has been filled with 10,0139 gr of dust. An overall mass of the dust of 20,1409 gr has been considered
- An amount of 90 ml of n-hexane has been put in the spherical vessel of the Soxhlet, while 115 ml have been put from the top of the extractor. An amount of 70 ml has been added during the extraction reaching an overall amount of 275 ml of hexane.
- After the extraction and the following evaporation, 2,4653 gr of oil have been collected with the following process efficiency:

$$\eta = \frac{2{,}4653}{20{,}1409} = 12{,}24\%$$

- An amount of 115 ml of hexane was left at the end.

Even this simulation lasted more time than the first one, that was the fastest one.

In addition, this last simulation seemed to be the most efficient.

Chapter 3

Transesterification Process

Studies over alternative biofuels are achieving important results since many years. The first generation of biofuels implies the use of edible feedstock like corn, soybean, sugarcane, and rapeseed. Second generation of biofuels comes from waste and lignocellulosic feedstocks, that have advantages over those of first generation such as higher stock yields and lower land requirements in terms of quality and quantity. On the contrary, the main problem associated with lignocellulose conversion to biofuels is its strong resistance to degradation. Thus, second generation biofuels still lack of economic viability at large scale.[3] Third generation biofuels are represented by micro- and macro-algae, which present further advantages over the previous two. In fact, terrestrial biomass-based biorefinery can rather worsen climate change when considering the life cycle of its final products. Fargione et al. (2008) and Dominguez-Faus et al. (2009) reported that direct and indirect land use change for energy crop cultivation induces a significantly high carbon debt and high water consumption. Thus, terrestrial biomass-based biorefinery seems not to be sustainable at present due to environmental as well as economic impacts.[7]

Marine biomass shows important advantages as it can grow on fresh, brackish, saline and wastewater streams and does not require use of arable land for the cultivation[2]. Macro-algae can convert solar energy into chemical energy with higher photosynthetic efficiency (6–8%) than terrestrial biomass (1.8– 2.2%) (FAO, 1997). Also, algae have a lower risk for the competition for food and energy than other energy crops like corn and wheat as seaweed markets are mainly in a few East Asia countries where seaweed is used for food, hydrocolloids, fertilizer, and animal feed.[7] In addition, algae can reach 2–20 times the production potential of conventional terrestrial energy crops. A negligible or low amount of lignin makes them less resistant to degradation than lignocellulosic feedstocks, and avoids the need for energy-intensive pretreatments before fermentation.[3] Macro-algae can tolerate a wide variety of environmental conditions and can be produced all over the year. [4] Furthermore, estimates indicate that the energy potential of marine biomass is more than 100 EJ per year, higher than the land-based biomass accounting only for 22 EJ.[22]

On the contrary, the use of marine biomass to produce biofuels face considerable obstacles: macro-algae have unique carbohydrates, which are strongly different from those of terrestrial biomass and so, terrestrial biomass-based technology cannot be directly applied to macroalgal biomass.[7] Another crucial parameter is their wide variation in nutrients content, which is related to several environmental factors: most of them vary according to season, and the changes under ecological conditions can stimulate or inhibit the biosynthesis of such nutrients.[23] Last but not least, seaweeds present very high values of moisture content (nearly 80%), that act by worsening every energy-related process from anaerobic digestion to biodiesel production. It's always crucial to determine the humidity content since transesterification process requires low levels of water in the reactants, where water leads to saponification reactions. According to all the above cited disadvantages, costly pre-treatment steps are mandatory in order to overcome such barriers and increase the production of related biofuels.

Among the biofuels that can be produced with algae, the present work will only focus on the production of biodiesel by means of a transesterification process.

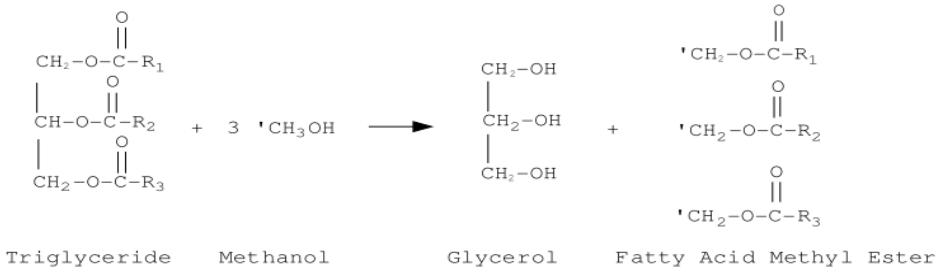

Figure 3.1 Transesterification process

The transesterification is the process in which the organic group of an ester is exchanged with the organic group of an alcohol: it essentially occurs by making triglyceride molecules react with an excess of alcohol in the presence of a catalyst to produce glycerin and fatty esters (Fatty Acid Methyl Esters).

The energy content of biodiesel is quite different from that one of fossil diesel: diesel LHV is around 42 MJ/kg while biodiesel LHV is around 38 MJ/kg. Pure biodiesel contains up to 10-12 % weight of oxygen, while diesel contains almost 0 % oxygen: the presence of oxygen allows a more complete combustion, which reduces HC, CO and particulate matter

emissions. On the other hand, higher oxygen content increases nitrogen oxides (NOx) emissions.[24]

The reduction in GHG emissions can reach 86% by implementing biodiesel and not petrodiesel. According to EPA (Environmental Protection Agency) the situation is described in the following table:

Pollutants	Emissions [%]
PM	-30
CO	-50
Ozone-forming (smog)	-50
PAH	-80
Unburned HC	-93
SO_2	-100

Figure 2.2 Reduced emissions in using biodiesel

Transesterification Process on Aspen Plus Software

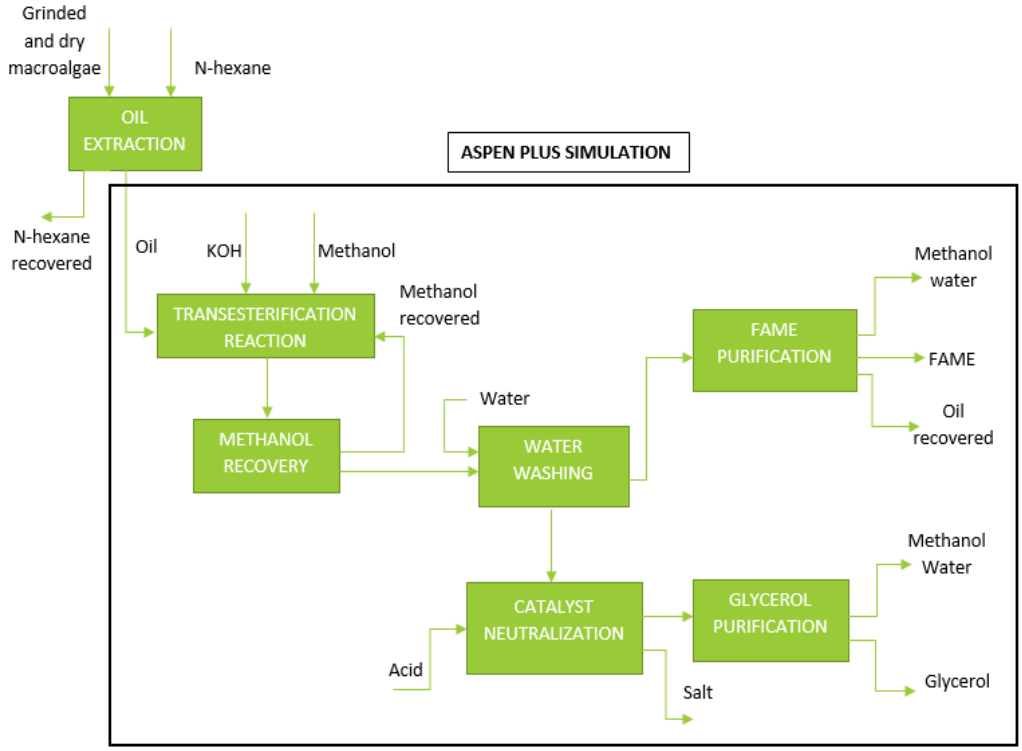

Figure 3.3 Transesterification process scheme

The entire transesterification process has been performed on Aspen Plus with the purpose of obtaining the energy required to perform the different steps. In order to simplify the process, the oil extracted from algae has been supposed as pure Triolein (or Trioleic Acid with formula $C_{57}H_{104}O_6$) because ASPEN Plus's database does not have thermodynamic or physical property data available for acids like palmitic acid, oleic acid, linoleic acid and arachidonic acid that are among the most present in *D. Antarctica*[15]. Actually, oleic acid is the most present (with a concentration of 25,36 ± 1,81 %)[15] and Triolein appears to be the best solution since it is composed of three oleic acid chains. Even the thermodynamics characteristics of Triolein can well represent the characteristics of the other acids, since they all have very similar boiling points.[25] The biodiesel produced, normally composed by several Fatty Acids Methyl Esters, as a consequence of the triglyceride utilized, is Methyl Oleate ($C_{19}H_{36}O_2$). The transformation from oil to biodiesel occurs at the presence of a catalyst,

the one chosen is Potassium Hydroxide (KOH). The following governing reaction is considered:

$$C_{57}H_{104}O_6 + 3CH_3OH \rightarrow 3C_{19}H_{36}O_2 + C_3H_8O_3$$

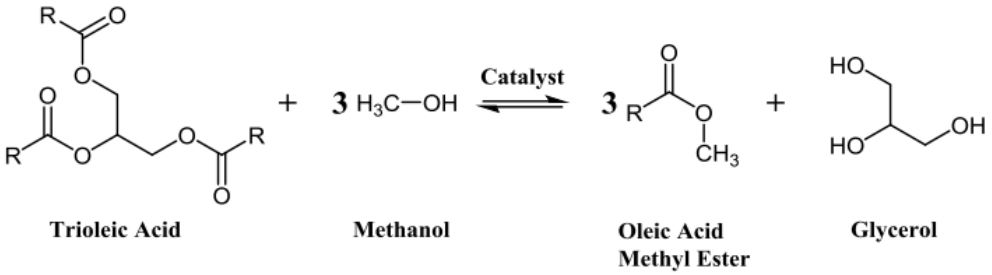

Figura 3.4 Transesterification chemistry

In accordance with the majority of industries involved in producing biodiesel from a minimum of 1000 kg/h to a maximum of 7000 kg/h, two main simulations have been performed in ASPEN: the first one leads to a production of around 1000 kg/h of FAME, scenario that has been assumed as the basic one where all the power needed is the minimum necessary to run the plant; the second simulation leads to around 6200 kg/h of FAME with an obvious increase in the overall energy needed. The two scenarios will put in evidence how different is the energy demanded, thus, in the following implementation of the plant that must provide the biodiesel process with the energy required, very diverse solutions will be proposed. It's worthy to assess that all the distillation processes work in an under pressured environment and that is dictated from the need to limit the temperature of the fluxes exiting the columns.

The two simulations are characterized by the same processes, with the only difference in the amount of chemical species involved. It's possible to split the process into 6 steps:

- *transesterification reaction*: it's where the reaction itself occurs by mixing methanol, catalyst and Triolein and letting them react at about 60 °C and 4 bars in a stochiometric reactor based on known fractional conversion of 95% of Triolein into Methyl Oleate. The reaction involved is the one already mentioned above: oil reacts with three moles of methanol leading to three moles of Methyl Oleate and glycerol.

- *methanol recovery*: it follows the reaction step and it's where most of methanol that has not reacted in the reactor is recovered and sent back to be mixed with "clean" methanol. It's a rigorous distillation column, to model the vacuum separation of excess methanol from the FAME and glycerol products and for which a 2 or 3-phase fractionation column has been used. For what concerns the operating specifications of the column, a vacuum environment has been supposed with a condenser pressure of 0,2 bar and a re-boiler pressure of 0,305 bar, 5 theoretical stages have been supposed, it has been put that the distillate rate is equal to the 94% of the methanol flow exiting the reactor and it has been chosen a reflux ratio of 2, that ensures that for every 1 mole of distillate produced, two moles from the splitting point are returned and recycled back in the column[25]
- *water washing:* while the recycled methanol is pumped back to be mixed with entering methanol and KOH, the remaining mixture is cooled down to 60 °C and undergoes water washing by means of a separator, to separate FAME from glycerol and the catalyst as well as the remaining methanol. A considerable amount of water must be injected in the system to better remove any soap that may have brought to possible saponification during the transesterification reaction. That is an important step, even though complete separation of FAME is impossible. The separator has been designed in order to give two streams with the following split fractions: the upper stream with all the FAME and all the oil and a small percentage of catalyst, water and methanol that are not separated; the bottom one with all the glycerol, 70% of catalyst, almost the whole amount of water (97%) and 90% of methanol. The water-washing step is followed by another separator designed to give the following streams: the one that goes to FAME purification composed by all the methanol, FAME and Triolein, 80% of water and a tiny amount (10%) of KOH that could not be separated completely; the downstream going to catalyst neutralization composed by all the glycerol and the remaining amount of water and catalyst.
- *catalyst neutralization:* The latter stream is then sent to a neutralization reactor to neutralize the alkali catalyst, KOH. This prevents further saponification reactions with glycerol and water, avoiding the formation of soap and foaming and maintaining the purity of the glycerol. During the neutralization reaction,

orthophosphoric acid H_3PO_4 is added to react with the catalyst and from salt precipitate K_3PO_4 according to the following reaction:

$$3KOH + H_3PO_4 \rightarrow K_3PO_4 + 3H_2O$$

The reactor has been designed to operate at 60°C and atmospheric pressure, with a conversion of 99% of the catalyst into potassium phosphate, which will subsequently be separated in a separator and removed to be sold as fertilizer, with acid and catalyst left.

- *glycerol purification:* The upper stream leaving the separator is sent to a distillation stage, after being preheated to 102°C to help water and methanol separation from glycerol.[25] The partial-vapor separation unit is designed to work at pressures of 0,105 bars for the top stage and 0,2 bars for the bottom stage, with 5 stages, a reflux ratio equal to 2 and a bottom rate equal to 98 kg/h is imposed. The result is an upper flux composed by water and methanol left into solution and a bottom flux of glycerol with a purity of around 100%.
- *FAME purification:* The upper stream exiting the separator after water washing undergoes a 3-phase fractionation to separate the principal product (biodiesel or FAME), the remaining oil and the useless mixture of water and methanol. The column condenser has a partial-vapor-liquid configuration: it means that only a fraction of the vapor generated in the column condenses, allowing for the methanol and water components to remain in the vapor phase, and the FAME product to condense earlier to the liquid phase, since it has a higher boiling point[25]. In addition, it is designed to work entirely at 0,105 or 0,105 and 0,2 bars (pressures respectively referred to the top stage and to the second stage of the distillation column), with 5 stages, a reflux ratio of 2 and a distillate ratio a little less than the FAME entering the separator. It's important that the FAME exiting the process has a minimum purity of 99,7wt%, to be compliant with the standard set by government regulatory committees[25].

Several simulations have been performed on Aspen to get the optimized configuration that allows for a correct and non-costly use of the different material fluxes, as well as a right expenditure of energy in the different stages. Once the best simulation is chosen, by looking

at the energy fluxes, it is evident that the distillation stages (methanol recovery, glycerol and FAME purification) are the ones that show the highest expenditure of energy.

I SIMULATION: Production of around 1000 kg/h of FAME

The process starts by mixing 120 kg/h of methanol with 10 kg/h of KOH and by bringing the mixture from atmospheric temperature and pressure to 4 bars. The mixture receives the recycled methanol that has been separated from the reaction products, obtaining an overall flow rate of 210 kg/h, given by the additional amount of recovered methanol of 90 kg/h. At the same time, 1100 kg/h of Triolein are brought to 60°C and the same pression of methanol-KOH mixture, that are the operative conditions of the reactor. The two streams are now sent to a Stochiometric Reactor, that is set up to work at 60 °C and 4 bars and is designed to operate a Triolein-FAME conversion of 95%. The transesterification process leads to 1049,76 kg/h of FAME. It follows the production of 108,7 kg/h of glycerol and what is left is an appreciable amount of methanol, which in part will be recovered, and a tiny amount of unreacted oil.

The following step is the methanol recovery, which works as a vacuum environment as already stated in the introduction part. A re-boiler pressure equal to 0,305 bars has been adopted in order to maintain FAME, glycerol and the other substances at a temperature lower than 150°C (in this case equal to 124,3°C). Higher temperatures could cause the degradation of FAME and glycerol and in case it happens, the two would be more difficult to separate in the following phases[25].

The stream after being cooled to 60°C undergoes the water washing stage where water is fed to the separator in a quantity equal to 170 kg/h, corresponding to the 14% of the stream that has to be washed, composed by FAME, glycerol and methanol and oil in a lower content. The water separation leads to the formation of two fluxes according to the percentage already assessed. The downstream of 286,5 kg/h (essentially composed by 57% of water, 38% of glycerol and 2,4% of KOH and 2% of methanol) is mixed with a flux of 1 kg/h of water and 2,7 kg/h of KOH coming from an additional separation stage, leading to a mixture of 290,2 kg/h (57% water, 37% glycerol, 3,3% KOH and 2% methanol).

At the neutralization phase, 8 kg/h of orthophosphoric acid are fed to the reactor, reacting with the catalyst present in the mixture and leading to the formation of 12,11 kg/h of potassium phosphate that is separated from the other constituents (with a purity of 83%) and recovered.

It follows the glycerol purification stage, where an amount of 98 kg/h of glycerol is separated as imposed in the bottom rate of the distillation column, with a purity of around 100%. The upper stream is composed by the glycerol that could not be recovered, the remaining methanol and almost the entire water fed in the washing phase.

Another stream equal to 1109,8 kg/h and composed by 94,6% of FAME, 5% of oil and a negligible amount of methanol and water leaves the water washing separator and undergoes FAME purification. As already said, the column is designed to work under pressure and two cases are analyzed: the first one where the entire operating pressure is 0,105 bars and the second one where re-boiler pressure is set to 0,2 bars. In both cases, all the different species are separated in three fluxes with the same flow rate: 1042,06 kg/h of FAME (purity of almost 100 %), 55 kg/h of oil (purity of 92%) that could be reutilized and a final flux of 7,35 kg/h composed by methanol, water and unseparated biodiesel. The two cases are only differentiated by the temperature of the recovered oil exiting the column: it equals 319,6°C and 347,6°C respectively.

Below, the tables show the power required by each process according to the two cases that have just been mentioned: i.e.

II SIMULATION: production of around 6000 kg/h of FAME

The simulation has been repeated increasing the production rate of the biodiesel. Thus, initial amounts of 720 kg/h of methanol and 60 kg/h of KOH are fed to the process, while 6600 kg/h of Triolein is used. All the operating parameters are kept the same, while the distillate and bottom rate of the distillation columns as well as all the species fed to the system are scaled accordingly to the augmented quantity of oil implemented: 1020 kg/h of water and 48 kg/h of acid are introduced. This second simulation leads to a biodiesel yield of 6252,4 kg/h and a glycerol production of 588 kg/h.

RESULTS: Energy Demand and Working Temperatures

The operating parameters are the same in both cases: there's no variation in pressure and temperature conditions by increasing the inlet amount of materials to produce more biodiesel. On the contrary, the energy needed to perform the different steps will change accordingly to the scale of the plant, in terms of the amount of fluxes undergoing the process, and accordingly to the working pressures. By considering the two different scenarios of each simulations (same pressure inside T-FAME or different values for condenser and re-boiler stage) and by looking only to the power that must be supplied to the system, the following situations are obtained:

Q SUPPLIED	kW	Q SUPPLIED	kW
HX1	18,798	HX1	18,798
T-METHANOL	135,006	T-METHANOL	135,006
SEP 1	0,209	SEP 1	0,209
T-FAME	538,911	T-FAME	494,314
NEUTR	5,844	NEUTR	5,844
HX3	23,271	HX3	23,271
T-GLYCEROL	223,65	T-GLYCEROL	223,65
TOT	945,689	TOT	901,092

Table 3.1 Thermal Needs of I scenario

And, for the second scenario:

Q SUPPLIED	kW	Q SUPPLIED	kW
HX1	113,206	HX1	113,206
T-METHANOL	810,035	T-METHANOL	810,035
SEP 1	1,255	SEP 1	1,255
T-FAME	3233,528	T-FAME	2965,884
NEUTR	35,066	NEUTR	35,066
HX3	139,627	HX3	139,627
T-GLYCEROL	1341,878	T-GLYCEROL	1341,888
TOT	5674,595	TOT	5406,961

Table 3.2 Thermal Needs of II scenario

By looking at the two tables, it's easy to see how the power required by the system increases proportionally to the amount of materials implemented: to produce more than 6 times the amount of biodiesel, it will be necessary to supply 6 times the overall power. For what concerns the two different cases in the same scenario, it can be noted that the case in which FAME purification column works at two different pressure is more convenient in terms of energy demand (494,3 kW against 538,9 kW for the first simulation and 2965,9 kW against 3233,5 kW for the second one). In addition, letting T-FAME working with two different pressures is more convenient even from the temperature point of view: in fact, imposing a lower re-boiler pressure inside the column, allows for a lower exiting temperature of the bottom flux (recovered oil). It is enough to assess the convenience of working at a lower re-boiler pressure, and for this reason in the following steps of the analysis only the second case of both simulations will be taken into account.

Besides considering the overall power required by the process, it's fundamental to know at which temperature the energy, towards process heat, must be supplied. That is a crucial part especially when choosing the best technology that must provide power to the system. The entire process can be divided in three ranges of temperature:

- Low temperature fluxes from ambient temperature to 60 °C: they are referred to the all the inlet fluxes from the environment (taken precisely at ambient temperature and pressure), as well as those processes that occurs between 50°C and 60°C like the transesterification reaction itself, all the separation processes and the neutralization step;
- Middle temperature fluxes from 102°C to 182°C: 102°C is the imposed temperature of the flux entering the glycerol purification column, 125°C is the temperature of the bottom flux exiting the methanol separation column as well as the upper stream exiting the glycerol purification column, the maximum temperature of this range is achieved in the T-FAME since it is relative to the fluxes of FAME and the mixture of water and methanol exiting the column.
- High temperature fluxes of 233°C and 319°C: these are the highest temperatures of the entire process, relative respectively to the glycerol flux at the outlet of the T-GLYCEROL and to the recovered oil exiting the T-FAME, having the highest temperature ever.

The lowest pressure of the cycle (equal to 10500 Pa) is achieved inside the distillation columns T-FAME and T-GLYCEROL and it is due to the need to limit as much as possible the operating temperatures or keep them within reasonable limits to prevent degradation of the substances as well as structural damages. The highest pressure evolving in the process is 40000 Pa, that is the working pressure of the transesterification reactor.

In the following phases of the work essentially two classifications will be made: low temperature fluxes up to 60°C and high temperature fluxes up to the highest temperature of the process. That is due to the fact that low temperature heat (up to 60°C) can be supplied in many ways and with several technologies, while higher grade heat is usually produced at temperatures higher than the ones implemented in the process (especially those in the middle range). Thus, heat at temperatures higher than 60°C will be degraded at lower temperatures in order to fulfill all the ranges.

In addition to the heat that must be supplied, the process requires a certain provision of mechanical work needed to run the pumps relative to the process itself, as well as those pumps necessary to circulate the water in the cooling system, i.e. to remove all the process heat. The pumps working in the only transesterification process require an overall of 0,53 kW for the first simulation and 2,6 kW for the second one.

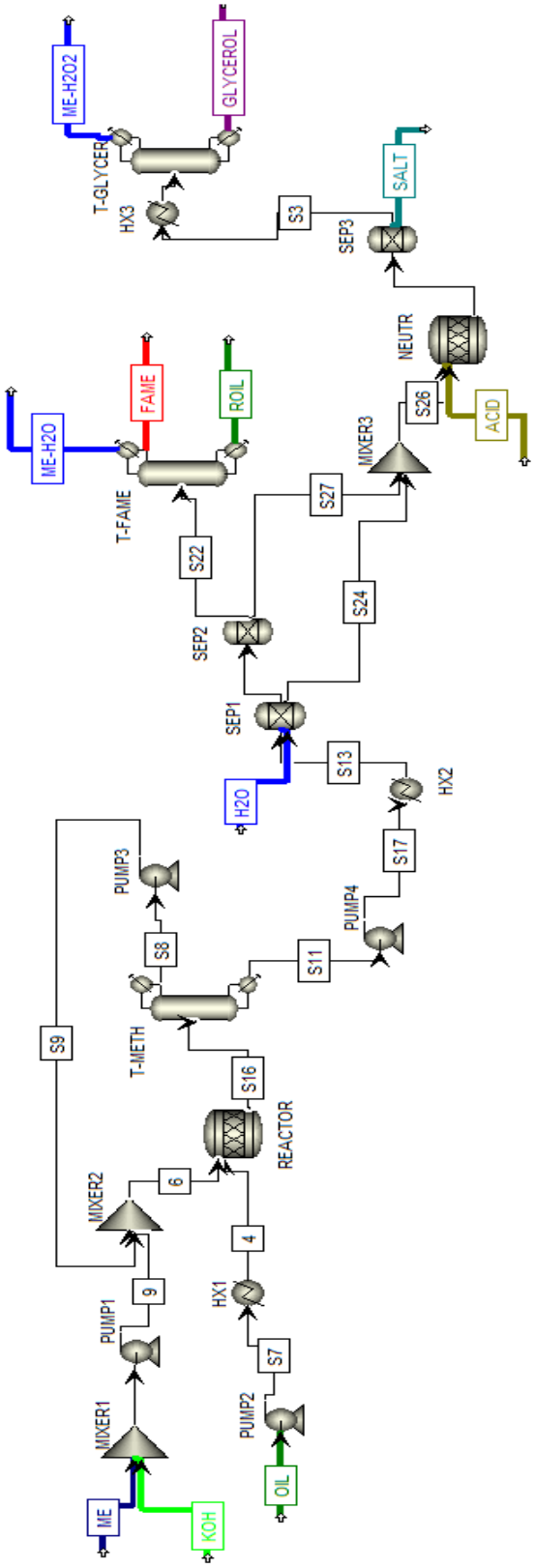

Figure 3.5 Aspen transesterification scheme

Chapter 4
Conventional Technologies to Supply Power to the Process

Recently, biodiesel has become more attractive because of its environmental benefits and by the fact that it is produced from renewable biomass. However, the production cost of biodiesel is the main obstacle for the marketing of the product since the whole biodiesel production process involves a significant energy demand, especially in the methanol recovery stage and in the purification stages of glycerol and FAME. [5] In the majority of cases, the biodiesel production chain is driven by electrical energy generated by means of fossil fuels.[26] That seems to be a contradiction in the particular case in which the process produces a sustainable and natural fuel by means of fossil fuels, with the aim of getting rid of a fossil fuel dependence.

As a consequence of this focal aspect, goal of this second part of the project is synthetizing biodiesel without or with a very limited use of fossil fuels. Different technological solutions are outlined and studied, with the aim of finding the best technology from an energy and economic point of view that is capable of providing the system with the required energy input, that, above all, is as greener as possible. The eco-efficient solution that will provide the process with the necessary energy demand trough an eco-friendly approach at the lowest cost will be considered as the optimum choice.

As a matter of fact, two very different paths will be undertaken:

1) Use of conventional technologies such as Internal Combustion Engine, Gas Turbine, Steam Turbine and Combined Cycle for the combined production of electrical energy and heat, as well as Heat Pumps;
2) Use of solar technologies such as Flat Solar Collectors and Concentrating Solar Panels for the only thermal purpose for the former and both heat and electricity for the latter.

The two cases are differentiated by several factors:

- In the first solution all the technologies, with the only exception of heat pumps, are cogenerative plants since they simultaneously produce electricity and heat: the former is used to run the pumps and all the electrical devices connected to the

system and to the whole firm (lighting etc..), the latter is used to provide the system with the required thermal energy.

All the four cases require a fuel and, in order to get rid of fossil fuels and make the system as greener as possible, the biodiesel itself produced in the process will be used. Obviously, the configuration will be acceptable when a maximum of 15-20% of the FAME produced is implemented in the electricity and heat generation: a major expenditure would be incoherent. An eventual surplus in the electricity production will be used to run heat pumps and provide additional thermal energy or will be sold to the electrical grid.

- In the second solution, no fuel is needed since the only source is the free and renewable solar radiation. Flat collectors will be used for the only production of low temperature thermal energy, assuming different configurations, while CSP can be implemented for the production of high temperature heat and will be coupled with an electricity production system. The main difference is that, while CSP plants can provide on their own all the energy inputs (high temperature heat as well as low temperature heat by means of a thermal degradation, as well as electricity), flat collectors can only produce low temperature heat and thus satisfy a small amount of the whole energy demand. This solution is affected by the relevant drawback that solar radiation is aleatory: conventional technologies must help in those cases such as night time or winter season.

Cogeneration Technologies

The first technological suggestion in terms of energy provision is given by those conventional and consolidated plants which operate in a cogeneration way, by producing electricity and heat simultaneously. Basically, a cogeneration process, also defined as Combined Heat and Power (CHP), consists in reutilizing hot flue gases exiting gas, steam turbines or engines, to produce thermal energy. That heat, otherwise released in the environment, can be used to produce hot water, superheated water, vapor or to heat up the temperature of a diathermic oil. These fluids, directly where they have been produced, or transported, can be utilized for a variety of purposes: heating of commercial, private buildings or industrial activities, as process heat for industrial uses, electricity generation in a topping cycle (in case of vapor) or even cold-water production by means of absorption cycles.

Usually the electrical energy produced is used for a self-consumption. But the electric system can be connected to the public grid so that the electricity can be exchanged in the two senses, freeing the production trend from the user needs trend. The thermal system is always supported by the use of typical boilers, which performs an integration function when the user absorption exceeds the thermal power produced by the plant.

In a general situation, variations in the user E/Q could arise and four operating conditions must be foreseen and managed:

- Surplus in electricity production: the surplus is given to the grid and can be transported to another location of the same user or be sold with a regular contract;
- Deficit in electricity production: the missing electricity is taken from the grid by means of an appropriate contract stipulated between the producer and the deliverer;
- Surplus in heat production: usually an over production of thermal energy is evacuated in the environment but it can be stored in the remote case in which there is a storage and be used when necessary,
- Deficit in heat production: when the thermal energy is not enough to satisfy the user demand, the heat is integrated with conventional boilers.

To better understand the convenience of installing a cogeneration plant, it's important to define parameters such as:

- Electrical efficiency: defined as the ratio between the electricity production and the inlet energy source coming from the fuel $\eta_{el} = \frac{P_{el}}{Q_{in}}$
- Thermal efficiency: defined as the ratio between the thermal useful recovered heat and the inlet energy source from the fuel $\eta_{th} = \frac{Q_{th}}{Q_{in}}$
- The electrical index as $\frac{P_{el}}{Q_{th}} = \frac{\eta_{el}}{\eta_{th}}$ (E/Q) as well as a thermal index $\frac{Q_{th}}{P_{el}} = \frac{\eta_{th}}{\eta_{el}}$ (Q/E), defined as the electricity produced with respect to the heat recovered and vice versa
- An overall cogeneration efficiency defined as $\eta_{cog} = \frac{P_{el}+Q_{th}}{Q_{in}}$
- The Energy Saving Index (ESI) (the Italian *IRE – Indice di Risparmio Energetico*) is introduced to clearly measure the advantages of cogeneration applications with respect to conventional ones in terms of fuel consumption:

$$ESI = \frac{Q_{in,el} + Q_{in,th} - Q_{in,cog}}{Q_{in,el} + Q_{in,el}} = 1 - \frac{Q_{in,cog}}{\frac{P_{el}}{\bar{\eta}_{el}} + \frac{Q_{th}}{\bar{\eta}_{th}}}$$

  Where $Q_{in,el}$ and $Q_{in,th}$ are the energy inputs for the separate production of electricity and thermal energy (a generic power plant and a boiler) and $\bar{\eta}_{el}$ and $\bar{\eta}_{th}$ respectively the electrical and thermal efficiency of the two plants. $Q_{in,cog}$ is the energy input in case of a cogeneration plant. The ESI index quantifies the fuel saving of a cogeneration plant with respect to a conventional one characterized by specific electrical and thermal efficiencies. As a matter of fact, it depends on the performances of the cogeneration process as well as on those of the conventional reference system.

Usually cogeneration activities are performed using gas turbines, steam turbines as well as combined plants and internal combustion engines. The fuels implemented in the process are natural gas, liquid fuels like diesel, oil or even biodiesel as well as mixtures. Obviously, all the different technologies are not interchangeable because they're characterized by different operating parameters such as the size of the plant, the E/Q ratio, the temperature at which heat must be supplied and the amount of fuel used.

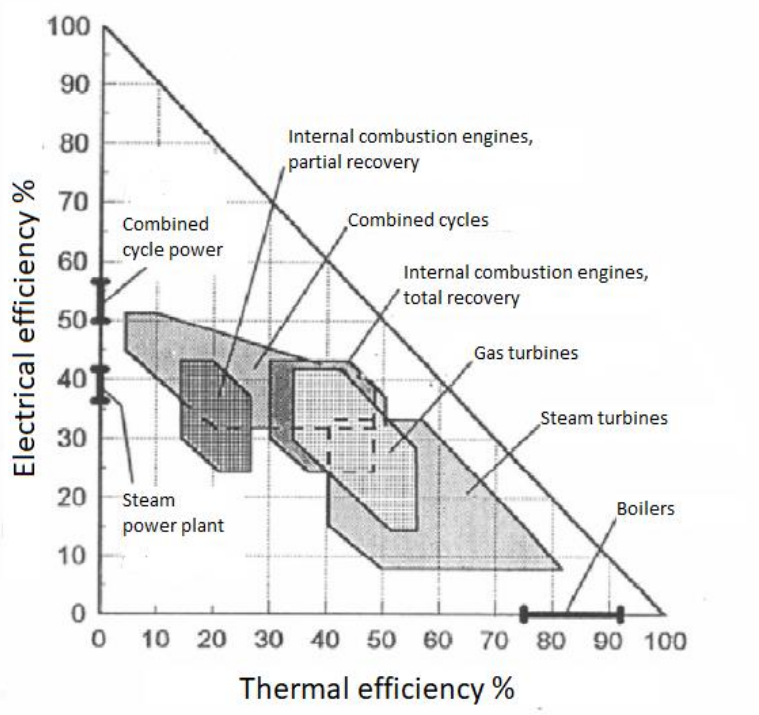

Figure 4.1 Thermal and electrical efficiencies of most common technologies

			Simple Plant	Cogeneration Plant			
		Power Range $[MW_{el}]$	η_{el} %	Q/E	η_{el} %	η_{th} %	η_{cog} %
INTERNAL COMBUSTION ENGINE	Partial Recovery	0.1-15	35-46	0.5-0.7	35-46	40-50	75-88
	Total Recovery	0.1-15	35-46	0.8-1.4	35-46	20-30	50-70
GAS TURBINE	Simple Recovery	1-400	25-40	1.5-3	25-40	40-60	70-85
STEAM TURBINE	Counter Pressure	1-100	30-43	4-10	12-30	75-85	75-97
	Condensation/bleedings	10-300	40-45	1-5	20-35	40-70	75-85
COMBINED CYCLES	Counter Pressure	10-250	43-55	1.2-2	35-50	20-40	65-85
	Condensation/bleedings	25-350	48-60	0.8-1.5	35-45	30-40	70-83

Table 4.1 Power ranges and efficiencies of conventional cogeneration technologies

From the table, it's easy to notice that for particular types of technologies the electrical efficiency does not change in the cogeneration configuration with respect to the only electricity configuration. That is the case of internal combustion engines and gas turbines, while for steam turbines or combined cycles η_{el} decreases.

ICEs and gas turbines, as well as counter pressure TV and counter pressure combined cycles, are included in the category A where there are all those plants where the thermal energy production does not entail any loss in the electricity production; steam turbines and combined cycles are included in the category B since any thermal production causes a reduction in electricity yield.

- A category: belong to this category all those cogeneration plants in which the thermal production takes place for heat recovery at the discharge of the plant without altering the conversion cycle. In fact, keeping the fuel supply constant, the electricity production remains constant and, considering the presence of a by-pass on the exhaust ports, the thermal production can vary from a minimum value (in particular nil, in correspondence of a completely open by-pass that excludes thermal production by the recuperator located at the engine exhaust) up to a maximum value (by-pass completely closed and then all the exhaust gases are conveyed into the recuperator that produces the maximum thermal energy).
- B category: belong to this group all those cogeneration plants where the thermal energy production is given by a heat withdrawal from the conversion cycle during the expansion stage that occurs in the turbine: it follows a reduction in the electricity production. In fact, keeping the fuel supplied constant, increasing the thermal

production, achieved through a greater steam extraction, electrical production progressively decreases due to the lower quantity of steam that undergoes the expansion in the turbine downstream of the extraction. On the other hand, a reduction of thermal production, realized by a progressive reduction of the extracted steam, increases the production of electricity due to the greater amount of steam that continues the expansion.

Cogenerative Internal Combustion Engine (ICE)

The internal combustion engine is a very consolidated technology and utilizes a wide variety of fuels. In the specific case what is considered is a Compression Ignition ICE since the fuel used is biodiesel. A compression ignition engine works in four steps:

- Intake stage: the air enters the combustion chamber
- Compression stage: the air is compressed and reaches a temperature of 700-800°C
- Combustion-expansion stage: nebulized fuel is injected in the chamber and the combustion takes place with the following expansion of the mixture
- Exhaust stage: the mixture is released and the chamber prepares to welcome fresh air

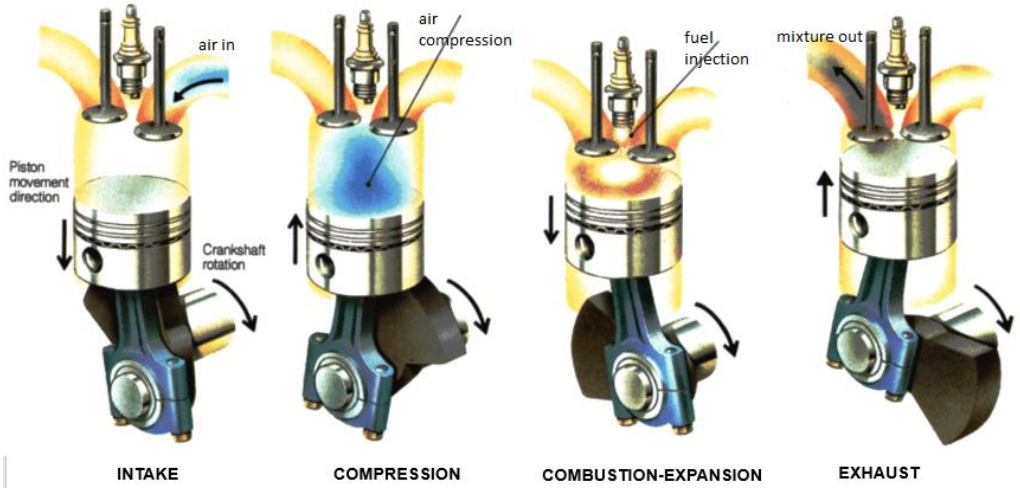

Figure 4.2 Operations of diesel ICE

The process can be summarized in the following graph:

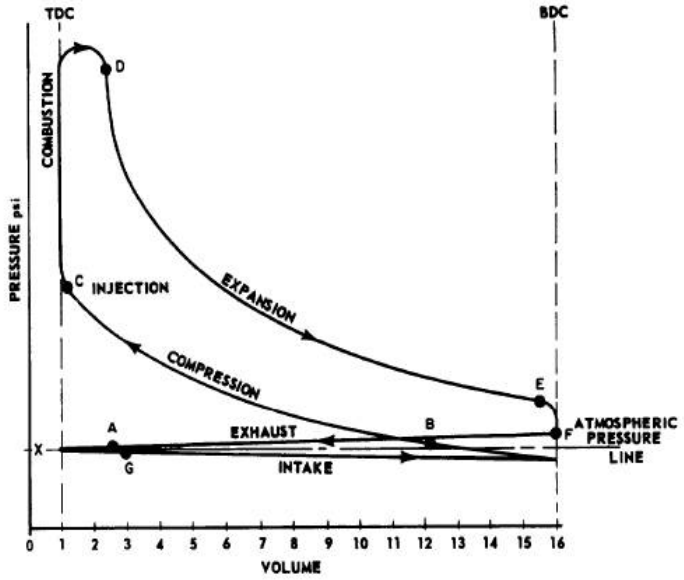

Figure 4.3 Pressure-volume diagram of diesel ICE

Where TDC and BDC are respectively the Top Dead Centre and the Bottom Dead Centre and they indicate the position of the piston inside the cylinder.

The power range of a combustion ignition ICE goes from 0,1 kWel to 20 MWel, it is characterized by high reliability, good conversion efficiencies as well as high operating flexibility and low investment costs. On the other hand, ICEs are affected by high maintenance costs (8-25 €/MWh), considerable pollutant emissions (NOx and CO) and noises and vibrations. They can work with conventional diesel, biodiesel, vegetable oil, and prior to technical modifications even with natural gas and biogas.

The present configuration takes into account the chance to operate the ICE in a cogeneration way with a 100% biodiesel load: the fuel is produced in loco and there's no need to buy it.

As already said, ICEs are included in the A category since the recovered heat does not affect the electricity production and it is uniquely linked to the electricity yield. Thermal recovery in ICEs does not influence the engine performances.

The heat can be recovered from four sources:

- From exhaust gases at a temperature higher than 400 °C
- From cooling water at a temperature between 90 and 95°C
- From lubricating oil at a temperature between 75 and 85°C
- From the intercooler (if present) at a temperature much lower (30-40°C)

In the present work, reference efficiencies for cogeneration ICEs have been assumed: η_{el} equal to 37% while η_{th} equal to 48%. According to the total energy entering the system and given by the fuel, the following graph shows how the energy balance is characterized:

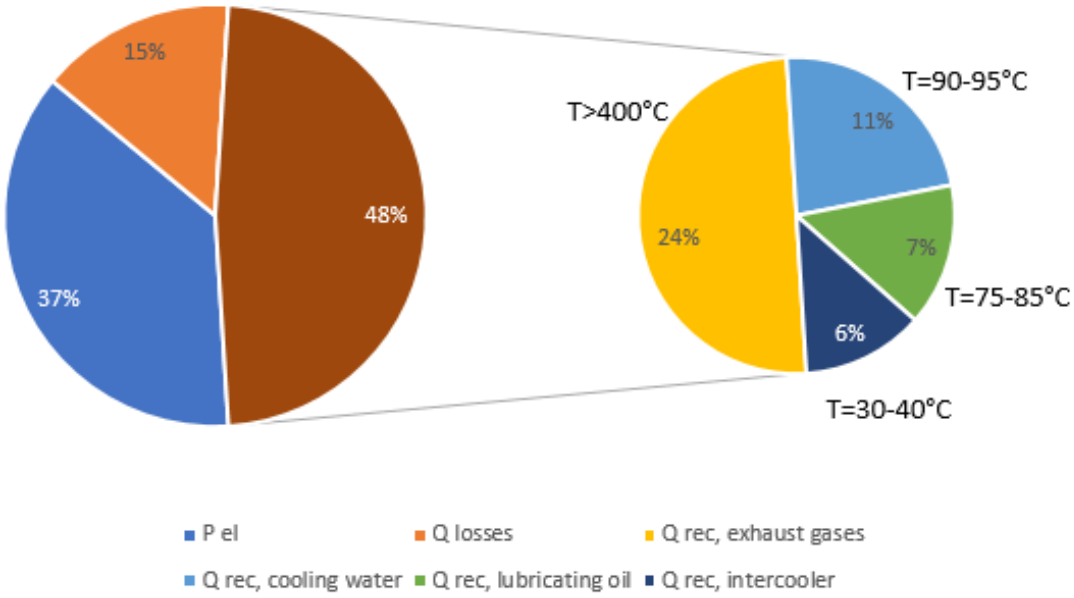

Figure 4.4 Energy balance of cogeneration diesel ICE

It's easy to notice that the biggest amount of recoverable heat is given by the thermal energy content of the flue gases, that is at very high temperature, while the 18% is given at a temperature of 80-90°C suitable for low-temperature processes, and the remaining 6% does not find any practical application in industrial situations.

In order to get 1000 kW of electrical power, 2700 kW must be given by the fuel in terms of its lower heating value and the following values of recovered heat can be computed: 648,65 kW at high temperature, 486,49 kW at middle temperature and 162,16 kW at low

temperature, for a total recoverable heat equal to 1297,29 kW. In a cogeneration ICE, it's possible to perform a total recovery, by recovering heat at all the different temperatures, or a partial recovery, by recovering only the high temperature heat. In the case in which it's performed a total recovery, the process brings to a η_{cog} equal to 85% and a Q/E equal to 1.3. If a partial recovery is performed, η_{cog} will be 61% and Q/E only 0,65.

Feasibility of Cogeneration ICE in Biodiesel Production Process

For what concerns the first scenario for the production of 1000 kg/h of biodiesel, it has already been said that a high temperature heat duty equal to 853 kW and a low temperature heat duty equal to 48 kW are necessary to perform the process.

The ICE will be designed giving priority to the supply of high temperature heat: in order to recover 853 kW, the ICE must be designed to supply 1315 kW of electricity by using an energy input equal to 3554 kW coming from the fuel. The amount of fuel implemented to have such performances is equal to 40% of the biodiesel produced by the plant, assuming a combustion efficiency of 80%, value much higher than what was set as maximum (20%). The recovered low-temperature heat (at 80-90°C) is equal to 640 kW, that is much higher than the one required by the process (equal to 48 kW). If the engine operates in a total recovery asset, a considerable amount of low-temperature heat must be rejected in the environment without any use. In addition, according to this configuration, there will be an excessive production of electrical energy with respect to what is required from the process: almost the entire electricity produced must be sold to the electrical grid.

It has been assumed an alternative situation in which the engine operates a partial recovery and the electricity generated is used to run a system of heat pumps aimed at providing heat at low temperature (65°C). A 50 kW_{th} heat pump must be considered and, assuming a coefficient of performance of 4,5 (equal to most of the pumps in the market), the pump will consume around 12 kW of electrical power.

For what concerns the second scenario aimed at producing around 6000 kg/h of FAME, the biodiesel engine should be designed to recover more than 5 MW of thermal power: to get this, an 8 MW_{el} engine must be chosen. This situation soon appears to be not so

convenient because there is an over production of electricity that must be sold almost entirely; in addition, besides the high temperature heat, there is a considerable amount of low temperature heat that must be rejected (the engine recovers almost 4 MW_{th} at 80 °C for the only 300 kW_{th} necessary). Furthermore, internal combustion engines are more suitable at lower power ranges: such high electrical demands bring to noisy and big machines, frequent maintenance operations and require a considerable fuel consumption.

Cogeneration Gas Turbine

Gas turbines are consolidated technologies and operate in a wide range of electrical output (from 30 kW to 400 MW). They're characterized by high simplicity, low weights and dimensions, low start and stop times, high conversion efficiencies and an appreciable variety of fuels utilizable. The typical configuration of a cogeneration gas turbine is the following:

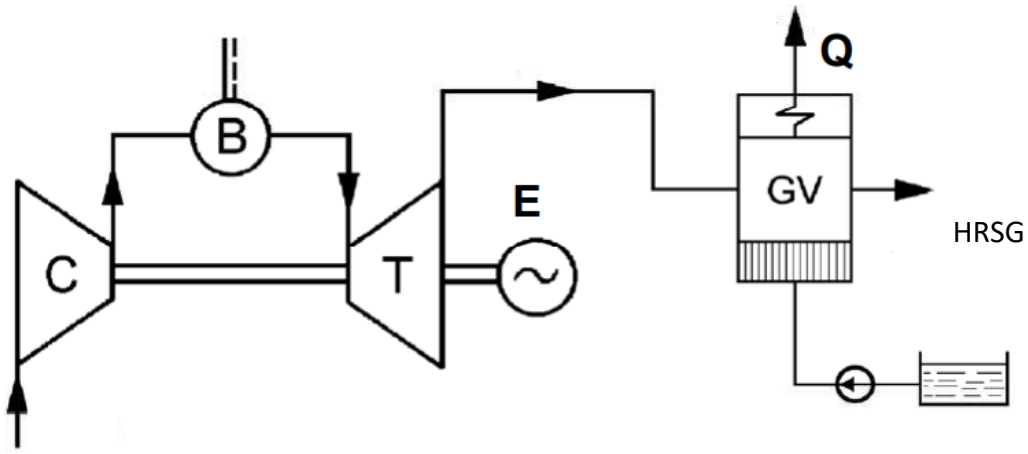

Figure 4.5 Cogeneration gas turbine scheme

A gas turbine can operate in two different ways:

- Direct use of the flue gases exiting the turbine in industrial processes such as high temperature ovens or drying processes
- Generation of a heat transfer fluid like steam, water or diathermic oil as it can be seen in the above scheme, that is the most common configuration.

The heat recovery in a gas turbine does not alter the electricity generated, except for load losses of flue gases inside the turbine, that bring to a counter pressure at the outlet of the turbine and to a consequent small electrical power production: in fact, in order to have exhaust gases at a temperature suitable for thermal uses, the turbine ejects gases at a higher pressure.

Similarly to ICE case, gas turbine is supposed to operate with the only biodiesel produced in loco. Obviously, when fueling gas turbine with a fuel different from natural gas, some technological modifications have to be accounted that affect the combustor. Generally, the technique most used by gas turbine manufacturers is the adoption of a lean-burn combustion, i.e. with air to fuel ratio higher than stoichiometric values, and an air blast fuel nozzle. The technique is aimed at maximizing mixing of fuel with air, minimizing the formation of CO and unburnt hydrocarbons.[27] In addition, important challenges involve the need of preventing harmful effects of ashes contained in heavy fuels like diesel: they cause corrosion, erosion and fouling on turbine blades. As a consequence, salts must be removed by water washing the fuel.[28]

It has been proved that with small technical and operating measures, biodiesel and diesel can be used interchangeably in a combustion chamber to make flue gases expand in a turbine: due to the lower heating value of the biodiesel, around 10 % additional fuel mass flow is needed for biodiesel to achieve the same exit temperature of the usual diesel fuel. Tests have proven that turbine exiting temperatures are quite similar for diesel and biodiesel, implying that the effect of the fuel change from diesel to biodiesel on turbine blades and nozzles is small and that the output of the turbine will be nearly the same by increasing of about 10 % the mass flow of the biodiesel[29].

The energy balance of a generic gas turbine is described in the following graph:

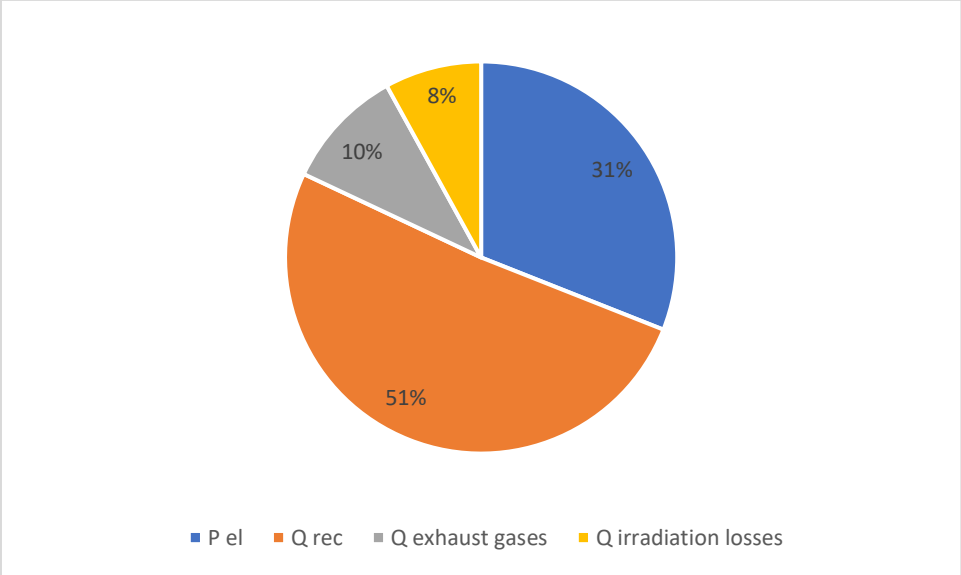

Figure 4.6 Energy balance of cogeneration gas turbine

From the above graph, it can be seen that the recoverable thermal heat is quite higher than the electricity production. In addition, differently from the previous case of ICEs, the entire amount of heat is given at the same temperature, that is the temperature of exhaust gases exiting the turbine (T>400°C) and thus, it's possible to perform the only total recovery in a gas turbine. In order to get 1000 kW of electrical power, 3226 kW must be given by the fuel and an amount of 1645 kW of thermal heat could be recovered. It's easy to see that a gas turbine shows better cogeneration performances with respect to the diesel engine: it has a higher thermal coefficient Q/E equal to 1.65 and a cogeneration efficiency equal to almost 85%.

Feasibility of Cogeneration Gas Turbine in Biodiesel Production Process

To guarantee the thermal energy demand in the first scenario of about 900 kW (that is the sum of high temperature and low temperature heat) the gas turbine must be designed to generate 550 kW_{el}, coming from a total energy input of 1766 kW. But, such a low power range is not feasible for a gas turbine.

In the second scenario the thermal energy demand is equal to 5407 kW and to assure this provision, the engine must generate around 3.3 MW_{el}.

The quantity of fuel used is 1255,5 kg/h considering the usual 80% efficiency in this second case, value that corresponds to 20% of the total biodiesel produced every hour, a value much more feasible than the previous one (40%). The only drawback in using such technology is that an amount of heat recovered must be degraded at lower temperature, since all the heat is recovered at very high temperature. That involves an expenditure in terms of energy as well as an increase in costs related to the degradation process.

An alternative solution can be seen in recovering only high temperature heat from the gas turbine, while providing low temperature one by means of apposite heat pumps. In this case, the thermal energy demand will be 5117 kW_{th} and the turbine must be designed to give 3.1 MW_{el}, with a following fuel consumption of 1188.16 kg/h, corresponding to 19% of biodiesel production. A 300 kW_{th} heat pump could be implemented in order to satisfy the thermal request of 289 kW_{th}. With a COP equal to 4.5, it would consume 68 kW_{el} and provide the process with continuous hot air at 65°C (enough to satisfy low-temperature thermal demands). The proposed heat pump is an existing model from Viessman company.

Cogeneration Steam Turbine

The steam cycle is very flexible with respect to the sources that can be used to produce energy as the different types of boilers (grid, bed fluid, powder, etc.) allow the use of all kinds of fuels, especially not valuable ones: natural gas, liquid fuels, oils, coal, biomass as well as municipal solid waste (waste-to-energy plants). Steam turbines are characterized by high

power ranges, from some MWs to over 1 GW with more turbines in parallel. These technologies allow the possibility to reach very high thermal efficiencies, but on the other hand, they are affected by high investment costs, high complexity, high difficulty in adapting to partial loads and require frequent maintenance.

The most known cogenerative solutions of steam turbines are:

- Counter pressure steam turbine: the entire steam flow rate required by the thermal user undergoes the process and thus a univocal link exists between electricity and thermal output. In these configurations, the condenser is not present since the steam exiting the turbine is used to supply thermal power to the user.

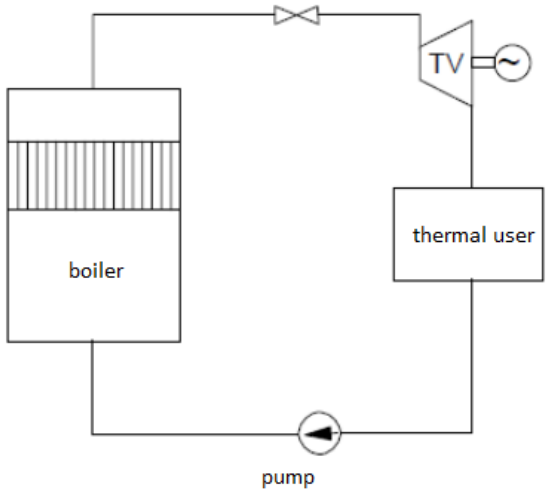

Figure 4.7 Counterpressure cogeneration steam turbine scheme

Counter pressure steam turbines are affected by low electrical efficiencies when operating in cogeneration (from 12% to 25%), while they can reach very high thermal efficiencies (from 75% to 85%). In order to generate 1000 kW_{el}, almost 6700 kW must be given by the fuel and more than 5300 kW_{th} are produced. The configuration shows a cogeneration efficiency equal to 95% and a thermal index equal to 5.3 (relevant with the common range that goes from 4 to 10).

- Condensation and bleeding steam turbines: a wide range of regulation is viable, making possible the optimization from and energy and economic point of view. By

extracting a precise quantity of vapor from the turbine, it's possible to produce only the necessary thermal power at the specified temperature and pressure conditions. Such turbines are included in the B category of cogeneration plants since by making bleedings from the turbine body, the thermal production will affect and decrease the electricity generated, letting expand in the turbine a lower amount of vapor.
This kind of steam turbines are less attractive in the field of cogeneration, since they exhibit lower values of cogeneration efficiencies and thermal indexes. By

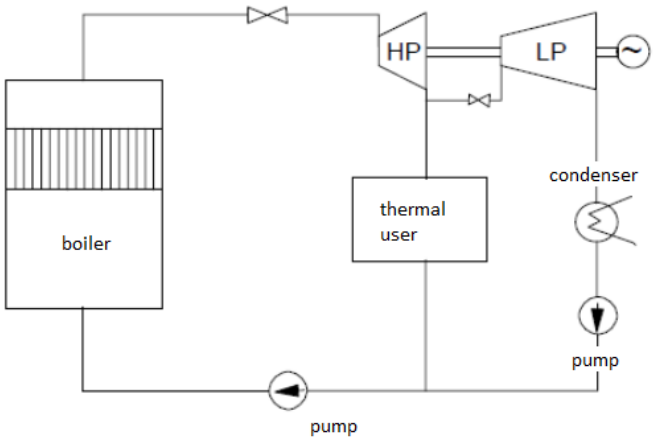

Figure 4.8 Condensation/bleedings cogeneration steam turbine scheme

considering an average η_{el} equal to 25% and an average η_{th} equal to 55%, it's possible to reach a cogeneration efficiency of 80% and a thermal index equal to 2.2. To get 1 MW_{el}, less energy in is necessary with respect to the counter pressure case (equal to 4000 kW) and the heat that can be recovered is equal to 2200 kW_{th}.

Feasibility of Cogeneration Steam Turbines

For what concerns the first scenario, neither counter pressure turbines nor condensation/bleeding turbines find technical applications. In fact, the smallest possible configuration in terms of power is 1 MW_{el} (for counter pressure turbines) that brings to a minimum of 5 MW_{th} recoverable, that is much higher than the energy required. Condensation/bleedings turbines are even less suitable since their minimum power output

is around 10 MW_{el}, which brings to a recover of 22 MW_{th}, more than twenty times higher than the necessary heat. As a result, steam turbines are not suitable in cases in which the magnitude of electrical and thermal powers are of much smaller order.

The operating size of condensation/bleeding turbines does not allow the adequacy neither for the second scenario, in fact a minimum of 22 MW_{th} are recovered with respect to the 5.4 MW_{th} required by the process: there would be an extreme energy loss that does not absolutely justify the employment of such technology. Even the electricity produced appears to be in an excessive amount (around 10 MW_{el}) and it should be completely sold to the grid. The condensation/bleeding turbine can be considered as the worst solution to supply energy to the transesterification process.

On the contrary, counter pressure steam turbines appear to be definitively suitable in the second scenario: it would be almost sufficient a 1 MW_{el} steam turbine to supply all the necessary thermal input to the process (5300 kW_{th} produced compared to 5407 kW_{th} required), after having degraded a small amount for low temperature purposes. In this case, there would be a fuel consumption of 800.38 kg/h, that corresponds to the only 13% of the total production. Instead of recovering all the necessary heat from the turbine and operating a degradation, it could be proposed to recover from the steam technology only the high temperature thermal energy and provide low temperature heat with additional devices such as heat pumps. This solution would avoid important energy losses for degradation purposes and employ the surplus electricity in a reasonable way, without selling it almost completely. As seen for GT configuration, a 300 kW_{th} heat pump can be implemented in order to satisfy the thermal request of 289 kW_{th}, with an electricity consumption of 68 kW_{el}. In this latter situation, fuel consumption will be equal to 789.47 kg/h which corresponds to 12.7% of the total biodiesel production, considering the minimum power range of 1 MW_{el}.

Cogeneration Combined Cycle

Combined plants are made of a topping gas cycle and a bottoming steam cycle, particular configuration that allows to obtain higher system efficiencies and a better reutilization of the high thermal content of flue gases exiting the first turbine. Combined cycles are born on the will of obtaining an increase of electricity production by exploiting the thermal energy of the gases, i.e. the electrical aspect is definitively privileged over the thermal demand. They are more suitable when the thermal demand is at low temperature. As a matter of fact, considering its energy purposes, combined cycles are the furthest technology in meeting the energy demand of the process. They exhibit among the lowest thermal recovery and cogeneration efficiencies, while showing very high values of electrical efficiencies.

In an analogous way as for steam turbines, combined cycles can adopt two different configurations: condensation/bleedings (most used) and counter pressure.

Gas and steam turbines show an average η_{el} equal respectively to 31% and 10%, while η_{th} is around 37%. Thus, to produce an overall of 1 MW_{el}, a fuel energy input equal to 2430 kW is necessary and only 902 kW_{th} can be recovered. Cogeneration efficiency is around 78%, while thermal index is 0.9, the lowest ever.

Feasibility of Cogeneration Combined Cycle

As already said, cogeneration combined cycles are characterized by the lowest cogeneration efficiency and thermal index. In addition, their high operating power ranges don't make them suitable for the cited scenarios, since the minimum size is 10 MW_{el}: with such electricity generation, an amount of 9 MW_{th} will be recovered, a value much higher even than the demand from the second scenario.

Chapter 5

Solar Technologies to Supply Power to the Process

The present study continues by analyzing the solar option in providing the plant with the necessary thermal input. The idea is born on the same assumption of getting rid of fossil fuels dependence and making the entire transesterification process as greener as possible. The intention of exploiting solar radiation comes from the fact that Chile has an extremely high potential, especially in the northern part of Atacama Desert. Relatively to photovoltaic energy, the solar energy industry in Chile is booming, providing very cheap electricity: in 2016, according to data from the national grid operator reported by the Bloomberg site, the electricity price reached zero for 113 days until April, in line with the year before, in which the 'zero' price was been reached for 192 days. The world record of solar electricity produced was recorded in the photovoltaic plant of El Romero, in the municipality of Vallenar, 645 km north of the capital Santiago. It is one of the largest solar plants for capacity in Latin America. El Romero is located in the Atacama Desert, an area particularly favorable to photovoltaics, since it is one of the driest places on the planet. In fact, it is known for the high level of irradiation - one of the highest in the world - and the very clean air that facilitates the capture of solar energy. That results in an already consolidated exploitation of this potential and makes the country pretty expert about the different solar technologies.

Figure 5.1 Chilean solar potential

The map on the right has been taken from Chile's *Ministerio de Energía* and shows the solar radiation potential of the country: it's easy to notice how big is the contribution of solar radiation in the north of Chile, where 7.5 kWh/m2/day can be reached. Valparaiso and Santiago de Chile occupy the central region of Chile and are affected by a solar radiation that goes from 4.5 to 5.5 kWh/m2/day, very similar to the Italian situation. It appears clear that Valparaiso, although it's not located in the most profitable part of the country,

has an appreciable solar potential that ca be exploited. Only the very south of the country does not show any interest in terms of solar conversion into thermal or electrical energy, due to the scarce radiation contribution.

Valparaiso is located in the southern hemisphere, precisely at a latitude of -33.1318 and a longitude of -71.5694; thus, the radiation profile shows an opposite trend with respect to what can be found in Europe. By considering a time frame that goes from 1st January 2004 to 31st December 2016, the Chilean *Ministerio de Energia* made possible to resume the different radiation contribution as follows:

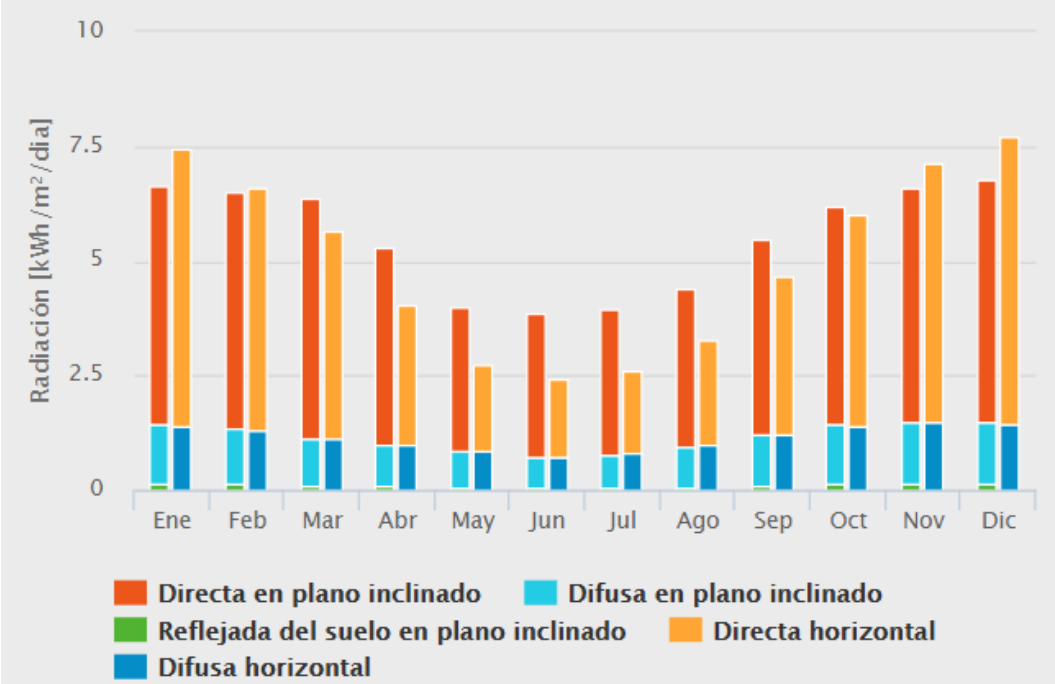

Figure 5.2 Different Radiation Contribution

Where the direct and diffuse tilted radiation (orange and light blue lines) have been obtained considering a panel tilt angle of 33° (equal to the latitudinal location of the city). The horizontal direct and diffuse radiation have been got supposing a 0° tilt angle of the panel. It's easy to see that during summer season the solar panel is able to catch more solar energy when horizontal, while during winter season the inclination is fundamental to make the system profitable.

The following table resumes all the different radiation contributions in the same time frame, given in W/m2:

W/m2	Global 33° tilted	Direct 33° tilted	Diffuse 33° tilted	Global horizontal	Direct horizontal	Diffuse horizontal	Direct normal
January	277,38	217,65	53,74	309,88	251,43	58,45	363,23
February	270,78	215,09	50,37	274,62	219,83	54,79	331,99
March	265,99	218,36	43,09	235,01	188,15	46,87	309,78
April	219,43	179,20	36,97	168,12	127,91	40,22	241,86
May	165,87	130,35	33,32	113,53	77,29	36,25	180,50
June	160,64	130,55	28,13	101,24	70,64	30,60	181,29
July	165,04	132,68	30,27	108,39	75,46	32,92	182,83
August	184,03	143,80	37,57	137,30	96,43	40,87	193,96
September	227,85	177,84	46,26	193,72	143,40	50,32	250,99
October	258,27	199,30	54,10	251,45	192,60	58,85	296,51
November	274,76	212,61	56,40	296,94	235,60	61,35	338,87
December	281,19	220,35	54,61	322,06	262,66	59,40	379,12

Table 5.1 Radiation Contribution in W/m^2

It's easy to notice that global radiation is nothing but the sum of direct (or beam) and diffuse radiation. In addition, it can be noted that the highest contribution is given by last column, that is the Direct Normal Irradiance (DNI): it's defined as the amount of solar radiation received per unit area by a surface that is always held perpendicular (or normal) to the rays that come in a straight line from the direction of the sun at its current position in the sky. Typically, the amount of irradiance annually received by a surface is maximized by keeping the panel normal to the incoming radiation: this quantity is used for concentrating solar thermal installations and installations that track the position of the sun.

Knowing the different radiation contributions is fundamental when choosing the technology: in fact, for instance, common solar collectors are able to catch both beam and direct irradiance and maximize their capturing capacity with a constant inclination angle. On the other hand, concentrating solar panels can only catch direct radiation, but by means of a particular tracking system, they move to stay all the time perpendicular to the sun rays, managing to capture a big amount of radiation.

Al already mentioned above, at this point of the analysis, the work aims at considering two different solar technologies which, however, are not mutually interchangeable: flat plate

collectors and concentrating solar panels. The formers are able to provide the process with the only low temperature heat, so the installation of conventional boilers for high temperature demands must be forecasted; the latters generate high temperature heat that satisfies the entire process thermal demand.

Thermal Energy Storage Systems (TES)

Because of the aleatory condition of solar source, every plant that exploits solar radiation must be designed assuming the presence of a thermal energy storage system. A TES system can basically store heat to be used later, to face the energy mismatch between energy generation and energy use. It essentially works in three steps: charge, storage and discharge. The characteristics that a storage system should have are:

- high energy density (high storage capacity)
- good heat transfer between HTF and the storage material (in case of a passive storage)
- mechanical and chemical stability of the storage material
- compatibility between the storage material and the container material
- complete reversibility of a number of cycles
- low thermal losses during the storage period
- easy control

To determine how convenient is a thermal storage, it's necessary to look at the thermal load reduction and the thermal/electricity energy savings. The former refers to the reduction of heat generation with respect to the case in which, under the same working conditions, any type of energy storage is employed. The latter simply refers to the thermal heat that is stored and may be reutilized, thus not needing to be generated again by the application.[30]

Essentially, three main types of thermal storage can be outlined:

- sensible heat storage: it consists in increasing the temperature of the storage material that could be water, air, oil, concrete etc.., all with high thermal capacity and abundant and cheap. The amount of stored energy is computed as:

$$Q = m \cdot c_p \cdot \Delta T$$

where Q is the amount of heat stored in the material (J), m is the mas of storage material (kg), c_p is the specific heat of the storage material (J/kg·K), and ΔT is the temperature change (K).

When selecting the appropriate material, it's important to look at density, specific heat, thermal conductivity and diffusivity, vapor pressure, compatibility with container materials, and chemical stability.[30]

Material	Density (kg/m^3)	Specific heat (J/kg·K)	Volumetric thermal capacity (10^6 J/m^3·K)
Clay	1,458	879	1.28
Brick	1,800	837	1.51
Sandstone	2,200	712	1.57
Wood	700	2,390	1.67
Concrete	2,000	880	1.76
Glass	2,710	837	2.27
Aluminium	2,710	896	2.43
Iron	7,900	452	3.57
Steel	7,840	465	3.68
Gravelly earth	2,050	1,840	3.77
Magnetite	5,177	752	3.89
Water	988	4,182	4.17

Figure 5.3 Characteristics of materials used for sensible heat storage

- latent heat storage where storage is performed by means of material transition of phase, usually solid-liquid phase change is used. The materials implemented are called phase change materials (PCM) and they gain heat by melting and release it by solidifying. The amount of stored heat is computed as:

$$Q = m \cdot \Delta h$$

where Q is the amount of heat stored in the material (J), m is the mas of storage material (kg), and Δh is the phase change enthalpy (J/kg). Usually PCM are selected based on the appropriate melting enthalpy and temperature, availability and costs.[30]

- thermochemical storage when a chemical reaction with high energy involved is used

Material	Melting temperature (°C)	Melting enthalpy (MJ/m^3)
Water-salt solutions	–100–0	200–300
Water	0	330
Clathrates	–50–0	200–300
Paraffins	–20–100	150–250
Salt hydrates	–20–80	200–600
Sugar alcohols	20–450	200–450
Nitrates	120–300	200–700
Hydroxides	150–400	500–700
Chlorides	350–750	550–800
Carbonates	400–800	600–1,000
Fluorides	700–900	> 1,000

Figure 5.4 Characteristics of materials used for latent heat storage

to store heat. It works by storing the products of the reaction and the heat stored, when necessary, has to be recovered by letting the reaction proceed in the opposite way: of course, only reversible reactions are suitable. Chemical energy conversion shows better energy storage performances than physical methods (sensible and latent heat storage): the most important challenge is to find the appropriate reversible chemical reaction for the energy source used. The main reactions studied are carbonation reaction, ammonia decomposition, metal oxidation reactions and sulfur cycles. In addition to chemical reactions, sorption systems can be used to store thermal energy in terms of adsorption on the surface of a porous material and absorption on liquids. [30]

Storages can even be seasonal and they're particularly efficient in countries characterized by a high solar potential during summer days, and a quite low solar radiation during winter season. It has been shown that seasonal thermal accumulation allows to obtain a significant reduction of the total collector surface. Sillman reported that the performances of a solar system with seasonal storage increase linearly with the tank size, to the point where the storage size is enough to store the entire thermal energy produced during summer days and not immediately used. A seasonal storage could satisfy 50-70% of the thermal energy

demand, with respect to the 10-20% of the daily storage plants, with a considerable reduction of fossil fuels consumption and environmental pollution. [31]

Big seasonal tanks are positively affected by economies of scale; in addition, they're generally more efficient than small scale plants with the same energy density, since the former presents a lower surface/volume ratio, and so lower thermal losses. On the other hand, it's difficult to precisely compute the thermal losses that affect seasonal tanks (they're usually buried or semi-buried and a precise estimation of thermophysical ground properties is not easy) and their realization is much more complex with respect to daily tanks.

Seasonal storage tanks are usually realized in steel or concrete, with an insulating layer on the surfaces. Usually, 500 m^3 cylindrical tanks are used, with a low surface/volume ratio and so low thermal losses per unit of stored energy; they're usually buried or semi-buried.[30]

In seasonal tanks, thermal power is transferred by injecting or extracting water directly from the storage system, or by means of exchangers that could be both internal or external. The following image shows three typical installations: the first one with an internal HX, the second one with an external HX while the third one with a shell and tube HX.

To face the problem of thermal losses, it's necessary to realize a good insulation in case of

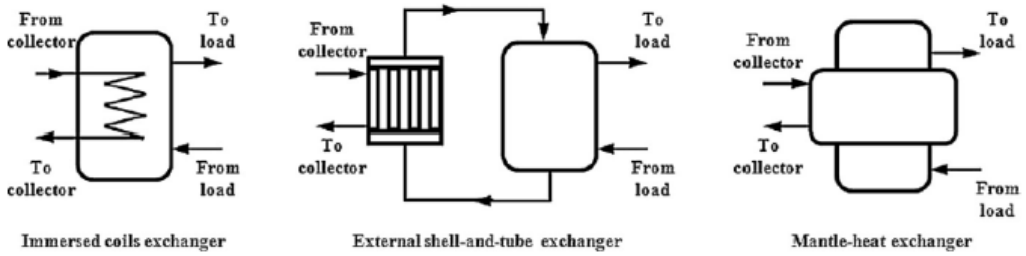

Figure 5.5 TES configurations for seasonal tanks

external tanks, or to bury the tanks or both the solutions. In case of buried tanks, the effect of thermal losses is a ground temperature increase, while the ground conductibility decreases for the diffusion of its humidity content along thermal gradients, which results in a less heat dispersion through tank walls. Buried tanks present the following advantages:

- they require a smaller volume with respect to systems that use rock materials or ground

- the thermal power is transferred with water flow rate
- they can be used in whatever climate conditions and ground characteristics
- the thermal insulation is relatively simple
- water penetration effects are negligible

on the other hand, buried tanks presents the following drawbacks:

- the ground around the tanks does not contribute to the insulation
- water losses due to cracking or corrosion can cause ground expansion
- when heat is extracted, wall external surface could be at lower temperature than ground one and this could cause condensation with losses in performances

It has been proved that a non-buried tank should be 1.9 times taller than a buried one, and it should have a double insulation to keep the same performances.

Flat Plate Solar Collectors

Solar collectors are devices that transform solar energy into heat, by means of a fluid which directly provides thermal energy or by means of a HTF which heats up another fuel.

Basically, a solar collector is composed by:

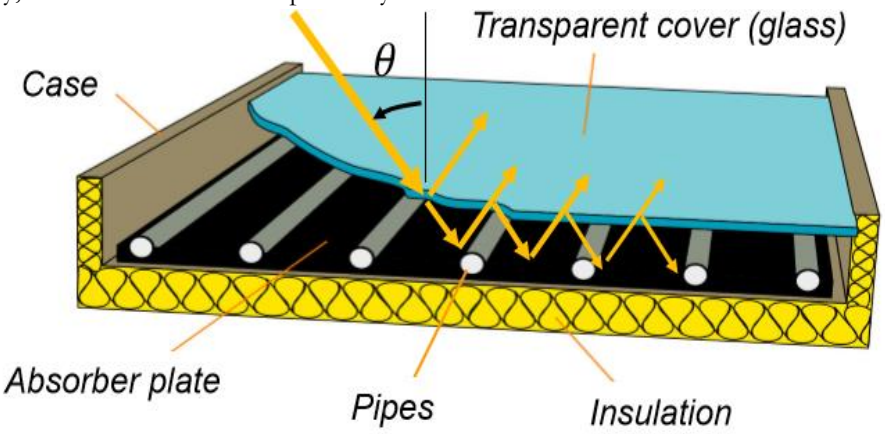

Figure 5.6 Flat plate collector

- A capturing energy system (absorbing or selective surface)
- An isolation system to minimize thermal losses
- A circulating system for the circulation of the transfer fluid

The operating principle of a solar collector is described as follows:

- Both beam and diffuse radiation cross the glass or polycarbonate cover
- The radiation hits the absorber plate which heats up and transfers heat to the fluid
- The transfer fluid increases its temperature

A solar collector must be resistant to the rain and humidity as well as to thermal and mechanical stresses. It must be easy to install, efficient in energy conversion, stable in performance and economic.

Three types of solar collector are commonly used depending on the intended use and the desired temperature range in the transfer fluid:

- Collectors for swimming pool temperature: without cover, suitable for low temperatures, and of relative low cost

- Flat plate collectors: most used for domestic or sanitary hot water, with transparent cover and insulation, suitable for medium fluid temperatures range (30 to 60 ° C)
- Vacuum tube collectors: used for sanitary hot water and to support industrial processes, higher cost, suitable for high fluid temperatures (up to 90 ° C)

The useful heat that can be generated through a solar collector is expressed as follows:

$$Q_u = A_c[S - U_L(T_p - T_a)]$$

Where A_c is the collector area, S is the generation term, U_L is the heat loss coefficient and T_p and T_a respectively the plate and the ambient temperature. Usually, the plate temperature is difficult to measure because it's an extreme ideal situation that the plate is entirely at an only temperature. So, the useful heat formula in expressed in an alternative way:

$$Q_u = F_R A_c[S - U_L(T_{fi} - T_a)]$$

Where T_{fi} is the fluid temperature at the inlet and F_R is a correction term, called heat removal factor, that takes into account the thermal resistance between the fluid and the plate. By doing some easy calculations, the removal factor is expressed as follows:

$$F_R = \frac{\dot{m}c_p}{A_c U_L}[1 - \exp\left(-\frac{F' A_c U_L}{\dot{m}c_p}\right)]$$

Where $\dot{m}$ and c_p are the nominal mass flow rate and the specific heat of the fluid inside the panel and F' is the collector efficiency factor, expression of the collector's ability to transfer heat from the fin to the fluid.

At times it is practical to refer to the fluid mean temperature (T_{fm}) rather than the fluid inlet temperature (T_{fi}). That is used in the European formulation and the formula undergoes a modification:

$$Q_u = F_{av} F_R A_c[S - U_L(T_{fm} - T_a)]$$

Where F_{av} is a correction factor expressed as:

$$F_{av} = \frac{2}{1 + \exp(-\frac{A_c U_L F'}{\dot{m} c_p})}$$

The generation term S for a generic tilted surface is expressed as:

$$S = 0.96(\tau\alpha)_{bn} K(\vartheta) G_T$$

Where G_T is the incident radiation on a tilted surface and $(\tau\alpha)_b$ is the transmission-absorption product, that account for that fraction of the transmitted radiation that is reflected back from the absorber plate and, subsequently, from the cover, until extinction, while $K(\vartheta)$ is the incidence angle modifier. In order to increase S, a good absorber plate absorptance is needed within the solar radiation wavelengths; at the same time, in order to decrease U_L, a poor absorber emissivity is needed within the infrared wavelengths. The characteristic of having high solar absorptance and low infrared emissivity is called selectivity.

General expression of the useful thermal energy given by a solar collector is:

$$Q_u = F_{av} F_R A_c [0.96(\tau\alpha)_{bn} K(\vartheta) G_T - U_L(T_{fm} - T_a)]$$

It has been chosen a generic collector and it has been calculated its thermal yield by using the following technical characteristics illustrated in its datasheet:

- a_1 equal to 3.88 $\frac{W}{m^2 K}$
- η_0 equal to 0.783
- $K(50°)$ equal to 0.92
- A_c equal to 3 m^2
- A nominal mass flow rate of 75 l/h equal to 0.022917 kg/s

Using the following formulas, it has been possible to estimate all the values to get Q_u

$$F_R U_L = \frac{a_1}{1 + a_1 \left(\frac{A_c}{2\dot{m} c_p}\right)} = 3.6598 \frac{W}{m^2 K}$$

$$F_R' U_L = F_{av} F_R U_L = \mathbf{3.5866} \frac{W}{m^2 K}$$

$$F_R 0.96(\tau\alpha)_{bn} K(50°) = \eta_0 \left(1 - F_R U_L \frac{A_c}{2\dot{m}c_p}\right) K(50°) = 0.6803$$

$$F_R 0.96(\tau\alpha)_{bn} K(50°) F_{av} = \mathbf{0.6667}$$

It has been chosen year 2014 as reference year. Initially two different configurations have been taken into account, just to see what was the best one: an initial inclination of 45° and a second one of 30°. The following graph shows the trend of the solar irradiance captured by the panels:

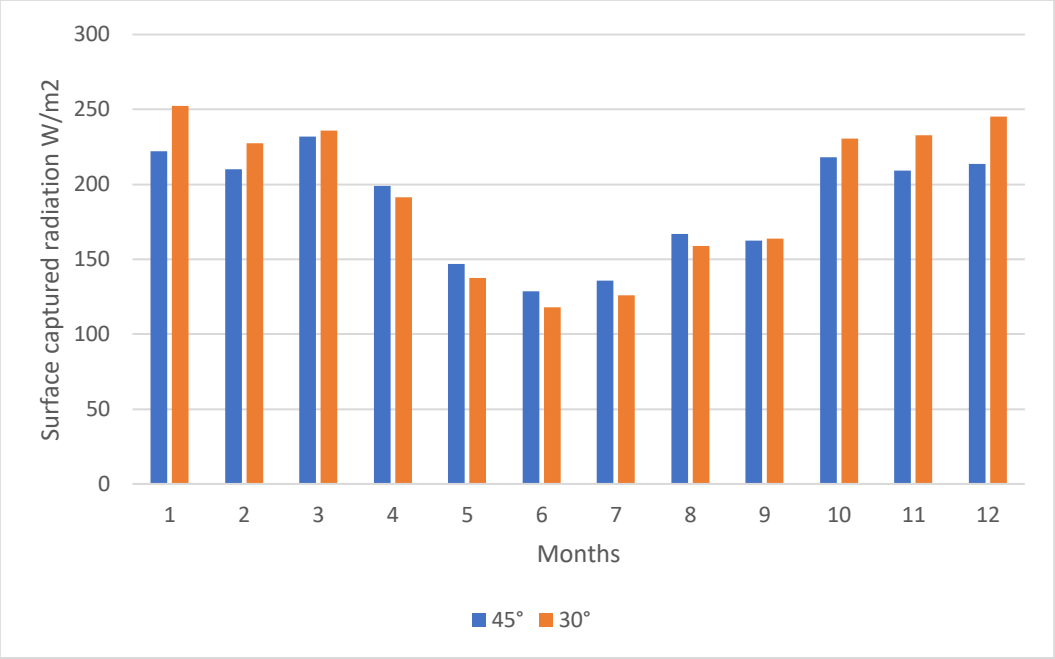

Figure 5.7 Captured radiation by surface at 45° and 30°

The 30° configuration is obviously preferred to the other since it is capable of absorbing more solar radiation during summertime and a lightly slower amount during winter months.

Solar flat collectors can only provide the process with low temperature heat, since the highest temperature the HTF can reach is around 90°C (in case of vacuum tube collectors). Therefore, according to the first scenario, the collectors must supply 48,12 kWh of thermal energy at 60°C while in the second scenario an amount of 289,154 kWh.

Three possible configurations have been proposed:

- the first one aimed at totally ensuring with the only solar plant the thermal supply during summer months, and by considering the implementation of a supporting tank to provide thermal energy during night time and whenever necessary in winter months. The solution will foresee the need to burn biodiesel in all those cases in which the thermal load stored during day time is not sufficient to meet the need during night time.
- the second one aimed at ensuring the supply even during winter season with the only solar collectors-solar tank system. The solution is an over sizing of the plant: it will ensure to meet the thermal need during cold months, while it will bring to a considerable thermal loss during summertime.
- the last one as an intermediate solution, aimed at satisfying with the only solar system the thermal load during both summer and winter by considering the implementation of a seasonal tank. The plant will be designed in order to store during summer months the required energy that will then be released gradually during winter time.

Flat plate collector configurations see the implementation of water storage tanks. That is the first kind of a TES system, where sensible heat of storage fluid is utilized to accumulate thermal energy. Water is a suitable material since it can reach a maximum temperature of 90°C, higher than the operating temperature of the system. To perform the calculations, the following data are considered:

- Water specific volume c_p equal to 4186 $\frac{J}{kgK}$
- water temperature at which heat must be supplied equal to 60°C (T_{use})
- temperature at which water is reintroduced in the tank equal to 15°C (T_{mains})
- water density ρ equal to 997 $\frac{kg}{m^3}$

Water potential of accumulating energy is expressed as the heat per unitary mass:

$$Q/m = c_p(T_{use} - T_{mains}) = 188.37\,\frac{kJ}{kg}$$

then heat is expressed per unitary volume as follows:

$$Q/_V = Q/_m \cdot \rho = 187.8 \frac{MJ}{m^3}$$

That dividing by 3600 brings to the water heat capacity as 52.17 $\frac{kWh}{m^3}$

I Configuration

The first approach looks at guaranteeing the thermal need during summer season by means of the only solar system. The plant will be dimensioned in order to completely fulfill the thermal request for both day and nighttime, without considering any additional source of heat (or at least considering it in the remote cases in which solar radiation is not sufficient to give energy).

The summer period is referred to the following six months: January, February, March, October, November and December. It has been chosen to include October and not April because from a meteorological history of the site, October was found to have a much higher solar potential. Thus, during these six months the solar system must generate the required energy to satisfy the thermal load during day hours but it must also include a storage tank to accumulate heat that will be released during nighttime. As already cleared, the system has been sized to respect this balance just for summer months: in winter season, the energy the solar system is not able to provide will be supplied by conventional boilers.

The number of collectors has been chosen considering that in all the six summer months, the thermal energy that can be stored must be always higher or slightly lower than what is demanded by the process. To get the portion of thermal energy that can be stored, from the useful heat the thermal demand of 48,12 kWh has been subtracted: the positive values represent the energy that the system is able to store every hour, while negative values represent the heat demand required by the process. The months have been divided into three slots each, to see more locally the behavior of heat stored and heat demanded. A number of 90 collectors has been chosen since it has been considered a good compromise.

Energy balance [MWh]	Energy balance [MWh]	Energy balance [MWh]	Energy balance [MWh]
JAN 1ST TERM	JAN 2ND TERM	JAN 3RD TERM	**JAN TOT**
7,555771353	7,218189802	7,7653736	**22,53933**
-6,552682371	-6,589550104	-7,320017857	**-20,4623**
FEB 1ST TERM	FEB 2ND TERM	FEB 3RD TERM	**FEB TOT**
7,859326182	7,104067398	5,826098465	**20,78949**
-6,605456473	-6,798149952	-5,4247746	**-18,8284**
MAR 1ST TERM	MAR 2ND TERM	MAR 3RD TERM	**MAR TOT**
7,143486245	7,228642108	6,74563071	**21,11776**
-6,867451408	-6,849034025	-7,77058235	**-21,4871**
OCT 1ST TERM	OCT 2ND TERM	OCT 3RD TERM	**OCT TOT**
6,499870965	5,843752068	7,552743446	**19,89637**
-6,956754839	-7,235932056	-7,468283927	**-21,661**
NOV 1ST TERM	NOV 2ND TERM	NOV 3RD TERM	**NOV TOT**
7,077075322	7,260727903	5,91906167	**20,25686**
-6,753949941	-6,709686341	-6,94007045	**-20,4037**
DEC 1ST TERM	DEC 2ND TERM	DEC 3RD TERM	**DEC TOT**
7,078757434	6,056571773	8,07181795	**21,20715**
-6,677251973	-6,719492342	-7,248381016	**-20,6451**

Table 5.2 Heat Stored and Heat Demanded for 90 Collector's' Configuration °

The above table shows that for January, February and December the stored thermal capacity is higher than the one requested, while for the other three months it is slightly lower: when necessary, conventional boilers must provide the required thermal energy. Only in the three months of March, October and November a tiny amount of biodiesel must be burned to generate the missing heat: respectively an amount of 35 kg, 167,17 kg and 13,91 kg of fuel will be necessary every month. Looking at the entire summer time, it can be noted that the overall thermal energy stored is higher than the one requested (125,8 MWh stored with respect to 123,5 MWh required).

In the period from April to September, the proposed configuration is able to provide the process with a total of 59,7 MWh out of the 147,7 MWh required. A thermal power equal to 88,05 MW must be provided with boilers: a biodiesel LHV equal to 38 $\frac{MJ}{kg}$ and a boiler efficiency equal to 100%. By looking at the single months, the following situation is outlined:

	ENERGY REQUIRED [MWh]	ENERGY STORED [MWh]	ENERGY DEFICIT TO SUPPLY WITH FUEL [MWh]	TOT FUEL CONSUMED [kg]
APRIL	22,05882592	15,52892592	6,5299	618,622105
MAY	25,47054609	8,20304609	17,2675	1635,86842
JUNE	25,84258147	6,80878147	19,0338	1803,20211
JULY	26,51421613	7,22371613	19,2905	1827,52105
AUGUST	24,6452305	10,7767305	13,8685	1313,85789
SEPTEMBER	23,20561842	11,14391842	12,0617	1142,68737
	147,7370185	59,68511853	88,0519	8341,75895

Table 5.3 Fuel consumed during winter months for 90 collectors' configuration

It's easy to notice that May, June and July are the worst months ever in terms of radiation potential: a considerable provision of biodiesel must be guaranteed to meet the thermal demand. The presence of storage tanks allows for a much lower use of biodiesel even during winter season. In case no tank is present, the situation is shown in the table below:

	ENERGY TO SUPPLY WITH FUEL [MWh]	MEAN HOURS WITH NO RADIATION	THERMAL ENERGY TO SUPPLY IN NIGHTTIME EVERY HOUR [kWh]	THERMAL ENERGY TO SUPPLY IN NIGHTTIME [kWh]	TOT FUEL DURING NIGHTTIME [kg]	THERMAL ENERGY TO SUPPLY IN DAYTIME [kWh]	TOT FUEL DURING DAYTIME [kg]
APRIL	22,05882592	14	48,122	20211,24	1914,749	1847,586	175,0345
MAY	25,47054609	14	48,122	20884,948	1978,574	4585,598	434,4251
JUNE	25,84258147	16	48,122	23098,56	2188,285	2744,021	259,9599
JULY	26,51421613	16	48,122	23868,512	2261,227	2645,704	250,6457
AUGUST	24,6452305	14	48,122	20884,948	1978,574	3760,283	356,2373
SEPTEMBER	23,20561842	14	48,122	20211,24	1914,749	2994,378	283,678
					12236,16		1759,98

Table 5.4 Fuel consumed during winter months if no storage is present

A total amount of 13996,14 kg of fuel would be needed if no tank was present.

For what concerns the supply of high temperature heat, solar collectors are not suitable since the transfer fluid can reach a maximum temperature of 90°C (only in particular cases). Therefore, the missing 852,97 kWh must be provided by burning biodiesel: 80,8 kg/h of fuel will be required to meet the thermal need, corresponding to the 10% of the hourly biodiesel production. During winter months, the percentage of biodiesel implemented for thermal purposes will be higher due to a lack of low temperature heat too, but anyway lower than 15%.

Considering the second scenario, a higher biodiesel yield brings to a higher thermal need and so, to an increasing number of solar collectors. An amount of 289,15 kW_{th} are necessary to produce around 6200 kg/h of biodiesel. Thus, to fully satisfy the thermal load in summer season during both day time and night time, a configuration with 550 solar collectors has been chosen. The following table shows the summer months divided into three terms:

Energy balance [MWh]	Energy balance [MWh]	Energy balance [MWh]	Energy balance [MWh]
JAN 1ST TERM	JAN 2ND TERM	JAN 3RD TERM	**JAN TOT**
46,6331	44,5699	47,9538	**139,1568**
-39,3211	-39,5462	-43,932	**-122,799**
FEB 1ST TERM	FEB 2ND TERM	FEB 3RD TERM	**FEB TOT**
48,4914	43,8284	35,9486	**128,2684**
-39,6469	-40,7769	-32,5505	**-112,974**
MAR 1ST TERM	MAR 2ND TERM	MAR 3RD TERM	**MAR TOT**
44,0781	44,6182	41,6716	**130,3679**
-41,2093	-41,1164	-46,635	**-128,961**
OCT 1ST TERM	OCT 2ND TERM	OCT 3RD TERM	**OCT TOT**
40,14	36,0959	46,6382	**122,8741**
-41,7501	-43,4217	-44,8219	**-129,994**
NOV 1ST TERM	NOV 2ND TERM	NOV 3RD TERM	**NOV TOT**
43,6772	44,7998	36,5688	**125,0458**
-40,5206	-40,2504	-41,6263	**-122,397**
DEC 1ST TERM	DEC 2ND TERM	DEC 3RD TERM	**DEC TOT**
43,6924	37,4309	49,815	**130,9383**
-40,0568	-40,3002	-43,4827	**-123,84**

Table 5.5 Heat Stored and Head Demanded for 550 Collectors' Configurations

In this second configuration it has been chosen to implement more than the proportionally required collectors (6 times the ones used for 1042 kg/h of biodiesel) because an excessive amount of fuel should be burned to meet the thermal request. As an overall, the system is capable of storing a total amount of 776,65 kWh out of the 740,96 kWh demanded by the process during nighttime. Only for October a total amount of 674,5 kg of biodiesel must be burned.

For what concerns winter months, the situation referred to the six single months is reported in the table below:

	ENERGY REQUIRED [MWh]	ENERGY STORED [MWh]	ENERGY DEFICIT TO SUPPLY WITH FUEL [MWh]	TOTAL FUEL CONSUMED [kg]
APRIL	132,3612158	96,00161	36,3596	3444,593911
MAY	152,845771	50,98606	101,8597	9649,867457
JUNE	155,0838571	42,31181	112,7721	10683,66803
JULY	159,0806895	44,85859	114,2221	10821,0411
AUGUST	147,8864092	66,79827	81,08814	7682,034199
SEPTEMBER	139,221621	69,05703	70,16459	6647,171932
	886,4795636	370,0134	516,4662	48928,37663

Table 5.6 Fuel consumed during winter months for 550 collectors' configuration

An amount of around 50 ton of biodiesel will be necessary during winter months.

In an analogous way as already seen for the first scenario, high temperature heat must be provided by burning biodiesel since solar collectors are not able in providing such high temperatures. To provide the process with more than 5 MW_{th}, a quantity of 484,77 kg/h of biodiesel has to be used.

As already said, the configuration includes the utilization of a storage system to accumulate thermal energy during daily hours to be released when no radiation is available. To assess the capacity of the tank, it has been chosen one of the day with the highest radiation potential, i.e. where a considerable amount of thermal energy is produced to be stored. For instance, by considering the 12th of January, an amount of 763,72 MWh is stored in the 9 hours of available solar radiation. By then dividing by the water thermal capacity per unit

volume, a tank of 14,64 m^3 results to be necessary. A 15 m^3 will be considered, being a size widely more diffused in the market.

By doing the same calculations for the second scenario, a 90,4 m^3 storage tank is now necessary.

II Configuration

A second approach sees the implementation of flat plate solar collectors in a way that the thermal request is satisfied all over the year, i.e. considering nil or a very limited use of biodiesel for low temperature purposes. On the one hand, the present configuration allows for a reduced use of the fuel produced that is implemented only for high temperature heat, on the other hand, over dimensioning the solar system brings to an excessive waste of thermal energy during summer season.

In order to ensure thermal energy provision from April to September, 160 solar collectors have been adopted: in fact, the system is able to store 149,77 kW_{th} out of the 141,93 kW_{th} required. During summer months, there will obviously be an over production of thermal energy that is lost in the environment without any use: 287,23 kWh are produced to be stored, while only 119,63 kWh are needed, with a huge thermal loss equal to 167,61 kWh.

Regarding the second scenario, 940 solar collectors are necessary to completely meet the thermal load during winter season: the system can store 871,73 kWh to the 853,9 kWh demanded. During summer months, the thermal load being lost is much higher: 1676,1 kWh are stored when only 719,51 kWh are necessary, leading to a thermal loss of 956,6 kWh.

The present configuration will account for the presence of a daily storage that must store thermal energy during day time and release it during night hours. The tanks for the two scenarios will be designed in order to guarantee thermal energy provision during nighttime: a 15 m^3 tank for the first scenario, that allows to store almost 0,8 MWh of thermal energy and a 85 m^3 tank for the second scenario, allowing to store around 4,5 MWh of thermal energy.

III Configuration

The last configuration that is proposed in the present work, sees the implementation of a seasonal energy storage tank.

For what concerns the first scenario, in order to perform a seasonal storage, 113 solar collectors must be installed: in fact, with such a configuration the system is able to store 56,63 MWh of thermal energy during summer time to the 56,54 MWh necessary during winter season. It's important to take into account the thermal losses that may occur due to the high storage volume. Assuming a thermal dispersion of 10%, 115 collectors will be necessary to meet the demand during winter time leading to a storage of 61,35 MWh. Considering the thermal losses, 55,22 MWh can be stored out of the 53,8 MWh necessary. To calculate the volume of the thermal tank, it's enough to divide the thermal energy that could be stored by the water heat capacity, leading to a seasonal tank of 1176,04 m^3 and 1176041,92 liters of water. A seasonal tank with a height equal to 10 m and a diameter of around 12 m could be implemented.

Referring to the second scenario, 690 collectors are necessary because they're able to provide 329,64 MWh (including the losses) out of the 324,66 MWh required. A storage tank of 7020,22 m^3 is required with a water consumption of 6999854,92 liters. Possible dimensions could be a height of 15 m and a diameter of around 24 m.

Compared to the first configuration where only daily storage tanks are used, the number of solar collectors must be augmented by 25% but a much lower use of biodiesel will be done, since seasonal thermal storage should provide the required heat during winter months.

Compared to the second configuration where no biodiesel is needed (except for remote cases) and daily tanks are implemented, there is a reduction of 36% to 41% of the number of solar collectors respectively for the I and II scenario. This will positively affect the overall cost of the plant while the presence of a seasonal storage will negatively do.

Concentrating Solar Panels (CSP)

Concentrating solar collectors are solar energy capturers equipped with devices, like reflecting mirrors or refractory lenses, able at conveying solar incident radiation towards an absorber whose area is smaller than the aperture area of the collector.

Flat plate useful heat has been expressed as:

$$Q = A_p S - A_p U_L (T_p - T_a)$$

Where thermal losses are directly proportional to the absorber area (A_p) and to the difference between operating temperature (T_p) and ambient temperature (T_a). In order to increase the operating temperature without increasing thermal losses, while keeping the same absorber area (A_p), the aperture area of the collector is increased (A_a).

$$Q = A_a S - A_p U_L (T_p - T_a) = A_a \left[S - \frac{U_L}{C_r} (T_p - T_a) \right]$$

Where C_r is defined as A_a / A_p and it's the geometrical concentration ratio. That formulations allows to increase the first term of the formula, i.e. the generation capacity of solar collectors, while keeping low values of the thermal losses term.

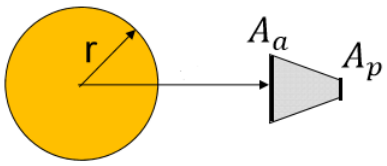

Figure 5.8 Aperture and absorber area of a CSP

As already seen for flat collectors, the formula can be rewritten in the following way:

$$Q = A_a F_R \left[S - \frac{U_L}{C_r} (T_{fi} - T_a) \right]$$

Where F_R is the removal factor and T_{fi} the fluid inlet temperature.

They are affected by the following advantages:

- the working fluid can reach higher temperatures compared to a flat system with the same solar energy collection surface, allowing to achieve greater thermodynamic efficiency
- higher thermal efficiency due to reduced thermal losses on the receiver surface
- the reflecting surface requires less material and has a simpler structure than a flat collector: the cost of a concentrating collector per unit of useful irradiated surface is less than for a flat collector
- considering the reduced surface of the absorber, surface treatments and the use of vacuum systems, designed to improve the efficiency of the system, are more economically viable
- the possibility to place the system "out of focus" allows to switch off the system, avoiding dangerous stagnation temperatures

on the other hand, CSP are affected by some drawbacks:

- they can only exploit direct solar radiation (DNI), collecting a percentage of diffuse radiation
- it's mandatory to provide the collectors with a sun tracking system for the sun, absent in flat collectors, which brings to higher costs
- reflective surfaces have a gradual deterioration of optical performance with time, mainly due to fouling, a more frequent maintenance is necessary
- the achievement of high temperatures, despite the considerable thermodynamic advantages, imposes necessary adjustments regarding the structure resistance to pressures and the heat storage at higher temperatures, with consequent economic/technological implications

Different types of concentrating collectors are present in the market and they can be classified according to the tracking system used:

- no tracking system: Compound Parabolic Concentrator (CPC)
- single axis tracker: Parabolic Trough Collector (PTC) and Linear Fresnel Reflector (LFR)

- double axis tracker: Parabolic Dish and Central Receiver Tower Reflector

To perform all the calculations, a parabolic trough collector has been chosen. PTCs allow to reach temperatures between 50 and 400 ° C, using relatively light and low-cost structures. The absorber is essentially a black metal tube, covered by a glass tube with an anti-reflecting coating to reduce heat losses, and it is positioned along the focal line of the receiver. When the parabolic trough is pointed towards the sun, the sun's rays, entering the aperture, are reflected by the mirror towards the absorber, which converts the energy into heat and transfers it to the HTF placed inside.

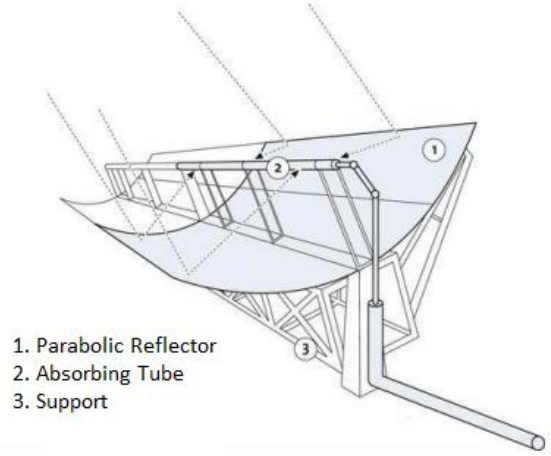

Figure 5.9 Parabolic Trough Collector

Different HTFs can be used in a PTC:

- water/vapor: it does not present any freezing problem, it's not corrosive and practically free; on the other hand, it leads to a high pressure inside the tube and to a difficult temperature control, water systems are not suitable for high working temperatures
- diathermic oil: very low freezing point (12-20°C), high thermal stability in the working temperature range, as well as low viscosity and no corrosive; on the other hand, it allows to reach a maximum temperature of 400°C, it's toxic and it forces to work at low pressures to avoid evaporation at working temperatures
- molten salts in binary mixtures (%m/m: 60% $NaNO_3$ and 40% KNO_3) or tertiary mixture such as Hitec and Hitec XL: they allow to work at low pressures and reach higher temperatures (600°C), they're cheap and not toxic; on the other hand, they have a very high freezing point that leads to an extreme difficulty to control it during night time
- carbon dioxide or other gases, only for experimental studies and prototypes.

The heat generation term has been computed as follows:

$$S = G_{b,a} \cdot \rho_n \cdot \gamma_n \cdot (\tau\alpha)_n \cdot IAM_{\rho\gamma\tau\alpha}$$

Where $G_{b,a} = G_{bn}\cos(\alpha_L)$ is the beam irradiance on the aperture area with α_L the aperture angle on the longitudinal plane, ρ_n is the mirror reflectivity with G_{bn} normal to the aperture, γ_n is the intercept factor with G_{bn} normal to the aperture defined as the ratio between the intercepted and reflected radiation, $\tau\alpha$ product with G_{bn} normal to the aperture and $IAM_{\rho\gamma\tau\alpha}$ the overall incident modifier.

CSPs are only able to absorb beam incident radiation but, being equipped with a sun tracking system, they are able to be perpendicular to the sun rays, being the radiation every hour normal to the collectors' surface. That's why, in order to compute the useful heat, the Direct Normal Irradiance (DNI) will be taken into account. DNI values of year 2014 of Valparaiso have been extrapolated from Chilean *Ministerio de Energía* website.

It's easy to notice from the values of the normal irradiance that while during summer months an appreciable radiation is reported for every daily hour (from 7 a.m. to 7 p.m.), for what concerns the winter season, cloudy days are much more frequent and the effective radiation captured by the collectors (that is only the beam one) is often 0 even during daily hours, not being the panel able in collecting the diffuse radiation. That brings to a winter scenario much more unfavorable than the case of flat plate collectors when, despite the incident radiation is lower, the panels can capture an appreciable amount of sun rays, being able to exploit diffuse irradiance.

To perform the calculations, the following values have been adopted:

- α_L equal to 25°
- ρ_n equal to 0,95
- γ_n equal to 0,95
- $(\tau\alpha)_n$ equal to 0,92 being τ 0,97 and α 0,95
- $IAM_{\rho\gamma\tau\alpha}$ equal to 0.7
- U_L equal to 1,50 $W/_{m^2K}$

- Considering that the aperture width (a) of the majority of collectors amounts to approximately 6 m and the module length (l) is between 12 and 14 m [32], the aperture area A_p has been calculated using the following formula (considering a module length of 12 m):

$$A_a = a \cdot l = 72\ m^2$$

- C_r equal to 66
- T_{fi} equal to 290°C
- F_R expressed as: $F_R = \frac{\frac{\dot{m}}{A_p} c_p}{U_L}\left[1 - \exp\left(-\frac{U_L \cdot F'}{\frac{\dot{m}}{A} c_p}\right)\right]$ that will assume two different values depending on the scenario

Differently from the case of plate collectors where it has been obviously considered that high temperature heat is generated by burning biodiesel, in this case concentrating panels are able to provide the process with the entire energy demand: it can heat up the working fluid up to 550°C, thus satisfying the high temperature demand, but the fluid can also be cooled down to the lower operating temperatures of the process (around 60°C).

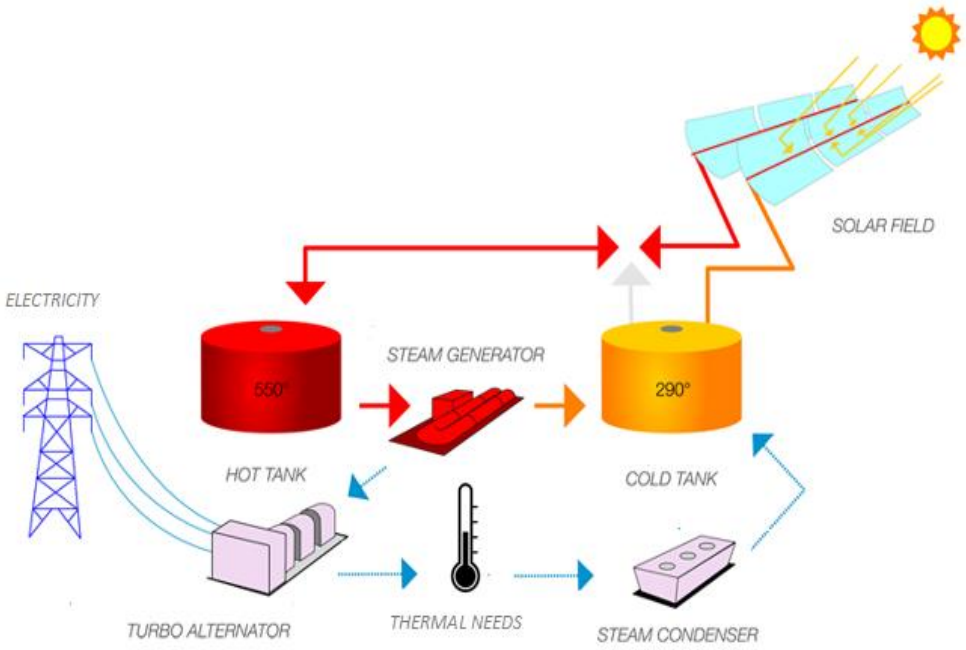

Figura 5.10 CSP + steam turbine scheme

In the present study it has been considered that molten salts are the heat transfer fluid which passes into the absorber and that is stored in apposite tanks. The energy content of molten salts will necessarily have to be transferred to water that undergoes a phase change: the vapor will then be expanded in a steam turbine with the following electricity generation.

The thermal needs will be satisfied by making three different bleedings at different operating temperatures and pressures. A simplified scheme for a condensation and derivation steam turbine is shown below:

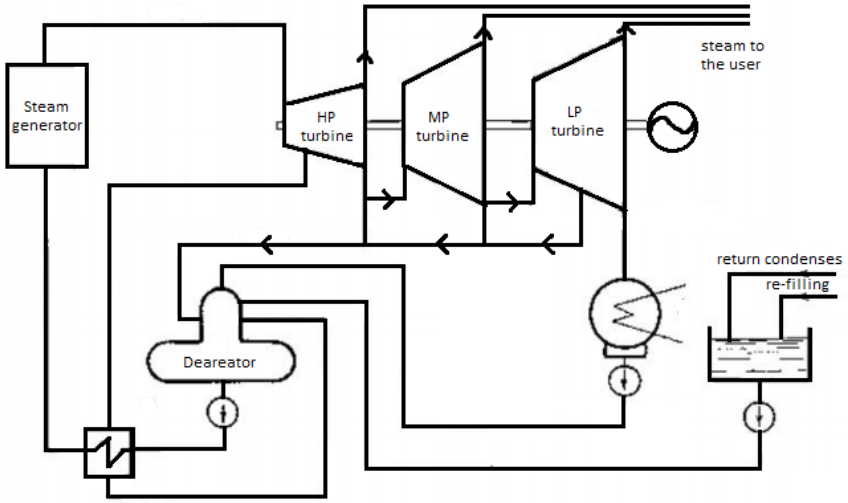

Figure 5.11 Condensation - derivation steam turbine scheme

Process thermal need has been classified into four temperatures range: 320°C, 240°C, 130°C and 65°C to provide heat at 319°C, 233°C and 182°C, 125°C and 60°C after opportune thermal degradation. In the present study has been considered a three bleedings configuration to satisfy the first three thermal needs, the last one will be then satisfied by using the condensation heat at 65 °C. Water T-s diagram has been precisely shown in the following graph:

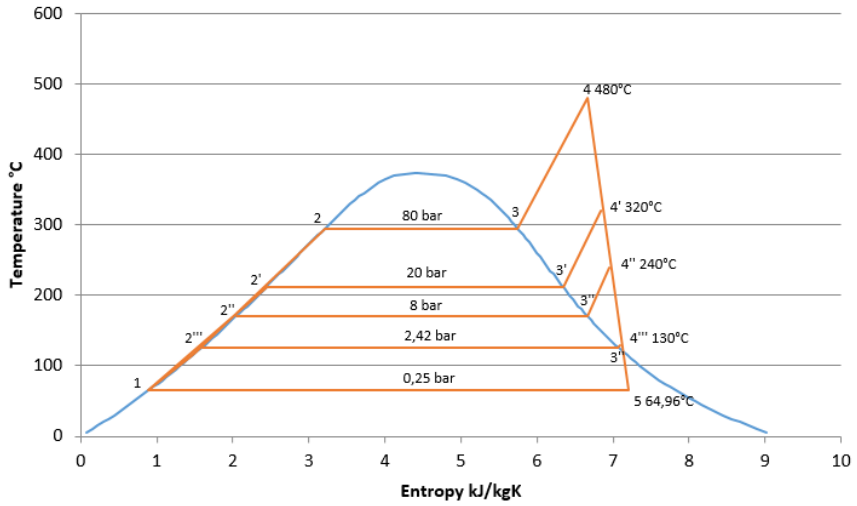

Figure 5.12 T-s diagram of steam turbine

Where the maximum vapor temperature (TIT) has been supposed equal to 480°C, making water heat up at a pressure of 80 bar. All the other pressures have been supposed in order to obtain vapor at the required temperatures: the three bleedings will be at a pressure of 20 bar, 8 bar and 2,42 bar while condensation pressure is set at 0,25 bar.

		Temperature [°C]	Pressure [bar]	Enthalpy [kJ/kg]	Entropy [kJ/kgK]	Vapor fraction
	1	64,96072	0,25	271,9147	0,893088	0
	1_pump	65	1	272,1306	0,8935	0
	2	295,0202	80	1317,142	3,207651	0
	3	295,0087	80	2758,611	5,744849	1
	4	480	80	3347,675	6,6586	1
	5	64,96328	0,25	2407,761	7,21	0,910602
I bleeding	2'	212,5881	20	908,5907	2,447024	0
	3'	212,3839	20	2798,384	6,339164	1
	4'	320	20	3068,941	6,8452	1
II bleeding	2''	170,3805	8	721,0272	2,045989	0
	3''	170,4132	8	2768,302	6,661542	1
	4''	240	8	2900,825	6,94311	1
III bleeding	2'''	126,1815	2,42	530,8164	1,595852	0
	3'''	126,3455	2,42	2715,003	7,063256	1
	4'''	130	2,42	2729,805	7,1	1

Table 5.7 Working physical conditions of steam turbine

Initial step of the analysis is calculating the amount of heat that must be provided at the different temperatures. The following simplifications have been taken into account:

- the entire low temperature heat is given at 60°C
- T-FAME heat is divided into 33% at 319°C, while the rest at 233-182°C
- T-GLYCEROL heat is divided into 50% at 233-182°C and 50% at 125°C
- T-METHANOL heat is entirely provided at 125°C

Once having obtained how much heat has to be given at every temperature, it has been computed the mass flow rate of vapor necessary to provide that heat, assuming an HX efficiency equal to 100% and a condenser efficiency equal to 95%.

As already seen in the plate collectors' situation, more than one configuration can be assessed even with CSPs. Two configurations will be considered:

- the first one aimed at satisfying the thermal load during summer months by means of daily storage tanks; during winter time and in all those cases in which solar plant is not enough to give the required energy, conventional boilers will be used
- the second one which sees the implementation of a seasonal storage tanks where all the surplus thermal energy produced during summer months, must be released during winter months

I Scenario

According to the first scenario with a biodiesel production of 1042 kg/h, the following heat proportion and relative mass flow rate of water have been computed:

- 163,12 kW must be provided at 319 °C by means of 0,075 kg/s of vapor
- 443,01 kW must be provided at 233-182°C by means of 0,205 kg/s of vapor
- 246,83 kW must be provided at 125 °C by means of 0,114 kg/s of vapor
- 48,122 kW must be provided at 60°C by means of 0,024 kg/s of vapor

A total amount of steam has been computed equal to 0,418 kg/s. In order to get the salt mass flow rate inside the solar panel and the total water undergoing the process, it has been imposed a minimum turbine power of 1 MW_{el} (that is the minimum power size of steam turbine): steam flow rate has been put equal to 1,264 kg/s and salt flow rate has been computed as 9,583 kg/s, which generates a thermal power of 3886,76 kW, assuming an HX efficiency of 100%, and makes water pass from saturated liquid at 65°C to superheated vapor at 480°C. Since the amount of vapor passing in the condenser is higher than the one

necessary to provide heat at 65°C, a portion of this thermal energy will be lost in the environment without any use.

The CSP plant will be able to produce both thermal and electrical energy. The gross electricity generated is computed as follows:

$$P_{el1} = 1{,}264 \cdot (h_4 - h_{4'}) = 352{,}25\ kW$$

$$P_{el2} = (1{,}264 - 0{,}075) \cdot (h_{4'} - h_{4''}) = 199{,}76\ kW$$

$$P_{el3} = (1{,}264 - 0{,}075 - 0{,}205) \cdot (h_{4''} - h_{4'''}) = 168{,}14\ kW$$

$$P_{el4} = (1{,}264 - 0{,}075 - 0{,}205 - 0{,}114) \cdot (h_{4''} - h_{4'''}) = 279{,}83\ kW$$

With a total of 1000 kW_{el} against the 1187,83 kW_{el} if no steam bleedings were performed.

Therefore, the solar plant has been simulated considering a salt flow rate evolving in the absorber equal to 9,58 kg/s.

Considering the first configuration, 100 solar panels, each one with an aperture area of 72 m^2, have been selected, so that they're able to fully satisfy thermal needs during January, February, November and December, while requiring an additional help from conventional boilers for March and October. That choice has been made because with an increasing number of collectors the thermal energy in excess during the 4 months would be considerable. With this configuration, both March and October present an energy lack of around 31 MWh that must be provided by burning around 3 ton of biodiesel for each month. While for winter months the situation is described in the above table.

	FUEL NECESSARY TO SATISFY THE LOAD [kg]
APR	5245,3063
MAY	24314,742
JUNE	26258,612
JULY	26854,78
AUG	22302,634
SEP	16683,113
	121659,19

Table 5.8 Fuel consumed during winter months for 650 collectors' configuration

Daily storage is designed to store a thermal energy of around 25 MWh, that is the highest excessive energy that could be generated throughout the year. Molten salts storage capacity has been computed as follows:

$$\frac{Q}{V} = \frac{c_p \cdot (550 - 290) \cdot \rho}{3600} = 0{,}18928 \ \frac{MWh}{m^3}$$

Where c_p of molten salts has been put equal to 1560 $\frac{J}{kgK}$ and ρ equal to 1680 $\frac{kg}{m^3}$.

The calculations brought to the need to install a 132,08 m^3 storage tank.

The second configuration sees the implementation of a molten salt seasonal tank: the idea is that all the surplus thermal energy produced during summer time is stored as molten salts at around 550°C to be used later one during winter time be means of the same steam turbine. A configuration with 113 panels have been accounted for, since the system is able to store 1043,42 MWh during summer season that become 939,08 MWh considering a 10% of thermal losses, while it requires an amount of 936.12 MWh during winter months. In such a situation, a 5512,59 m^3 storage tank is required (with a height of 12 m and a diameter of around 24 m), but no diesel has to be burned (except for remote cases).

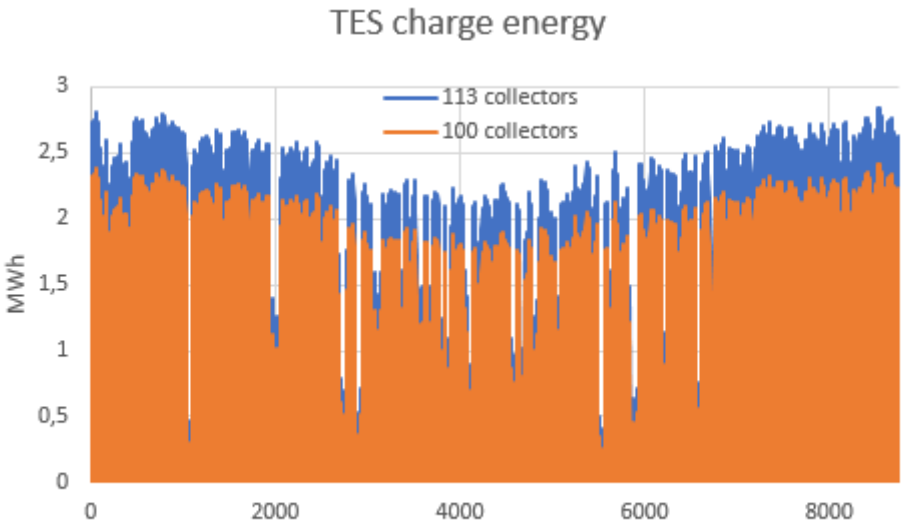

Figure 5.13 Heat captured by the two configurations for I scenario

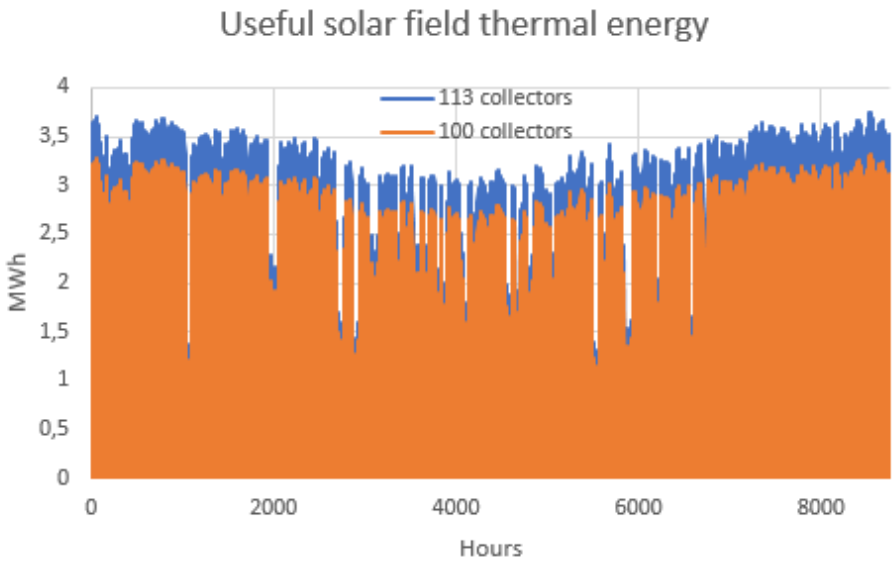

Figure 5.14 TES charge energy for the two configurations for I scenario

II Scenario

Looking at the second scenario and performing the same calculations as before, the following values have been got:

- 978,74 kW must be provided at 319 °C by means of 0,453 kg/s of vapor
- 2658,09 kW must be provided at 233-182°C by means of 1,23 kg/s of vapor
- 1480,98 kW must be provided at 125 °C by means of 0,685 kg/s of vapor
- 289,15 kW must be provided at 60°C by means of 0,142 kg/s of vapor

For a total steam flow rate of 2,511 kg/s. In this case, it has been done the simplification by considering that the steam undergoing the process can exactly be the one required, since it brings to a reasonable steam turbine power size. Salt flow rate has been computed equal to 19,04 kg/s, leading to a thermal energy of 7724,16 kW. CSP electrical turbine will generate 1233,59 kW_{el} compared to the 2360,57 kW_{el} if the entire steam flow rate expands in the

turbine. Actually, the steam evolving in the process must be slightly higher considering the bleedings from the turbine towards the deaerator.

The solar plant has been simulated considering a salt flow rate of 19,04 kg/s.

For the first configuration, 600 panels have been implemented. As the previous case, only for March and October an addition thermal power must be supplied by burning fuel: a total of 17 ton of biodiesel are necessary for every month. Daily storage has been designed in order to be able to store around 150 MWh of thermal energy, so that a 740 m^3 tank must be used. The following fuel will be then needed to satisfy the load during winter months, leading to a total fuel consumption of 725 tons.

	Fuel necessary to satisfy the load [kg]
APR	30603,37
MAY	145168,1
JUNE	156840,9
JULY	160432,1
AUG	133054,1
SEP	99315,48
	725414,1

Table 5.9 Fuel Consumed during Winter Months

According to the second configuration, 677 panels are supposed to be the best situation. They will be able to store a seasonal thermal energy of 6284,9 MWh (equal to 5656,42 MWh if losses are considered), out of the 5592,21 MWh demanded during winter season.

A seasonal tank equal to 33204,29 m^3 is necessary. The tank could have the following dimensions: a height of 25 m and diameter of around 42 m.

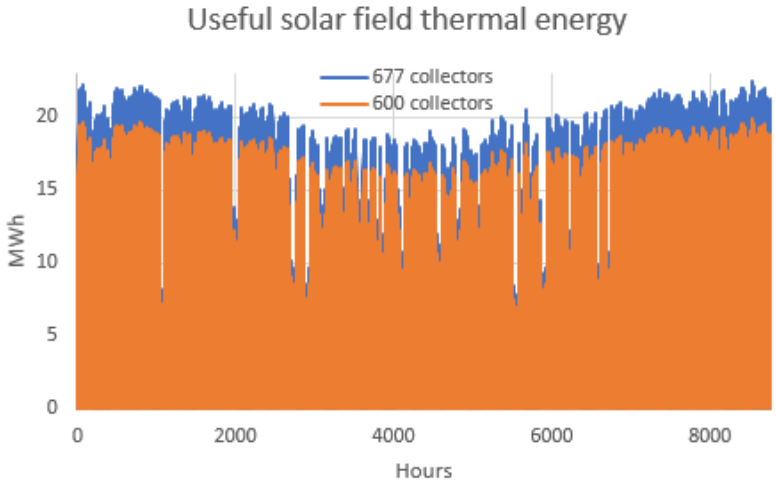

Figure 5.15 Heat captured by the two configurations for II scenario

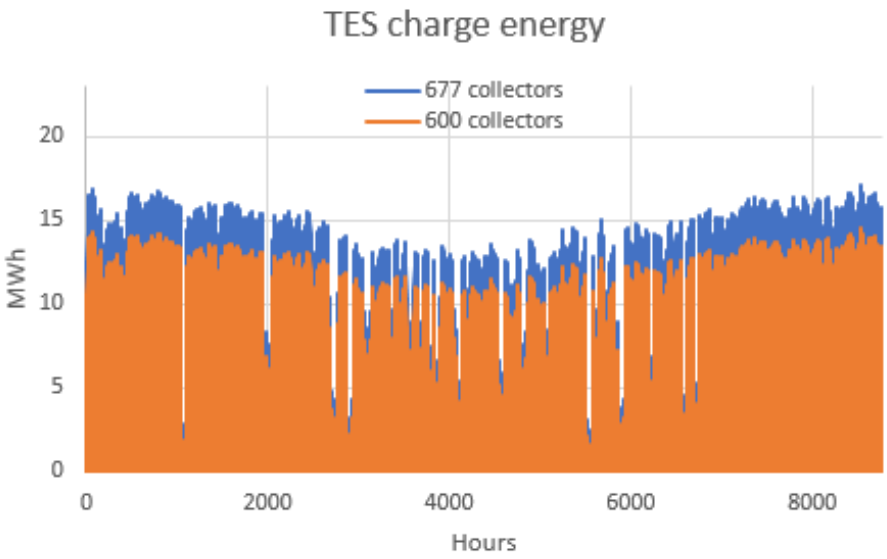

Figure 5.16 TES charge energy for the two configurations for II scenario

Chapter 6

Economic Analysis

Last step of the present work is performing an economic analysis aimed at evaluating the costs affecting the transesterification process as well as the technologies providing thermal energy. The latter step is performed to see which configuration is affected by the lowest costs, that, thus, can be considered the best solution to provide the process with the required thermal energy.

The economic analysis, besides obtaining Investment and O&M costs, will be essentially based on the calculation of the following values:

- NPV (Net Present Value) that is defined as the difference between the present value of cash inflows and the present value of cash outflows over a period of time; it is used in capital budgeting to analyze the profitability of a projected investment or project. Defined as:

$$NPV = \sum_{t=1}^{T} \frac{C_t}{(1+r)^t} - C_0$$

  Where C_t is the net cash inflow during period t, C_0 is the total initial investments cost, r the discount rate and t the number of time periods.

  A positive net present value indicates that the earnings generated by a project or investment exceeds the anticipated: generally, an investment with a positive NPV will be profitable, and an investment with a negative NPV will result in a net loss.
- IRR (Interest Rate of Return) that is a metric used in capital budgeting to estimate the profitability of potential investments; it is essentially a discount rate that makes the net present value (NPV) of all cash flows equal to zero. The higher a project's internal rate of return, the more desirable it is to undertake.
- PBP (Pay Back Period) that is the time required to recover the cost of an investment. The payback period of a given investment or project is an important determinant of whether to undertake the position or project, as longer payback periods are typically not desirable for investment positions.

Before going through a mere economic study, the following considerations will be taken into account:

- The only conventional technology that will be studied for I scenario is a biodiesel boiler, that is considered as the "base-case" of the present simulation. It limits to burn part of the biodiesel produced to supply energy to the process. An important drawback is the need to buy electricity from the national grid.
- In order to avoid excessive thermal losses, neither gas turbines nor steam turbines will be studied for 1042 kg/h biodiesel scenario, since they cannot be designed at such a low power range (less than 1 MW_{el}). The only apparently suitable technology is the internal combustion engine, but its use would require 40% of the total biodiesel produced by the plant every hour, a value definitively too high to be economically affordable. No conventional cogeneration technology will be studied for thermal provision of 1042 kg/h of biodiesel.
- Both gas turbines and steam turbines are feasible solutions in providing the necessary heat to the 6200 kg/h biodiesel scenario. To avoid thermal losses as much as possible, both the technological configurations are designed to recover only high temperature heat (from 320°C to 125°C), while heat at 65°C will be supplied by means of apposite heat pumps. The two technologies mainly differ for the amount of necessary fuel, which corresponds to 19,16% in the former case and 12,21% in the latter one.
- Flat plate collectors will be studied for the three different configurations proposed and for the two scenarios, where high temperature heat can be supplied by means of a conventional cogeneration technology to generate electricity too (gas or steam turbine), or by simply burning biodiesel in a boiler.
- CSP configuration is the only configuration where low temperature heat, high temperature heat and electricity can be supplied with a unique technology. For this reason, the present plant appears to be the most energetically-wise, but on the contrary, it will show considerable costs related to the particular type of technology. It will be studied according to the two different cases for each scenario.

For what concerns conventional technologies such as conventional boiler, Gas and Steam Turbines, the following values have been accounted:

Plant Lifetime	25	years
Inflation Rate OPEX	0,5	%
Discount Rate	8	%
Tax Rate	40	%
Ammortization	12	years
Construction Time	2	years
Investment Costs Split	0,55	first year
	0,45	second year
Fuel Price	1,5/1,3	USD$/L
Electricity Price for Selling	0,08	USD$/kWh
Electricity Price for buying (only boiler)	0,13	USD$/kWh

Table 6.1 Economic Values for Conventional Technologies

Economic Analysis of the Transesterification Process

The following analysis has been conducted in order to evaluate which are the costs that affect the process and thus calculate the Net Present Value and the Pay Back Period of the plant. For the only present case study, the economic evaluation has been performed by using Aspen Plus, the same software used to simulate the entire process. In fact, Aspen Plus presents an economic division called Aspen Process Economic Analyzer (APEA), which is able to evaluate all the annual costs (fixed and variable), revenues, cash flows and the net present value. The following costs have been computed:

- The *Total Project Capital Cost*: its calculation has been made possible because the software contains a database with the equipment costs of all the different devices. The total cost is composed of the following costs:

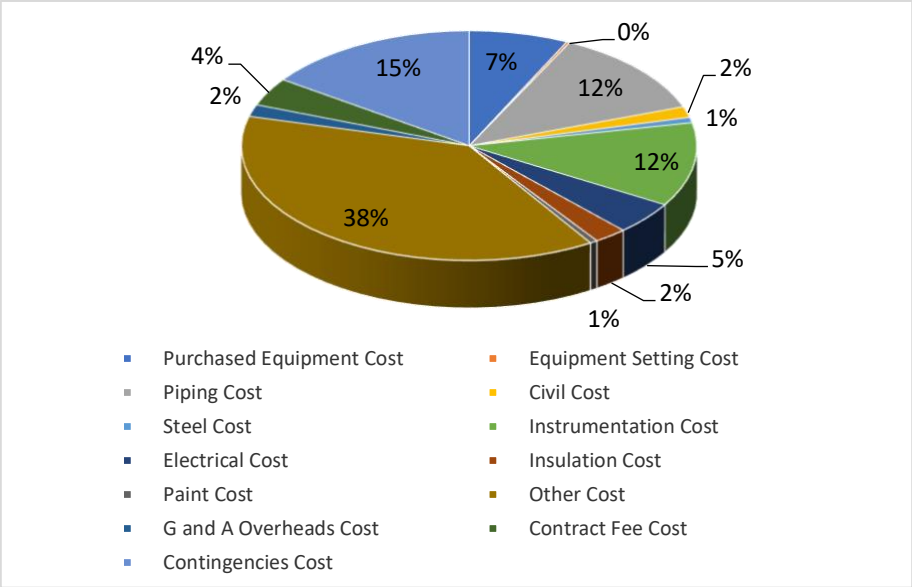

Figure 6.1 Installation Costs split for Biodiesel Process

- The *Total Operating Labor and Maintenance Cost* given by labor, maintenance and supervision.
- The *Total Operating Cost* that represents the highest contribution of the costs system: it takes into account all the costs related to the functioning of the plant.
- The *Total Utilities Cost* that refers to the use of electricity, cooling water and steam necessary to perform the different processes: electricity will be used especially to run pumps, the water inside the condensers and the steam in the distillation columns.
- The *Total Raw Materials Cost* and the *Total Products Sales Cost* have been obtained by imposing stream costs to the different materials entering the system, and to those products given by the process, as shown in the table on the right.

	USD $/kg	Reference
Cost Triolein	0,780437	[33]
Cost Methanol	0,286601	[33]
Cost KOH	0,61509	[33]
Cost Water	0,000353	[33]
Costa Acid	0,132277	[33]
Cost Glycerol	0,33	[33]
Cost FAME I SCENARIO	1,5	supposed
Cost FAME II SCENARIO	1,3	supposed

Table 6.2 Material streams costs

As it can be easily seen from the table above, the cost of biodiesel produced has been assumed at two different values: the lower price of the second scenario is essentially due to economies of scale, that is a proportionate saving in costs gained by an increased level of production (from 1042 kg/h to 6200 kg/h). In fact, by performing a fast evaluation of the costs affecting the process in the two cases, it can be demonstrated that the biodiesel cost in the first scenario is augmented by at least 10%. INSERISCI 33 REFERENCE

The software has supposed plant operating hours of 8760 hours and a lifetime period of 20 years; it assumes a 26 weeks duration for the EPC (Equipment Purchasing Cost) phase, a 20 weeks period for starting-up the plant and a 15 weeks period as the duration of construction. The calculations have been then adjusted by considering a two-years duration of the construction phase, as well as the following values:

Plant Lifetime	25	years
r inflation OPEX	3,5	%
r inflation Revenue	5	%
r interest	20	%
r tax	40	%
Construction time	2	years
Investment costs	55%	first year
	45%	second year

Table 6.3 Economic Values for the Transesterification Process

I Scenario

According to the first scenario, the following table shows the obtained cost values:

Total Project Capital Cost	USD $	9346450
Total Raw Materials Cost	USD $/year	7934620
Total Products Sales	USD $/year	13990700
Total Operating Labor and Maintenance Cost	USD $/year	865971
Total Utilities Cost	USD $/year	101651
Total Operating Cost	USD $/year	10306900

Table 6.4 Biodiesel Plant related costs for I Scenario

Where the following graph shows the PBP:

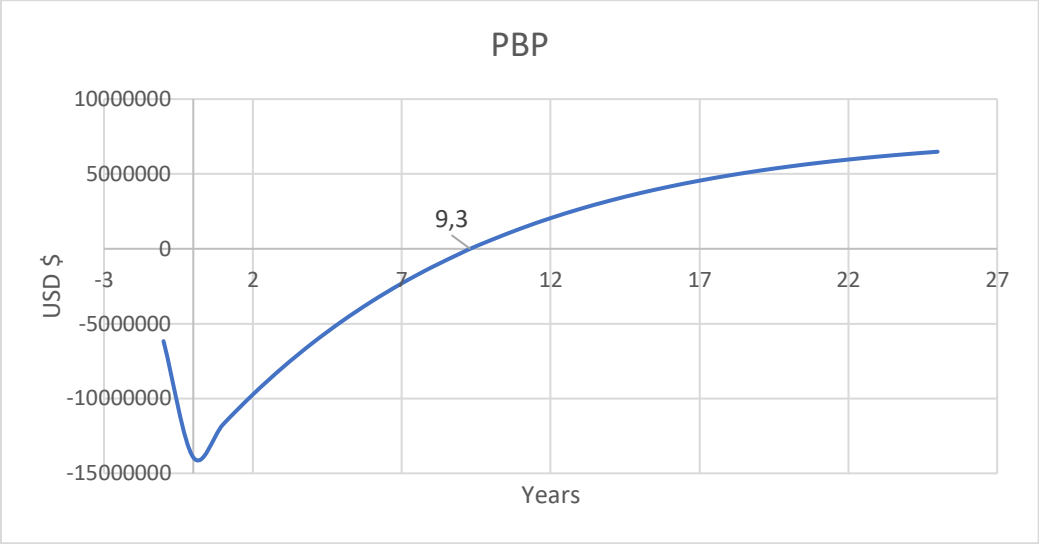

Figure 6.2 Biodiesel plant PBP for I scenario

A NPV equal to 7.514.257,53 $ and an IRR equal to 26% are obtained.

II Scenario

For what concerns the 6200 kg/h biodiesel scenario, the following costs have been computed trough APEA:

Total Project Capital Cost	USD $	11715800
Total Raw Materials Cost	USD $/year	47335000
Total Products Sales	USD $/year	72978200
Total Operating Labor and Maintenance Cost	USD $/year	899939
Total Utilities Cost	USD $/year	415699
Total Operating Cost	USD $/year	53253500

Table 6.5 Biodiesel plant related costs for II Scenario

An NPV equal to 77.757.138,20 $ and an IRR of 50% are obtained. It will be evident that NPV and IRR values for the economic analysis of the transesterification process alone are the highest one that can be reached: that is obvious considering that the evaluation does not account for the energy-providing technology that will work by increasing the costs, and thus decreasing NPV and IRR.

The economic evaluation of the two scenarios shows an evident convenience of the second configuration with respect to the first one: the process leads to the production of more biodiesel that could be sold at a lower price, and thus be more competitive in a market where fossil fuels have much lower prices. In addition, with the second scenario the plant is able to recover the investment costs in one third the time of the first one, making it far more profitable.

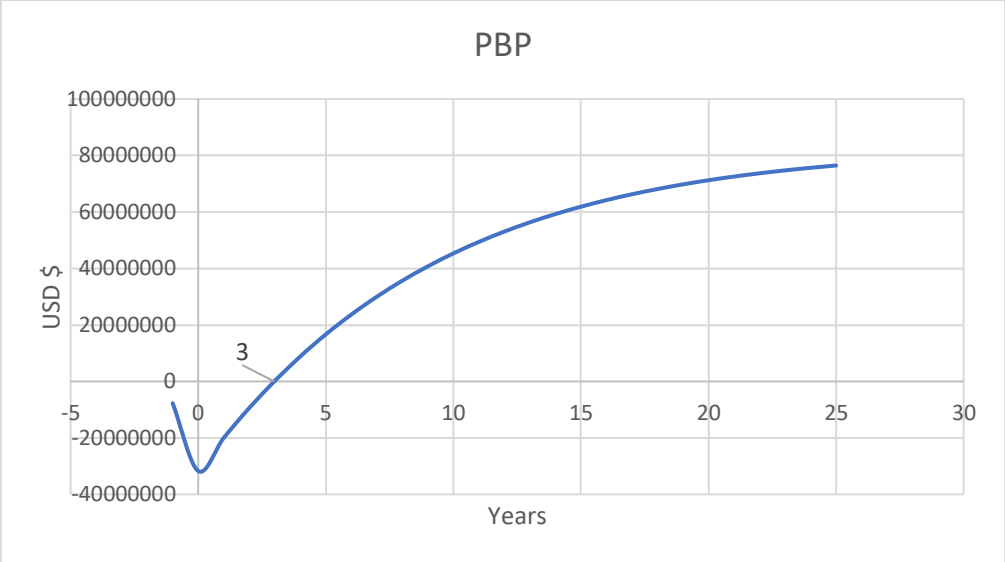

Figure 6.3 Biodiesel plant PBP for II scenario

Economic Analysis of "Base-case" with Boiler

Before going into the analysis of the cogeneration technologies that have been proposed, it will be considered the "base-case" of coupling the biodiesel process with the technology that surely appears to be the most obvious, since thermal energy is the main requirement: conventional boiler. The same economic values of gas and steam turbines will be considered, with the only exception of the need to buy electricity from the national grid.

I Scenario

A 950 kWt conventional boiler is necessary and the following values have been considered:

- An investment cost equal to 50 $/kW
- An O&M cost equal to 800 $ at which it has to be summed up the costs related to the electricity bought
- An electricity capacity that must be bought equal to 87600 kWh_{el} at 0,13 $/kWh
- An amount of burned fuel equal to 85,37 kg/h

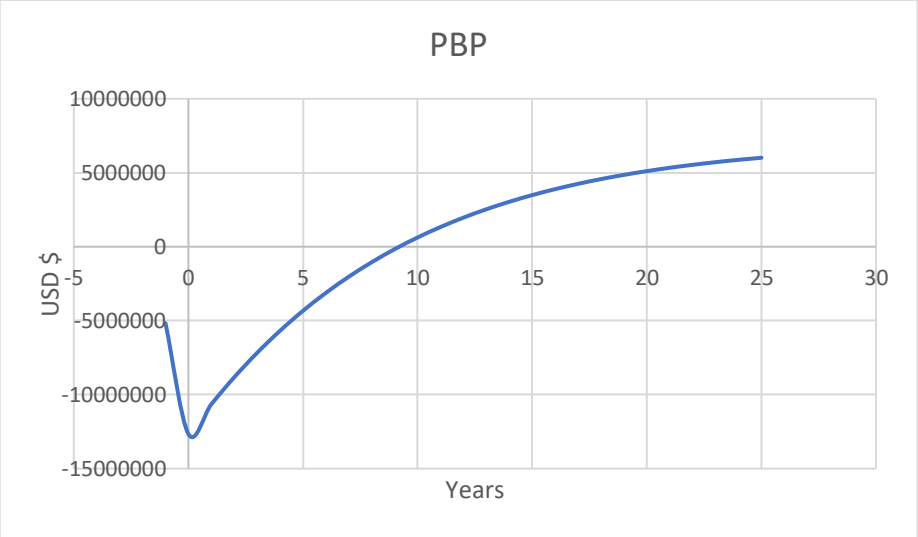

Figure 6.4 Base-case PBP for I scenario

It has been calculated an NPV of 6.014.115,87 $ and an IRR of 25%.

II Scenario

A 5500 kW_{th} conventional boiler has been supposed with the same operating values, except for the O&M cost of the boiler equal to 1500$ and the fuel burned equal to 512,24 kg/h.

A much more convenient situation is delineated with a PBP of around 3 years, a NPV equal to 70.072.942,38$ and an IRR of 48%.

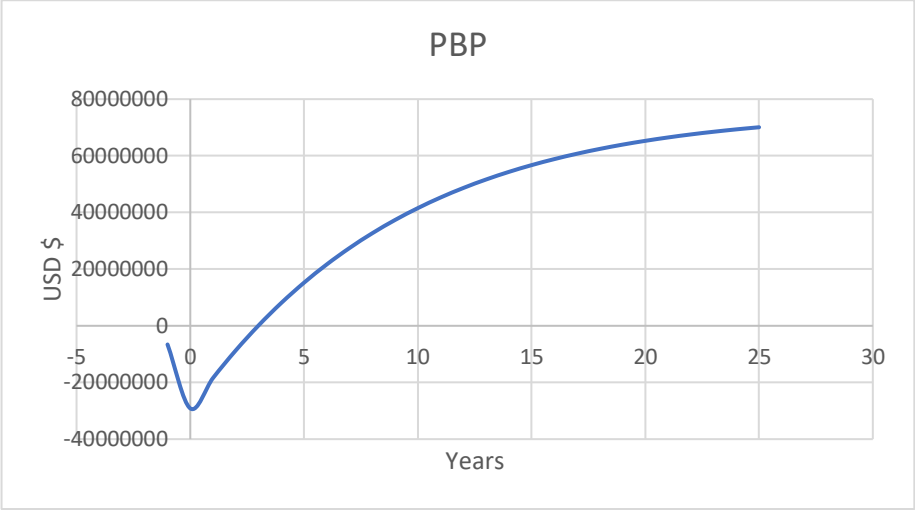

Figure 6.5 Base-case PBP for II scenario

Economic Analysis of the Integration between Biodiesel Process and Gas Turbine

To assess the costs related to the use of a 3110 kW_{el} cogeneration gas turbine, the following values have been considered:

- An investment cost equal to 2000 $^{\$}/_{kW_{el}}$ (conventional gas turbine is 1700 $/kW but the costs have been augmented considering that the present turbine must work with biodiesel and not natural gas and the combustor needs some modifications)

- An O&M cost equal to 0,01 $\$/_{kWh}$
- A total installed capacity of 27269880 $kWh/_{year}$
- A total electrical sold capacity of 26586600 $kWh/_{year}$ since the remaining energy is used to run a heat pump for low temperature purposes and for auxiliaries
- An amount of burned fuel equal to 10408 ton per year

By considering the integration of transesterification process and gas turbine, the situation is described below:

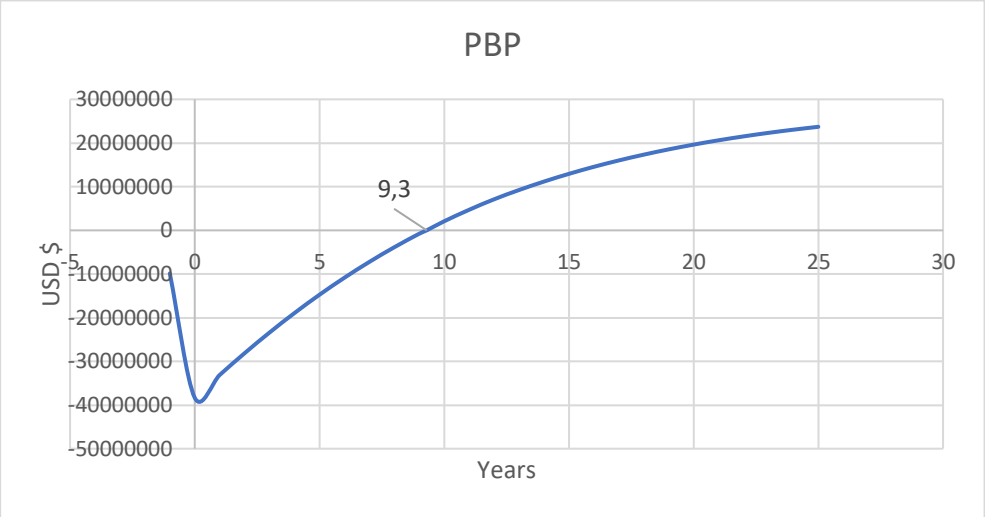

Figure 6.6 Biodiesel-gas turbine PBP

NPV equal to 23.716.292,97$ and IRR of 25%.

Economic Analysis of the Integration between Biodiesel Process and Steam Turbine

To assess the costs related to the use of a 1000 kW_{el} cogeneration steam turbine, the following values have been considered:

- An investment cost equal to 3000 $^{\$}/_{kW_{el}}$
- An O&M cost equal to 0,01 $^{\$}/_{kWh}$
- A total installed capacity of 8760000 $^{kWh}/_{year}$
- A total electrical sold capacity of 8076720 $^{kWh}/_{year}$ since the remaining energy is used to run a heat pump for low temperature purposes and for auxiliaries
- An amount of burned fuel equal to 6915,8 ton per year

Differently from the previous case, a much higher investment cost per kW_{el} installed leads to a lower total investment cost due to a lower size of the plant. In this case the situation is described by the following graphs:

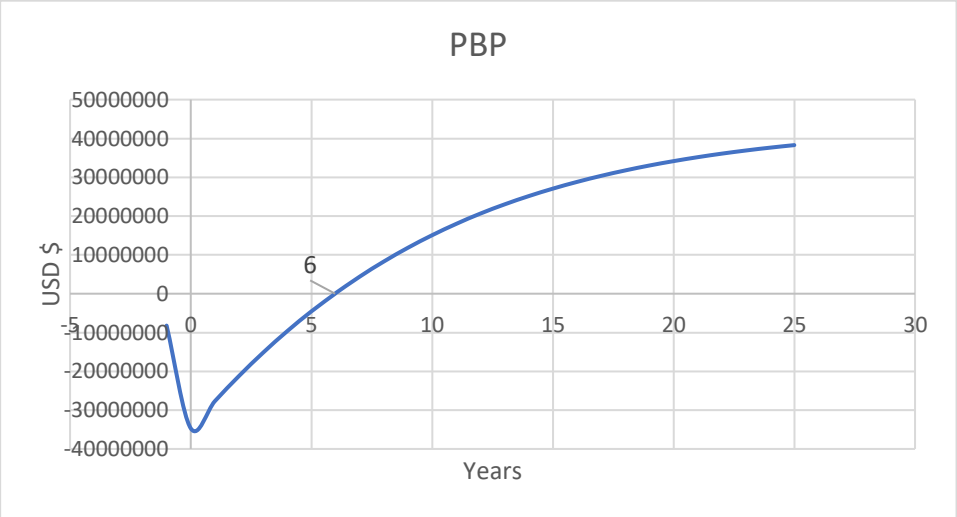

Figure 6.7 Biodiesel-steam turbine PBP

From the analysis it's immediate to notice that the integration of the biodiesel plant with a steam turbine appears to be much more profitable since the entire plant is able to recover

all the investment costs 3 years earlier than the case with a gas turbine. That is mainly due to three aspects:

- the lower investment costs of the steam turbine compared to the gas turbine, even if the former has a higher cost per unit of installed capacity
- the lower Operating & Maintenance Cost of the steam turbine since the plant is affected by a lower overall electricity capacity and less fuel is implemented
- the higher profits in the second case, as a consequence of being able to sell much more biodiesel, since a lower amount must be burned to run the turbine

NPV has been computed equal to 38.412.607,93 $ with an IRR of 32%.

Economic Analysis of the Integration Between Biodiesel Process and Solar Technologies

Plant Lifetime	25	years
Inflation Rate OPEX	3,5	%
Discount Rate	8	%
Tax Rate	40	%
Ammortization	12	years
Incentive	0,12	$/kWh installed
Construction Time	2	years
Investment Costs Split	0,55	first year
	0,45	second year
Electricity Price for Selling	0,08	USD$/kWh
Electricity Price for Buying (only for flat plate)	0,13	USD$/kWh

Table 6.6 Economic Values for Solar Technologies

For the only flat plate configuration storage the following specific costs have been considered:

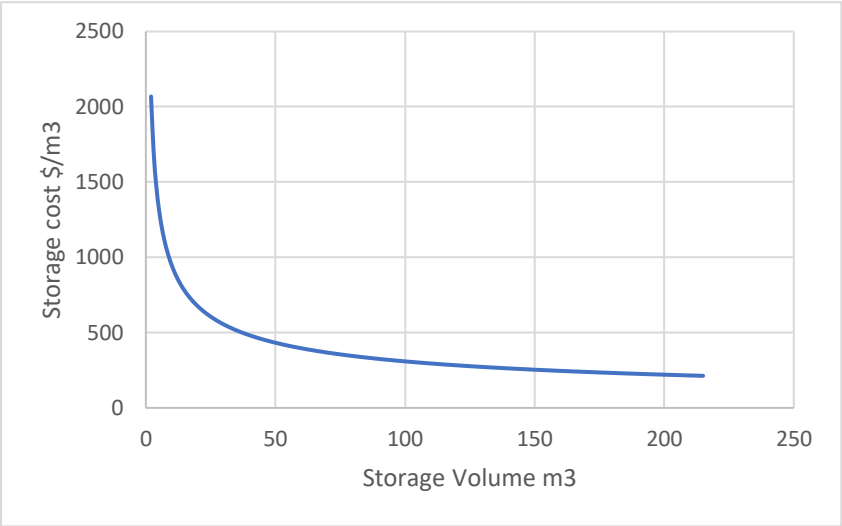

Figure 6.8 Water storage cost wrt storage volume

Economic Analysis of the Integration between Biodiesel Process and Solar Flat Plate Collectors

For what concerns the economic evaluation of solar flat plate collectors, the following values have been accounted for the two scenarios and the three different configurations:

- an investment cost of solar panels equal to 800 $/m2
- a boiler of 853 kW for the I scenario and 5200 kW for the second one
- a specific cost of high temperature boiler of 50 $/kW for I scenario and 70 $/ kW for the second one

The following table shows the situation regarding the first scenario:

I SCENARIO				
		I CONFIGURATION	II CONFIGURATION	III CONFIGURATION
A coll	m2	270	480	345
Q heat useful	kWh	335816,06	597006,33	429098,3
Fuel used	kg/h	81,78	80,81	80,81
Volume storage	m3	15	15	1176,04
Specific storage cost	$/m3	777	777	215
Cost storage	$	11655	11655	252848,6
OPEX flat+boiler+storage	$/year	2000	2000	2500
CAPEX flat+boiler+storage	$	270305	438305	571498,6
CAPEX biodiesel	$	9346450	9346450	9346450
NPV	$	**2.627.116,22**	**2.759.710,95**	**2.526.558,36**
IRR	%	**21**	**21**	**20**

Table 6.7 Flat Plate Collectors' Configurations for I scenario

From the PBP graph below it can be seen that the three configurations are very similar, it can be noted that the last configuration is the one with the lowest NPV due to the implementation of a seasonal storage tank.

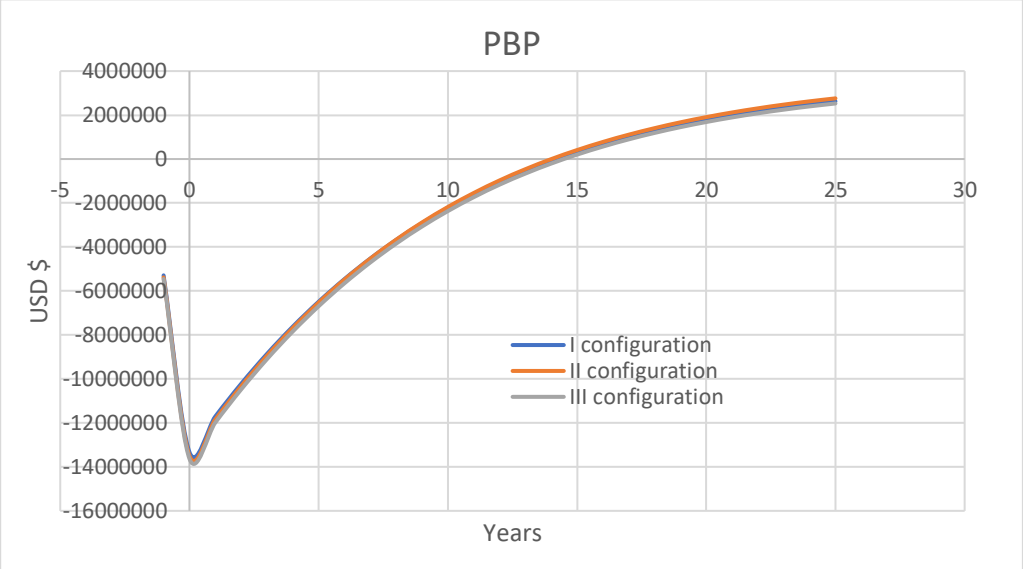

Figure 6.9 Flat plate collectors' PBP for I scenario

Regarding the second scenario the situation is described below:

		II SCENARIO		
		I CONFIGURATION	II CONFIGURATION	III CONFIGURATION
A coll	m2	1650	2880	2070
Q heat useful	kWh	2052209,2	3507412,2	2574589,8
Fuel used	kg/h	490,43	484,8	484,8
Volume storage	m3	90	85	7020
Specific storage cost	$/m3	325	335	215
Cost storage	$	29250	28475	1509300
OPEX flat+boiler+storage	$/year	2000	2000	2500
CAPEX flat+boiler+storage	$	1713250	2648475	3529300
CAPEX biodiesel	$	11715800	11715800	11715800
NPV	$	**52.681.319,56**	**53.391.041,58**	**52.010.163,70**
IRR	%	**38**	**38**	**37**

Figure 6.8 Flat plate collectors' configurations II scenario

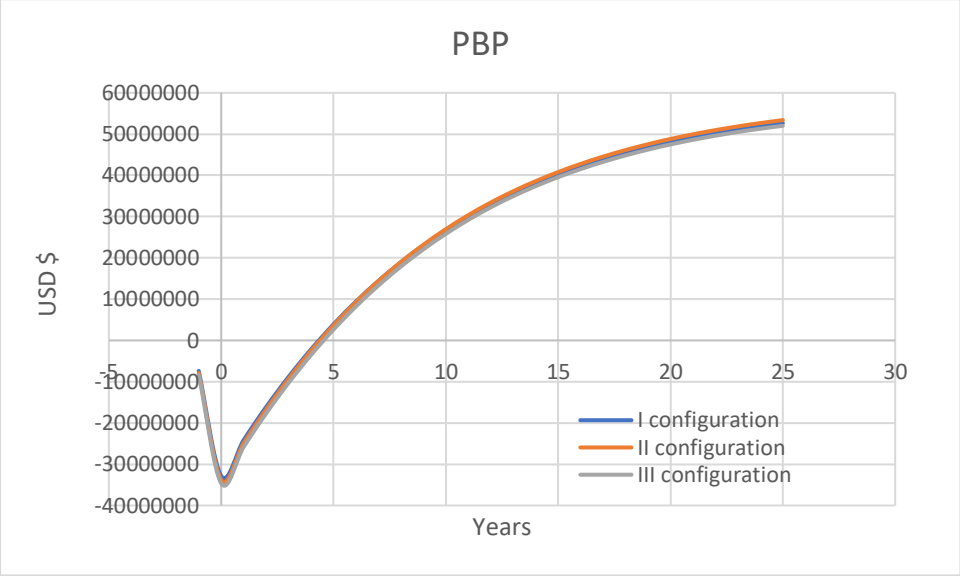

Figure 6.10 Flat plate collectors' PBP for II scenario

As predictable, the II scenario is able to recover all the investment costs in a time much shorter than I scenario.

To give completeness to the economic study, it has been supposed to couple solar flat plate collectors with gas and steam turbines in order to evaluate the behavior and compare it with collectors-boiler configuration. Before performing the simulation it's already known that the configurations will be less convenient than the boiler one, but it's worthy to assess some important differences:

- the collectors - gas/steam turbine configuration does not need to buy any electricity from the grid, being able to produce it by itself
- Revenues related to gas or steam turbines technology are higher since the plant is able to sell the surplus electricity to the grid
- An important drawback in performing such a solution is given by the much higher consumption of biodiesel produced (1203,31 kg/h for gas turbine and 789,47 kg/h for steam turbine compared to the only 490,43 kg/h with boiler configuration) that leads to a biodiesel process revenue much lower
- Obviously, in the case in which solar collectors are not able to generate the minimum thermal energy, gas or steam turbine will be used by generating themselves surplus heat and degrading it to the user temperature
- Actually, steam turbine appears to be more convenient because it was already overdesigned to give a minimum power of 1 MW, and in the present configuration it does not need to be redesigned to supply low temperature heat when solar collectors are not sufficient

From the PBP graph it's evident how the configuration that couples solar thermal collectors with steam turbine is much more suitable: the turbine stays the same, it is able to sell a lower amount of electricity, but it is affected by a quite lower capital cost and uses a definitively lower amount of biodiesel, allowing to sell a higher amount of fuel. The NPV of the I configuration is 23.316.955,49 $ with an IRR of 24%, while NPV for steam turbine is 39.091.641,00 $ with an IRR of 31%.

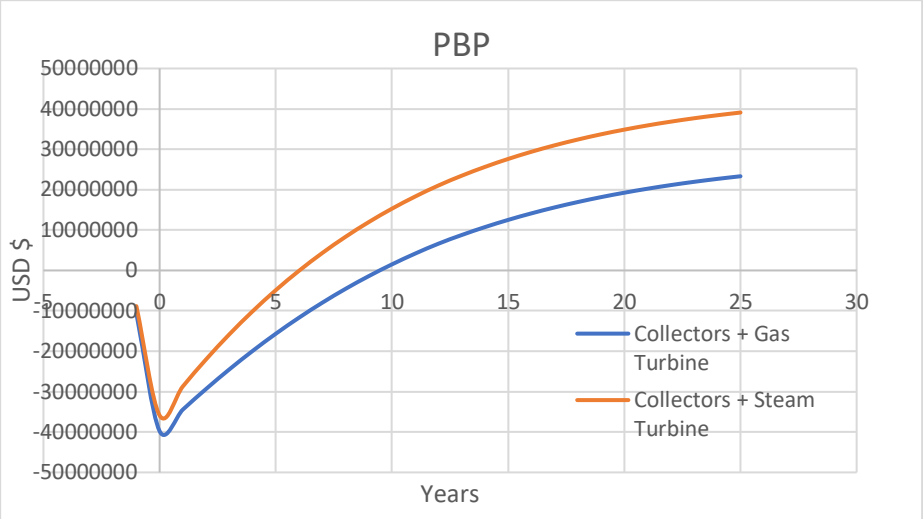

Figure 6.11 Flat plate collectors-gas/steam turbine PBP

Economic Analysis of the Integration Between Biodiesel Process and Concentrating Solar Panels

Last step of the economic analysis is the evaluation of all those variables related to the implementation of CSP technology. Before going in the economic evaluation, it's important to say that CSP currently requires much higher capital investments than the other energy sources, especially in a country like Chile where the technology is not mature and there are no real providers. What it's expected to obtain is a scenario not so convenient where the installation costs are paid back in many years.

The only constant value in the evaluation is the O&M costs equal to 0,04 $/kWh[34], because the investment costs have been differentiated for every configuration considering that:

- In the same scenario, the first configuration has a unique value of investment cost, that includes a storage of maximum 15 hours, while the second one has a value referred to the only CSP system and another value referred to the seasonal storage
- The same configurations exhibit different values of investment costs because the costs of the II scenario have been decreased considering savings coming from economies of scale.

The total installed costs of a Parabolic Trough technology are split as follows:[34]

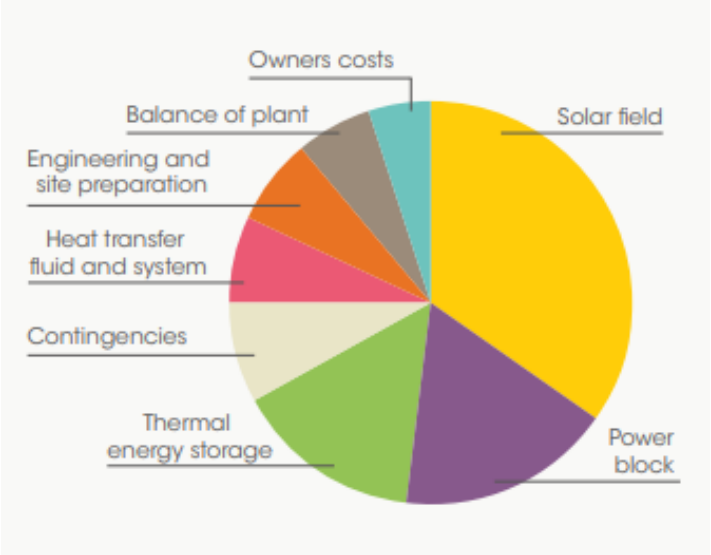

Figure 6.12 Installation costs split for CSP technology

		I SCENARIO	
		I CONFIGURATION	II CONFIGURATION
P el	kW	1187,83	1187,83
Q heat useful	kWh/year	7087455,834	8008825,093
Fuel used	kg/h	14,55	0
Capacity sold	KWh	8672400	8672400
Investment cost CSP[34]	$/kWh	11000	10500
Investment cost storage	$/m3	-	300
CAPEX CSP	$	13066130	15779768,4
CAPEX 2 seasonal storages	$	-	3307553,4
CAPEX biodiesel	$	9346450	9346450
NPV	$	**3.127.960,62**	**2.662.978,85**
IRR	%	**18**	**17**

Figure 6.9 CSP Collectors' Configurations for I scenario

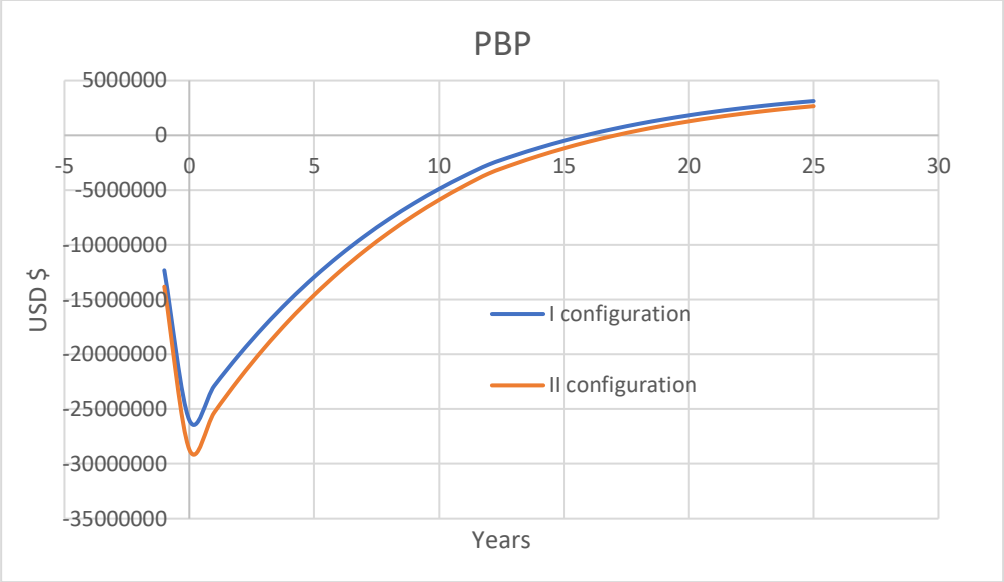

Figure 6.13 CSP Collectors' PBP for I scenario

		II SCENARIO	
		I CONFIGURATION	II CONFIGURATION
P el	kW	7126,98*	7126,98*
Q heat useful	kWh/year	42592035,33	48058013,2
Fuel used	kg/h	86,6	0
Capacity sold	KWh	10718648,4	11668811
Investment cost CSP	$/kW	10800	10400
Investment cost storage	$/m3	-	290
CAPEX CSP	$	76971384	93379080,2
CAPEX 2 seasonal storages	$	-	19258488,2
CAPEX biodiesel	$	11715800	11715800
NPV	$	**26.327.333,48**	**16.144.489,94**
IRR	%	**21**	**19**

Figure 6.10 CSP Collectors' Configurations for II scenario

* actually, the electric power of the II scenario steam turbine is much lower because there's no need to produce such an electrical output, but to have a clear idea of the economic variables it has been supposed as if the turbine is 6 times the one of the I scenario. That is

due to the fact that the investment cost of the CSP plant is referred to the electricity output, and the calculations must be carried out considering a normal CSP plant where the aim is electricity production and not thermal energy.

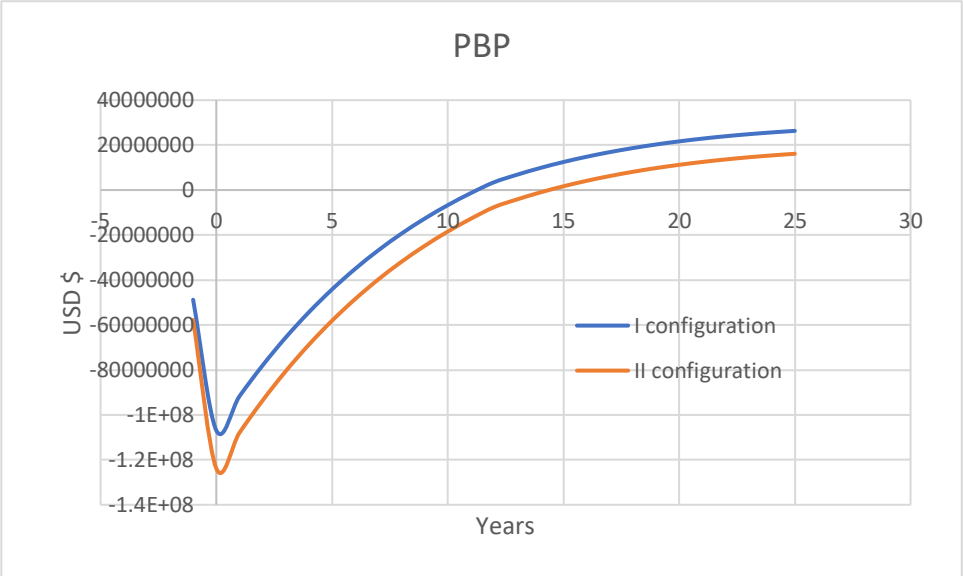

Figure 6.14 CSP Collectors' PBP for II scenario

Chapter 7

Conclusions

The present work is born as a way to exploit the multitude of macro-algae that every year settle on Chilean sea shores. In fact, Chile is experiencing consistent problems related to algae accumulation: they inhibit tourism and require a big cost effort for collection and disposal. In the only year 2011 more than 415 thousand tons of macro-algae have been found of Chilean beaches, from the very North part of the country to the regions of lakes at the South. That brought population to introduce macro-algae in the alimentation: in fact, *Durvillaea Antarctica*, commonly known as *Cochayuyo*, is largely consumed all over the country for its richness in nutrients and vitamins. But an advantageous way in exploiting the high energy potential of macro-algae is by converting them into biofuels, i.e biogas or biodiesel.

This paper particularly focuses on the conversion of oil extracted from macro-algae into FAME (Fatty Acid Methyl Esters, biodiesel) by means of a transesterification process. Two scenarios have been considered: the first with a biodiesel production of 1042 kg/h and the second with 6200 kg/h. The process, simulated using Aspen Plus, took into account the oil-biodiesel conversion step as well as methanol recovery and FAME and glycerol purification steps. That was due to the need of calculating the energy consumption demanded by the entire process, in order to find possible solutions in providing that energy. In fact, the majority of biodiesel-generating plants, makes use of fossil fuel based technologies to provide the process with the necessary thermal energy. Main objective of the present study is to suggest alternative solutions that may get rid of fossil fuels dependence and make the process as green as possible.

As a matter of fact, cogenerative solutions such as ICE, gas turbine and steam turbine have been proposed that make use of the same biodiesel produced in loco; they rely on the general assumption of making the plant self-sustainable by producing electricity too. For I scenario, the only suitable technology was the ICE, but it has been discarded because of the high consumption of biodiesel. For what concerns the II scenario, ICE has not been considered because it would generate an over production of electricity and it is more suitable for low power ranges, while both cogenerative gas and steam turbines have been accounted. It has

been supposed to provide only high temperature heat and ensure low temperature needs by using heat pumps: a 3.1 MW_{el} gas turbine while a 1 MW_{el} steam turbine will be necessary, leading to a biodiesel consumption respectively of 19% and 12,7% of the total produced.

In addition, solar technologies have been supposed with the aim of exploiting the high solar potential of V region and providing the plant with clean and sustainable energy. Two solar technologies have been considered: flat plate collectors for the only low-temperature heat and CSP technology for the supply of the entire thermal need as well as electricity.

Regarding solar collectors' configuration, three scenarios have been proposed: the first one aimed at ensuring thermal needs during summer season, the second one aimed at totally supplying thermal need during both summer and winter season, while the last one which includes the implementation of a seasonal storage tank to store surplus thermal energy during summer months and release it during winter months. A configuration with respectively 90, 160 and 115 panels have been proposed for I scenario and 550, 940 and 690 for the II one.

Regarding CSP solution, two scenarios have been followed: the first one aimed at satisfying the thermal load during summer season, while the second one with molten salts seasonal tanks to guarantee a complete supply. A configuration with respectively 100 and 113 panels have been obtained for I scenario and 600 and 677 for the II one.

Third step of the present study have been the economic analysis of the different configurations proposed. At all the scenarios, a "base-case" with conventional boiler providing thermal energy has been added, just to have a comparison term: obviously, it showed the highest NPV, being the technology the cheapest and most consolidated one for the present purpose. Gas and steam turbines configurations showed respectively a NPV equal respectively to one third and half of the base-case, and will be paid back in 9 and 6 years while the base-case recovers its costs in less than 3 years. The configuration with solar collectors showed a maximum of NPV equal to 2.759.710,9 USD $ for the I scenario with a reduction of almost 63% with respect to the base-case. On the other hand, for what concerns II scenario, the maximum achievable NPV is 53.391.041,58 USD $, with a reduction of 30% with respect to the base-case. Integration scenarios with solar collectors and gas or steam turbines have been also analyzed: the integration with gas turbine lead to a NPV slightly

lower than only-turbine configuration, while the collectors-steam turbine integration brought to a NPV of 39.091.641 USD $, higher than the only-steam turbine configuration. That is mainly due to the fact that there's no need of oversizing the turbine (being already oversized in the stand-alone case), the plant can sell almost the entire electricity generated (not having to run a heat pump) and being solar collectors a renewable technology, they benefit from national subsidies. Eventually, economic evaluation of CSP technologies have been performed: even if it seems to be the most suitable configuration, being able to provide the process with all the required energy inputs, it resulted to be the least convenient in terms of NPV and IRR. The plant would recover its initial costs in 17 years for the I scenario and in 12 and 15 years for the I and II configuration in the II scenario. That is mainly due to the fact that in Chile this technology is not yet mature and there are no suppliers.

For what concerns I scenario, the general aim of getting rid of fossil fuels and exploiting renewable solar source has been found in solar collectors-conventional boiler configuration, having a NPV equal to 2.759.710,95 USD $.

Even for II scenario, the economic evaluation suggested that the optimal scenario is given by solar collectors-conventional boilers, showing a NPV of 70.072.942,38 USD $.

It's even possible to think of the optimal solution by introducing the need to make the plant self-sustainable. For the only II scenario, that optimal compromise has been reached in the combination of flat plate collectors and steam turbine:

- Solar collectors will provide the process with low temperature heat, leading to a limited use of biodiesel;
- Steam turbine will provide the process with high temperature heat; it will also generate electricity to run auxiliaries and the surplus one will be sold, leading to a mayor revenue.

List of Figures

Figure 1.1 – Botryocladia Sp.

Figure 1.2 – Laminaria Digitata

Figure 1.3 – Production of algae

Figure 1.4 – World production of different kinds of biomass

Figure 1.5 – Carbohydrate composition of macroalgae, microalgae and lignocellulosic biomass

Figure 1.6 – Algae accumulation along Chilean coasts every year

Figure 1.7 – Algae accumulation along Chilean coasts in year 2011

Figure 1.8 – Algae accumulation according to regions

Figure 1.9 – Algae accumulation in the city of Valparaiso

Figure 1.10 – Fatty acid content of D. Antarctica

Figure 1.11 – Fatty acid content of L. Nigrescens

Figure 2.1 – Parts of Soxhlet extractor

Figure 2.2 – Operation of Soxhlet extractor

Figure 2.3 – Oil recovery from algae at different rates of dryness

Figure 2.4 – Unsaturated fatty acid content of pistachio oil obtained by Soxhlet technique

Figure 2.5 – Durvillaea Antarctica

Figure 2.6 – Lessonia Nigrescens

Figures 2.7-2.8 – Pressing phase with pressing machine

Figure 2.9 – Drying stove

Figures 2.10-2.11-2.12 – Drying of pressed Durvillaea, non-pressed Durvillaea, Lessonia Nigrescens

Figure 2.13 – Mixer

Figure 2.14 – Dehumidifier

Figure 2.15 – Thin algal dust

Figure 2.16 – At the beginning of the process

Figure 2.17 – During the process

Figure 2.18 – At the end of the process

Figure 2.19 – Rotaevaporator

Figure 3.1 – Transesterification process

Figure 3.2 – Reduced emissions in using biodiesel
Figure 3.3 – Transesterification process scheme
Figure 3.4 – Transesterification chemistry
Figure 3.5 – Aspen transesterification scheme
Figure 4.1 – Thermal and electrical efficiencies of most common technologies
Figure 4.2 – Operations of diesel ICE
Figure 4.3 – Pressure-volume diagram of diesel ICE
Figure 4.4 – Energy balance of cogeneration diesel ICE
Figure 4.5 – Cogeneration gas turbine scheme
Figure 4.6 – Energy balance of cogeneration gas turbine
Figure 4.7 – Counter-pressure cogeneration steam turbine scheme
Figure 4.8 – Condensation/bleedings cogeneration steam turbine scheme
Figure 5.1 – Chilean solar potential
Figure 5.2 – Different radiation contributions
Figure 5.3 – Characteristics of materials used for sensible heat storage
Figure 5.4 – Characteristics of materials used for latent heat storage
Figure 5.5 – TES configurations for seasonal tanks
Figure 5.6 – Flat plate collectors
Figure 5.7 – Captured radiation by surface at 45° and 30°
Figure 5.8 – Aperture and absorber area of a CSP
Figure 5.9 – Parabolic trough collector
Figure 5.10 – CSP + steam turbine scheme
Figure 5.11 – Condensation – derivation steam turbine scheme
Figure 5.12 – T-s diagram of steam turbine
Figure 5.13 – Heat captured by the two different configurations for I scenario
Figure 5.14 – TES charge power for the two configurations for I scenario
Figure 5.15 – Heat captured by the two different configurations for II scenario
Figure 5.16 – TES charge power for the two configurations for II scenario
Figure 6.1 – Installation costs split for biodiesel process
Figure 6.2 – Biodiesel plant PBP for I scenario
Figure 6.3 – Biodiesel plant PBP for II scenario
Figure 6.4 – Base-case PBP for I scenario

Figure 6.5 – Base-case PBP for II scenario
Figure 6.6 – Biodiesel-gas turbine PBP
Figure 6.7 – Biodiesel-steam turbine PBP
Figure 6.8 – Water storage cost wrt storage volume
Figure 6.9 – Flat plate collectors' PBP for I scenario
Figure 6.10 – Flat plate collectors' PBP for II scenario
Figure 6.11 – Flat plate collectors-gas/steam turbine PBP
Figure 6.12 – Installation costs split for CSP technology
Figure 6.13 – CSP collectors' PBP for I scenario
Figure 6.14 – CSP collectors' PBP for II scenario

List of Tables

Table 1.1 – D. Antarctica and L. Nigrescens chemical composition

Table 3.1 – Thermal needs of I scenario

Table 3.2 – Thermal need of II scenario

Table 4.1 – Power ranges and efficiencies of conventional cogeneration technologies

Table 5.1 – Radiation contributions in W/m2

Table 5.2 – Heat stored and heat demanded for 90 collectors' configuration

Table 5.3 – Fuel consumed during winter months for 90 collectors' configuration

Table 5.4 – Fuel consumed during winter months if no storage is present

Table 5.5 – Heat stored and heat demanded for 550 collectors' configuration

Table 5.6 – Fuel consumed during winter months for 550 collectors' configuration

Table 5.7 – Working physical conditions of steam turbine

Table 5.8 – Fuel consumed during winter months for 650 collectors' configuration

Table 5.9 – Fuel consumed during winter months

Table 6.1 – Economic values of conventional technologies

Table 6.2 – Material streams costs

Table 6.3 – Economic values for the transesterification process

Table 6.4 – Biodiesel plant related costs for I scenario

Table 6.5 – Biodiesel plant related costs for II scenario

Table 6.6 – Economic values for solar technologies

Table 6.7 - Flat plate collectors' configurations for I scenario

Table 6.8 - Flat plate collectors' configurations for II scenario

Table 6.9 – CSP collectors' configurations for I scenario

Table 6.10 – CSP collectors' configurations for II scenario

References

1. Wei N, Quarterman J, Jin YS. Marine macroalgae: An untapped resource for producing fuels and chemicals. *Trends Biotechnol.* 2013;31(2):70-77. doi:10.1016/j.tibtech.2012.10.009.

2. Lobban CS, Harrison PJ. Seaweed Mariculture. *Seaweed Ecol Physiol.* 1994:283-297.

3. Montingelli ME, Tedesco S, Olabi AG. Biogas production from algal biomass: A review. *Renew Sustain Energy Rev.* 2015;43:961-972. doi:10.1016/j.rser.2014.11.052.

4. Astals S, Musenze RS, Bai X, et al. Anaerobic co-digestion of pig manure and algae: Impact of intracellular algal products recovery on co-digestion performance. *Bioresour Technol.* 2015;181:97-104. doi:10.1016/j.biortech.2015.01.039.

5. León JA, Montero G, Coronado M, et al. Solar Energy for a Solvent Recovery Stage in a Biodiesel Production Process. *Int J Photoenergy.* 2016;2016. doi:10.1155/2016/1048095.

6. Angelidaki I, Ahring BK. Thermophilic anaerobic digestion of livestock waste: the effect of ammonia. *Appl Microbiol Biotechnol.* 1993;38(4):560-564. doi:10.1007/BF00242955.

7. Jung KA, Lim SR, Kim Y, Park JM. Potentials of macroalgae as feedstocks for biorefinery. *Bioresour Technol.* 2013;135:182-190. doi:10.1016/j.biortech.2012.10.025.

8. Whittick A. The Biology of Seaweeds. *Phycologia.* 1983;22(4):455-456. doi:10.2216/i0031-8884-22-4-455.1.

9. FAO. *The State of World Fisheries and Aquaculture*. Vol 2014.; 2014. doi:92-5-105177-1.

10. Ross AB, Jones JM, Kubacki ML, Bridgeman T. Classification of macroalgae as fuel and its thermochemical behaviour. *Bioresour Technol.* 2008;99(14):6494-6504. doi:10.1016/j.biortech.2007.11.036.

11. Bruton T, Lyons H, Lerat Y, Stanley M, Rasmussen MB. A Review of the Potential of Marine Algae as a Source of Biofuel in Ireland. *Sustain Energy Irel Dublin*. 2009:88. doi:10.1016/j.envint.2003.08.001.

12. Black WAP. The seasonal variation in weight and chemical composition of the common British Laminariaceae. *J Mar Biol Assoc United Kingdom*. 1950;29(01):45. doi:10.1017/S0025315400056186.

13. Quitral V, Morales C, Sepúlveda M, Schwartz M M. Propiedades nutritivas y saludables de algas marinas y su potencialidad como ingrediente funcional. *Rev Chil Nutr.* 2012;39(4):196-202. doi:10.4067/S0717-75182012000400014.

14. Chapman VJ. *Seaweeds and Their Uses*.; 1980. doi:10.1007/s13398-014-0173-7.2.

15. Ortiz J, Romero N, Robert P, et al. Dietary fiber, amino acid, fatty acid and

toccopherol contents of the edible seaweeds *Ulva lactuca* and *Durvillaea antartica*. *Food Chem*. 2006;33(5):575_583. doi:DOI 10.1016/j.foodchem.2005.07.027.

16. Mishra VK, Temelli F, Ooraikul B, Shacklock PF, Craigie JS. Lipids of the Red Alga, Palmaria palmata. *Bot Mar*. 1993;36(5):2011-2013. doi:10.1515/botm.1993.36.2.169.

17. IFOP. Cochayuyo y huiros. 2009:1-5.

18. Gomez I, Westermeier R. Energy contents and organic constituents in Antarctic and south Chilean marine brown algae. *Polar Biol*. 1995;15(8):597-602. doi:10.1007/BF00239653.

19. Marina DDB, Ciencias F De, Católica U, Acuicultura D De, Ciencias F De. The chemical composition of Lessonia berteroana (ex L . nigrescens) in kelp harvest management and open access areas near Coquimbo , Chile The chemical composition of Lessonia berteroana (ex L . nigrescens) in kelp harvest management and open access a. 2018;46(May). doi:10.3856/vol46-issue1-fulltext-2.

20. Suganya T, Nagendra Gandhi N, Renganathan S. Production of algal biodiesel from marine macroalgae Enteromorpha compressa by two step process: Optimization and kinetic study. *Bioresour Technol*. 2013;128:392-400. doi:10.1016/j.biortech.2012.10.068.

21. Abdolshahi A, Majd MH, Rad JS, Taheri M, Shabani A, Teixeira da Silva JA. Choice of solvent extraction technique affects fatty acid composition of pistachio (Pistacia vera L.) oil. *J Food Sci Technol*. 2015;52(4):2422-2427. doi:10.1007/s13197-013-1183-8.

22. Chynoweth DP, Owens JM, Legrand R. Renewable methane from anaerobic digestion of biomass. *Renew Energy*. 2000;22(1-3):1-8. doi:10.1016/S0960-1481(00)00019-7.

23. Marinho-Soriano E, Fonseca PC, Carneiro MAA, Moreira WSC. Seasonal variation in the chemical composition of two tropical seaweeds. *Bioresour Technol*. 2006;97(18):2402-2406. doi:10.1016/j.biortech.2005.10.014.

24. Myint L. Process analysis and optimization of Biodiesel production from vegetable oils. *Texas A&M Univ*. 2007;(May):100. http://medcontent.metapress.com/index/A65RM03P4874243N.pdf.

25. Kick C, Kline A, Hladky H, Aller B. Using AspenPlus Resources to Model Biodiesel Production Applicable for a Senior Capstone Design Project. *ASEE North-Central Sect Conf*. 2013.

26. Agee BM, Mullins G, Swartling DJ. Use of solar energy for biodiesel production and use of biodiesel waste as a green reaction solvent. *Sustain Chem Process*. 2014;2(21):1-10. doi:10.1186/s40508-014-0021-2.

27. Rollbuhler RJ. *COMBUSTION CHARACTERISTICS OF GAS TURBINE ALTERNATIVE FUELS*.; 1987.

28. Jones R, Goldmeer J, Monetti B. Addressing gas turbine fuel flexibility. *GE Energy*. 2011;GER-4601 (:1-20. http://site.ge-energy.com/prod_serv/products/tech_docs/en/downloads/GER4601.pdf.

29. Szalay D, Fujiwara H, Palocz-andresen M. Using biodiesel fuel for gas turbine combustors. 2015;65(65):65-76. doi:10.3220/LBF1443169529000.

30. Cabeza LF, Martorell I, Miró L, Fernández AI, Barreneche C. *Introduction to Thermal Energy Storage (TES) Systems*. Woodhead Publishing Limited; 2014. doi:10.1533/9781782420965.1.

31. Sillman S. Performance and economics of annual storage solar heating systems. *Sol Energy*. 1981;27(6):513-528. doi:10.1016/0038-092X(81)90046-3.

32. Günther M, Joemann M, Csambor S. Advanced CSP Teaching Materials Chapter 5 Parabolic Trough Technology Authors. *2011*. 2011:1-43.

33. Haas MJ, McAloon AJ, Yee WC, Foglia TA. A process model to estimate biodiesel production costs. *Bioresour Technol*. 2006;97(4):671-678. doi:10.1016/j.biortech.2005.03.039.

34. Koch K, Thiel M, Tellier F, Hagen W, Graeve M, Tala F. Species separation within the Lessonia nigrescens complex (Phaeophyceae , Laminariales) is mirrored by ecophysiological traits. 2015;(May). doi:10.1515/bot-2014-0086.